THE ASTROPHYSICAL JOURNAL

An International Review of Spectroscopy and Astronomical Physics

FOUNDED IN 1895 BY GEORGE E. HALE AND JAMES E. KEELER

EDITORS

HENRY G. GALE
Ryerson Physical Laboratory of the University of Chicago

FREDERICK H. SEARES
Mount Wilson Observatory of the Carnegie Institution of Washington

OTTO STRUVE
Yerkes Observatory of the University of Chicago

COLLABORATORS

WALTER S. ADAMS, *Mount Wilson Observatory;* JOSEPH S. AMES, *Johns Hopkins University;* WILLIAM W. CAMPBELL, *Lick Observatory;* HENRY CREW, *Northwestern University;* CHARLES FABRY, *Université de Paris;* ALFRED FOWLER, *Imperial College, London;* EDWIN HUBBLE, *Mount Wilson Observatory;* HEINRICH KAYSER, *Universität Bonn;* ROBERT A. MILLIKAN, *Institute of Technology, Pasadena;* HUGH F. NEWALL, *Cambridge University;* FRIEDRICH PASCHEN, *Reichsanstalt, Charlottenburg;* HENRY N. RUSSELL, *Princeton University;* FRANK SCHLESINGER, *Yale Observatory;* HARLOW SHAPLEY, *Harvard College Observatory*

VOLUME 86

JULY–DECEMBER 1937

THE UNIVERSITY OF CHICAGO PRESS
CHICAGO, ILLINOIS

THE CAMBRIDGE UNIVERSITY PRESS, LONDON
THE MARUZEN COMPANY LIMITED, TOKYO
THE COMMERCIAL PRESS, LIMITED, SHANGHAI

PUBLISHED JULY, SEPTEMBER, OCTOBER, NOVEMBER, DECEMBER 1937

COMPOSED AND PRINTED BY THE UNIVERSITY OF CHICAGO PRESS
CHICAGO, ILLINOIS, U.S.A.

Astron Obs
Wake

CONTENTS

NUMBER I

PAGE

THE BOUNDARY-VALUE PROBLEM OF THE THEORY OF STELLAR ABSORPTION LINES. Bengt Strömgren 1

REGIONAL STUDY OF INTERSTELLAR SODIUM. Paul W. Merrill . . . 28

ANALYSIS OF THE INTENSITIES OF THE INTERSTELLAR D LINES O. C. Wilson and Paul W. Merrill 44

PHYSICAL PROCESSES IN GASEOUS NEBULAE. II. THEORY OF THE BALMER DECREMENT. Donald H. Menzel and James G. Baker 70

THE OPACITY IN THE INTERIOR OF A STAR. S. Chandrasekhar . . . 78

THE ANNUAL VARIATION IN THE INTENSITY OF THE ZODIACAL LIGHT. C. T. Elvey 84

AN EMISSION NEBULA NEAR σ SCORPII. Otto Struve 94

NOTES

NOTE ON A POSSIBLE EFFECT OF THE RECENT INCREASE IN BRIGHTNESS OF γ CASSIOPEIAE. W. W. Morgan 100

NOTE ON THE DUPLICITY OF NOVA HERCULIS. G. P. Kuiper . . . 102

REVIEWS 106

NUMBER II

MAGNESIUM HYDRIDE IN ARCTURUS AND ANTARES. Dorothy N. Davis. 109

THE TRAPEZIUM CLUSTER OF THE ORION NEBULA. W. Baade and R. Minkowski 119

SPECTROPHOTOMETRIC INVESTIGATIONS OF SOME O- AND B-TYPE STARS CONNECTED WITH THE ORION NEBULA. W. Baade and R. Minkowski 123

REGIONAL STUDY OF THE INTERSTELLAR CALCIUM LINES. Roscoe F. Sanford 136

SPECTROGRAPHIC ORBITS OF FIVE FAINT VARIABLE STARS. Roscoe F. Sanford 153

INTENSITIES OF THE INFRARED *Ca* II TRIPLET IN STELLAR SPECTRA. O. C. Wilson and Paul W. Merrill 162

THE ORBITS OF FIVE VISUAL BINARIES BELONGING TO THE HYADES. G. P. Kuiper 166

PAGE

On the Hydrogen Content of Clusters. G. P. Kuiper 176

A Spectrographic Observation of the Reflection Effect in Close Binaries. Otto Struve 198

The Degree of Variability of Calcium Content in Atmospheres of A-Type Stars. J. W. Abrams and E. Öpik 203

Notes

The Color Index of the Night Sky. Jessie Rudnick 212

Reviews 215

NUMBER III

On the Masses of Nebulae and of Clusters of Nebulae. F. Zwicky 217

Photoelectric Magnitudes and Colors of Extragalactic Nebulae. Joel Stebbins and Albert E. Whitford 247

Intensities and Displacements of Interstellar Lines. Paul W. Merrill, Roscoe F. Sanford, O. C. Wilson, and Cora G. Burwell . . 274

The Spectrum of H_2 from λ 4225 to λ 4756. Norton A. Kent and Reginald G. Lacount 311

Photochemistry of Planetary Atmospheres. Rupert Wildt . . . 321

Note on the Temperature of Venus. Arthur Adel 337

Notes

The Nuclear Star Cluster in 30 Doradus. Harlow Shapley and John S. Paraskevopoulos 340

The Photoelectric Color of the Zodiacal Light. C. T. Elvey and Paul Rudnick 342

NUMBER IV

The Sodium Content of the Head of the Great Daylight Comet Skjellerup 1927 K. Arthur Adel, V. M. Slipher, and R. Ladenburg 345

Radial Velocities of Cepheid Variable Stars. Alfred H. Joy . . 363

The Testing of Diffraction Gratings by Knife Edge and by Interferometer. Henry G. Gale 437

The Behavior of Forbidden Oxygen Lines in Novae. N. T. Bobrovnikoff and J. M. MacQueen 446

Photometry of the G Band in Representative Stellar Spectra. W. A. Rense and J. A. Hynek 460

On the Origin of the Solar System. W. J. Luyten and E. L. Hill . . 470

PAGE

NOTES

CONSIDERATIONS REGARDING INTERSTELLAR MOLECULES. P. Swings and L. Rosenfeld 483

NOTE ON THE INTERPRETATION OF UNIDENTIFIED INTERSTELLAR LINES. Eugene H. Eyster 486

NUMBER V

THE CONTOURS OF $H\gamma$ AND $H\delta$ IN δ CEPHEI. C. J. Krieger 489

PHOTOGRAPHIC STUDIES OF NEBULAE. John C. Duncan 496

THE EXCITATION OF EMISSION LINES IN LATE-TYPE VARIABLES. A. D. Thackeray 499

INFRARED STELLAR SURVEYS AND INDEX SEQUENCES. Charles Hetzler . 509

COLOR INDICES OF REFLECTION NEBULAE. O. C. Collins 529

THE VARIATION OF THE LIGHT FROM THE NIGHT SKY AND ITS EFFECT. C. T. Elvey and Paul Rudnick 562

THE INTERPRETATION OF ϵ AURIGAE. G. P. Kuiper, O. Struve, and B. Strömgren 570

A NEW SLIT SPECTROGRAPH FOR DIFFUSE GALACTIC NEBULAE. Otto Struve 613

NOTES

THE SPECTRA OF THE NORTH AMERICA NEBULA AND OF THE γ CYGNI NEBULA. J. L. Greenstein and L. G. Henyey 620

NOTE ON THE SPECTRUM OF PERIODIC COMET ENCKE. G. Van Biesbroeck and L. G. Henyey 622

PARTIALLY DEGENERATE STELLAR CONFIGURATIONS. S. Chandrasekhar 623

REVIEWS 626

ERRATUM 627

INDEX 628

THE ASTROPHYSICAL JOURNAL

AN INTERNATIONAL REVIEW OF SPECTROSCOPY AND ASTRONOMICAL PHYSICS

VOLUME 86 JULY 1937 NUMBER 1

THE BOUNDARY-VALUE PROBLEM OF THE THEORY OF STELLAR ABSORPTION LINES

BENGT STRÖMGREN

ABSTRACT

The problem of the *theoretical calculation of intensities within absorption lines* is considered. The case when the ratio of continuous absorption to continuous-plus-line absorption is *variable through the atmosphere* in such a way that the relative changes are not very large but are otherwise arbitrary is considered. For this case convenient formulae for the calculation of absorption-line intensities in the integrated spectrum are derived. With the aid of the relations derived, the relative *influence of the various layers of the atmosphere* on the intensities within absorption lines is discussed. The relations are specialized for comparison with equations previously derived by Eddington and Unsöld. The accuracy and *range of applicability* of the procedure developed is discussed.

I

The theory of stellar absorption lines gives the relation between the ratio r of the intensity at any point within an absorption line to the intensity of the adjacent continuous spectrum, on one hand, and the ratio η of the line-absorption coefficient to the coefficient of continuous absorption, on the other. As is well known, the simple case that the ratio η is constant throughout the atmosphere can be treated analytically in a simple way. This case has been discussed by Eddington and Milne. Eddington[1] has shown that the case, when $1/(1+\eta)$ is a linear function of the optical depth τ in the continuous spectrum, can also be treated analytically, the ratio r being expressible with the aid of Bessel functions. Woolley[2] has used the method of computing r, just referred to, in a number of cases of practical importance, and has also used the method in the case when

[1] *M.N.*, **89**, 620, 1929. [2] *Ibid.*, **92**, 482, 1932; **93**, 691, 1933.

$1/(1+\eta)$ can be put equal to a linear function of the optical depth for the part of the atmosphere above a certain boundary depth, and equal to a linear function differing from the first below that boundary depth.

When η is given numerically as a function of optical depth, the ratio r can always be found with the aid of numerical integrations. This method has been used by Pannekoek.[3]

In many problems of quantitative analysis of stellar absorption-line spectra it is of importance to be able to carry out calculations of r values in a convenient, and yet not too inaccurate, way. The simplest method is to choose the value of η at some representative point—say at $\tau = 1/3$—and compute r as if η were constant throughout the atmosphere and equal to that value. This method, however, may lead to results that are considerably in error. Unsöld[4] has developed a very convenient method for calculating accurate r values in the extreme wings of stellar absorption lines ($r > 0.85$). This method is of great value in the discussion of broad absorption lines for which contours can be measured. In the case of fainter lines, where only equivalent widths can be determined experimentally, the method naturally fails. Those parts of the contour for which $r < 0.85$ contribute largely to the equivalent width, except in the case of extremely weak lines, which in general would not be measurable.

Minnaert[5] has developed Unsöld's method for the extreme wings, with the purpose of making possible accurate predictions of the variation of the intensities in the extreme wings over the solar disk.

Ten Bruggencate[6] has treated the general boundary-value problem of stellar absorption lines in a purely analytical way, subdividing the atmosphere into a large number of separate layers. Wellmann[7] has developed analytical methods for calculating r values and has shown that they can be used in practical cases.

In the present paper we shall consider the case that the ratio $1/(1+\eta)$ of continuous absorption to continuous-plus-line absorp-

[3] *Ibid.*, **91**, 139, 519, 1930–1931; *Pub. Astr. Inst. Amsterdam*, No. 4, 1935.

[4] *Zs. f. Ap.*, **4**, 339, 1932.

[5] *Ibid.*, **12**, 313, 1936.

[6] *Ibid.*, **4**, 159, 1932.

[7] *Ibid.*, **12**, 140, 1936.

tion is variable through the atmosphere, in such a way that the relative changes of $1/(1+\eta)$ throughout the relevant parts of the atmosphere are not very large but are otherwise arbitrary. For this case convenient formulae for the calculation of r values are derived. It is shown that the changes of η can be rather large without serious error in the computed r value. Though cases may occur in which the variation of η is such that the method fails, a great many cases of practical importance are covered with sufficient accuracy.

A number of examples of the use of the method here developed for calculating r values may be found in a forthcoming paper by the author on the hydrogen content of stellar atmospheres.

The procedure here developed can be applied to the theory of the continuous spectrum for the general case when the absorption coefficient is an unrestricted function of depth and wave-length. An investigation of this problem is, however, outside the scope of the present paper.

II

The theory of stellar absorption lines[8] leads to the following differential equation for the intensity I_ν within an absorption line:

$$\cos\theta \frac{dI_\nu}{\rho dx} = (k_\nu + l_\nu)I_\nu - k_\nu B_\nu - (1-\epsilon)l_\nu J_\nu - \epsilon l_\nu Q B_\nu . \qquad (1)$$

Here I_ν is the intensity at a certain geometrical depth x below the surface of the atmosphere, in a direction making the angle θ with the outward normal to the atmosphere (considered as plane-parallel). Further, ρ is the density, k_ν the coefficient of continuous absorption at the frequency ν, l_ν the coefficient of line absorption at frequency ν, B_ν the Planck intensity corresponding to the local temperature and J_ν the mean intensity (i.e., I_ν averaged over all directions), both at frequency ν. The quantity ϵ is a measure of the influence of electron capture on the upper stationary state of the line considered and of collision transition to that state upon the intensities within the line, while Q is a measure of the deviation from a Planck spectrum

[8] Cf. A. S. Eddington, *The Internal Constitution of the Stars*, Cambridge, 1926; E. A. Milne, *Handbuch d. Astrophysik*, **3**, 1, Berlin, 1929; S. Rosseland, *Astrophysik*, Berlin, 1931; B. Strömgren, *Handbuch d. Astrophysik*, **7**, Berlin, 1936; S. Rosseland, *Theoretical Astrophysics*, Oxford, 1936.

of the ionizing continuous spectrum at the point considered. The exact definition of the quantities ϵ and Q can be found in a paper by the author;[9] in the present discussion we shall only make use of the fact that ϵ is a small quantity, usually less than 0.01, while Q is usually somewhat larger than 1 but of the order of magnitude 1.

The equation of transfer (1) is the most general equation for the case of lines originating from the ground state, when line fluorescence is neglected.

When the system of differential equations (1) is treated according to Eddington's method of approximation, the following equations are obtained. Averaging (1) over all directions, one finds

$$\frac{dH_\nu}{\rho dx} = (k_\nu + \epsilon l_\nu)J_\nu - (k_\nu + \epsilon l_\nu Q)B_\nu , \tag{2}$$

H_ν being defined as

$$H_\nu = \int I_\nu \cos\theta \frac{d\omega}{4\pi} \tag{3}$$

or

$$H_\nu = \frac{1}{4\pi} F_\nu , \tag{4}$$

where F_ν is the net flux. Averaging (1) after multiplication by $\cos\theta$, we get

$$\frac{dK_\nu}{\rho dx} = (k_\nu + l_\nu)H_\nu , \tag{5}$$

K_ν being defined as

$$K_\nu = \int I_\nu \cos^2\theta \frac{d\omega}{4\pi} . \tag{6}$$

Introducing Eddington's approximation $K_\nu = \frac{1}{3}J_\nu$ in (5), we obtain

$$\frac{dJ_\nu}{\rho dx} = 3(k_\nu + l_\nu)H_\nu . \tag{7}$$

[9] *Zs. f. Ap.*, **10**, 237, 1935.

Now J_ν can be determined from (2) and (7), when use is made of the boundary conditions of the problem. It is convenient at this stage to introduce the optical depth in the line at the frequency ν:

$$dt_\nu = (k_\nu + l_\nu)\rho dx \tag{8}$$

or

$$t_\nu = \int_0^x (k_\nu + l_\nu)\rho dx \,. \tag{9}$$

The following simplifying notation is used:

$$\eta_\nu = \frac{l_\nu}{k_\nu}, \tag{10}$$

$$\lambda_\nu = \frac{1 + \epsilon\eta_\nu}{1 + \eta_\nu} \,. \tag{11}$$

Then equations (2) and (7) take the form

$$\frac{dH_\nu}{dt_\nu} = \lambda_\nu\left(J_\nu - \frac{1 + \epsilon\eta_\nu Q}{1 + \epsilon\eta_\nu} B_\nu\right) \tag{12}$$

and

$$\frac{dJ_\nu}{dt_\nu} = 3H_\nu \,. \tag{13}$$

Eliminating H_ν between (12) and (13), we find

$$\frac{d^2J_\nu}{dt_\nu^2} = 3\lambda_\nu\left(J_\nu - \frac{1 + \epsilon\eta_\nu Q}{1 + \epsilon\eta_\nu} B_\nu\right). \tag{14}$$

The factor $(1 + \epsilon\eta_\nu Q)/(1 + \epsilon\eta_\nu)$, because of the smallness of ϵ, does not differ appreciably from unity, except in the case of very large η_ν values, i.e., at frequencies near the center of strong absorption lines. The results of the present investigation are intended mainly for use in calculations of equivalent widths of absorption lines. In these calculations the factor in question can be put equal to unity without appreciable loss of accuracy, the corresponding small changes of the intensity near the center of the lines leading to

very small changes in the equivalent width only. For the sake of convenience we shall, therefore, in the following analysis omit the factor $(1 + \epsilon\eta_\nu Q)/(1 + \epsilon\eta_\nu)$. If for other purposes it should be desirable to take account of this factor, one can do so simply by interpreting B_ν in the relations derived below as the Planck intensity corrected by multiplication with $(1 + \epsilon\eta_\nu Q)/(1 + \epsilon\eta_\nu)$. We therefore write (14) as

$$\frac{d^2 J_\nu}{dt_\nu^2} = 3\lambda_\nu (J_\nu - B_\nu) \,. \tag{15}$$

The proper particular solution of (15) is fixed by the following boundary conditions: (1) As $t_\nu \to \infty$, $J_\nu - B_\nu$ must not increase exponentially (in important simplified cases $J_\nu - B_\nu$ then tends to zero). (2) For $t_\nu = 0$, $J_\nu = 2H_\nu$ (Eddington's approximate expression of the fact that on the surface there is no ingoing radiation):

$$(J_\nu)_{t_\nu = 0} = 2(H_\nu)_{t_\nu = 0} \,. \tag{16}$$

Making use of (13), the second boundary condition can be written in the following form:

$$\frac{2}{3}\left(\frac{dJ_\nu}{dt_\nu}\right)_{t_\nu = 0} = (J_\nu)_{t_\nu = 0} \,. \tag{17}$$

When J_ν has been found as a function of t_ν, I_ν can be determined as a function of t_ν and θ from (1). When it is sufficient to find the intensity in the integrated spectrum radiated by the star, it is not necessary to go through the latter analysis, as was pointed out by Eddington. The net flux F_ν for $t_\nu = 0$, which is proportional to the intensity in the integrated spectrum, is, according to (4) and (13) or (16), given by

$$\left(\frac{F_\nu}{\pi}\right)_{t_\nu = 0} = \frac{4}{3}\left(\frac{dJ_\nu}{dt_\nu}\right)_{t_\nu = 0} = 2(J_\nu)_{t_\nu = 0} \,, \tag{18}$$

and can thus be found immediately, when J_ν has been determined as a function of t_ν.

III

The mathematical boundary-value problem of the theory of stellar absorption lines can thus be stated as follows: One has to find that solution of the differential equation

$$\frac{d^2J_\nu}{dt_\nu^2} = 3\lambda_\nu(J_\nu - B_\nu) \tag{19}$$

which satisfies the boundary condition that $J_\nu - B_\nu$ does not increase exponentially as t_ν goes to infinity, and the further boundary condition that

$$\frac{2}{3}\left(\frac{dJ_\nu}{dt_\nu}\right)_{t_\nu=0} = (J_\nu)_{t_\nu=0}\,. \tag{20}$$

The intensity within the spectral line in the integrated spectrum of the star is given by $(J_\nu)_{t_\nu=0}$. In (19) λ_ν and B_ν should be considered as known functions of t_ν.

For the sake of convenience we shall drop the index ν of all quantities in the analysis following. Let

$$y = J - B\,. \tag{21}$$

Then, from (19),

$$\frac{d^2y}{dt^2} = 3\lambda y - \frac{d^2B}{dt^2}\,. \tag{22}$$

The boundary conditions are now that y must not increase exponentially as t goes to infinity, and, according to (20),

$$\frac{2}{3}\left(\frac{dy}{dt}\right)_{t=0} - (y)_{t=0} = (B)_{t=0} - \frac{2}{3}\left(\frac{dB}{dt}\right)_{t=0}\,. \tag{23}$$

Introduce

$$a = (B)_{t=0} \tag{24}$$

$$p = \left(\frac{dB}{dt}\right)_{t=0}, \tag{25}$$

then

$$\frac{2}{3}\left(\frac{dy}{dt}\right)_{t=0} - (y)_{t=0} = a - \tfrac{2}{3}p\,. \tag{26}$$

Finally, (18) becomes

$$\left(\frac{F}{\pi}\right)_{t=0} = \frac{4}{3}\left(\frac{dy}{dt}\right)_{t=0} + \tfrac{4}{3}p = 2(y)_{t=0} + 2a\,. \tag{27}$$

Again λ and d^2B/dt^2 are to be considered as given functions of t. The simplified case first studied by Eddington and Milne corresponds to λ equal to a constant, independent of t, and $d^2B/dt^2 = 0$, i.e., $B = a + pt$. In that case it follows immediately that

$$y = -\frac{a - \frac{2}{3}p}{1 + \frac{2}{3}\sqrt{3\lambda}}\, e^{-\sqrt{3\lambda}\,t}, \qquad \left(\lambda = \text{const};\ \frac{d^2B}{dt^2} = 0\right). \tag{28}$$

Then, from (27),

$$\tfrac{1}{2}\left(\frac{F}{\pi}\right)_{t=0} = a - \frac{a - \frac{2}{3}p}{1 + \frac{2}{3}\sqrt{3\lambda}} \tag{29}$$

or

$$\left(\frac{F}{\pi}\right)_{t=0} = \frac{\frac{4}{3}a\sqrt{3\lambda} + \frac{4}{3}p}{1 + \frac{2}{3}\sqrt{3\lambda}}\,. \tag{30}$$

The introduction of the values of a and p following from a discussion of the Planck intensity as a function of the optical depth t then completes the calculation.

We shall consider in the following the case when the variation of λ is small compared with λ. The boundary-value problem can then be solved with the aid of standard perturbation methods of the theory of differential equations. The first part of the analysis, up to equation (51), is, however, perfectly general.

Let

$$\lambda = \lambda_0 + \delta\,, \tag{31}$$

where λ_0 is some properly chosen constant value, not necessarily the value of λ for $t = 0$. Then (22) becomes

$$\frac{d^2y}{dt^2} = 3\lambda_0 y + 3y\cdot\delta - \frac{d^2B}{dt^2}\,. \tag{32}$$

We can write the general solution of (32) in the form

$$y = Ce^{\sqrt{3\lambda_0}\,t} + De^{-\sqrt{3\lambda_0}\,t}, \tag{33}$$

where C and D are functions of t. From (33) it follows that

$$\frac{dy}{dt} = \sqrt{3\lambda_0}\,Ce^{\sqrt{3\lambda_0}\,t} - \sqrt{3\lambda_0}\,De^{-\sqrt{3\lambda_0}\,t}, \tag{34}$$

provided we fix C and D by the usual condition

$$0 = \frac{dC}{dt}\,e^{\sqrt{3\lambda_0}\,t} + \frac{dD}{dt}\,e^{-\sqrt{3\lambda_0}\,t}. \tag{35}$$

Then

$$\left.\begin{aligned}\frac{d^2y}{dt^2} &= 3\lambda_0 Ce^{\sqrt{3\lambda_0}\,t} + 3\lambda_0 De^{-\sqrt{3\lambda_0}\,t} \\ &\quad + \sqrt{3\lambda_0}\,\frac{dC}{dt}\,e^{\sqrt{3\lambda_0}\,t} - \sqrt{3\lambda_0}\,\frac{dD}{dt}\,e^{-\sqrt{3\lambda_0}\,t};\end{aligned}\right\} \tag{36}$$

and therefore, according to (32), one must have

$$3y\cdot\delta - \frac{d^2B}{dt^2} = \sqrt{3\lambda_0}\,\frac{dC}{dt}\,e^{\sqrt{3\lambda_0}\,t} - \sqrt{3\lambda_0}\,\frac{dD}{dt}\,e^{-\sqrt{3\lambda_0}\,t}. \tag{37}$$

Solving (35) and (37) for the derivatives of C and D, one finds

$$\frac{dC}{dt} = \frac{1}{2\sqrt{3\lambda_0}}\,e^{-\sqrt{3\lambda_0}\,t}\cdot 3y\cdot\delta - \frac{1}{2\sqrt{3\lambda_0}}\,e^{-\sqrt{3\lambda_0}\,t}\cdot\frac{d^2B}{dt^2} \tag{38}$$

and

$$\frac{dD}{dt} = -\frac{1}{2\sqrt{3\lambda_0}}\,e^{\sqrt{3\lambda_0}\,t}\cdot 3y\cdot\delta + \frac{1}{2\sqrt{3\lambda_0}}\,e^{\sqrt{3\lambda_0}\,t}\cdot\frac{d^2B}{dt^2}. \tag{39}$$

These two differential equations can be solved by quadratures:

$$C = -\frac{1}{2\sqrt{3\lambda_0}}\int_t^{c_1} e^{-\sqrt{3\lambda_0}\,t}\cdot 3y\cdot\delta\cdot dt + \frac{1}{2\sqrt{3\lambda_0}}\int_t^{c_1} e^{-\sqrt{3\lambda_0}\,t}\cdot\frac{d^2B}{dt^2}\cdot dt \tag{40}$$

and

$$D = -\frac{1}{2\sqrt{3\lambda_0}}\int_{c_2}^{t} e^{\sqrt{3\lambda_0}\,t}\cdot 3y\cdot\delta\cdot dt + \frac{1}{2\sqrt{3\lambda_0}}\int_{c_2}^{t} e^{\sqrt{3\lambda_0}\,t}\cdot\frac{d^2B}{dt^2}\cdot dt. \tag{41}$$

From (33), (40), and (41) one finds that the general solution of the differential equation (32) can be written in the form

$$\left.\begin{aligned} y = &- \frac{1}{2\sqrt{3\lambda_0}} e^{\sqrt{3\lambda_0}\,t} \int_t^{c_1} e^{-\sqrt{3\lambda_0}\,t} \cdot 3y \cdot \delta \cdot dt \\ &+ \frac{1}{2\sqrt{3\lambda_0}} e^{\sqrt{3\lambda_0}\,t} \int_t^{c_1} e^{-\sqrt{3\lambda_0}\,t} \cdot \frac{d^2B}{dt^2} \cdot dt \\ &- \frac{1}{2\sqrt{3\lambda_0}} e^{-\sqrt{3\lambda_0}\,t} \int_{c_2}^{t} e^{\sqrt{3\lambda_0}\,t} \cdot 3y \cdot \delta \cdot dt \\ &+ \frac{1}{2\sqrt{3\lambda_0}} e^{-\sqrt{3\lambda_0}\,t} \int_{c_2}^{t} e^{\sqrt{3\lambda_0}\,t} \cdot \frac{d^2B}{dt^2} \cdot dt \,. \end{aligned}\right\} \quad (42)$$

The two constants of the general solution are c_1 and c_2. The next step is to determine c_1 and c_2 in such a way that the boundary conditions are satisfied. As t tends to infinity, the two terms involving c_2 will be of the order of magnitude of y. Hence, the sum of the two terms involving c_1 must not increase exponentially with t. Suppose that c_1 were finite. Then the sum of the two integrals involving c_1 would tend toward a finite limit as t goes to infinity, and the sum of the two terms involving c_1 would increase exponentially as t goes to infinity, in contradiction with the result derived from the boundary condition. Hence c_1 has to be replaced by ∞. Then the first boundary condition is satisfied.

Putting c_2 equal to zero, allowing for this by adding a constant times the factor of the integrals involving c_2, one can now write the solution as

$$\left.\begin{aligned} y = &- \frac{1}{2\sqrt{3\lambda_0}} e^{\sqrt{3\lambda_0}\,t} \int_t^{\infty} e^{-\sqrt{3\lambda_0}\,t} \cdot 3y \cdot \delta \cdot dt \\ &+ \frac{1}{2\sqrt{3\lambda_0}} e^{\sqrt{3\lambda_0}\,t} \int_t^{\infty} e^{-\sqrt{3\lambda_0}\,t} \cdot \frac{d^2B}{dt^2} \cdot dt \\ &- \frac{1}{2\sqrt{3\lambda_0}} e^{-\sqrt{3\lambda_0}\,t} \int_0^{t} e^{\sqrt{3\lambda_0}\,t} \cdot 3y \cdot \delta \cdot dt \\ &+ \frac{1}{2\sqrt{3\lambda_0}} e^{-\sqrt{3\lambda_0}\,t} \int_0^{t} e^{\sqrt{3\lambda_0}\,t} \cdot \frac{d^2B}{dt^2} \cdot dt + \gamma e^{-\sqrt{3\lambda_0}\,t}, \end{aligned}\right\} \quad (43)$$

where γ is a constant of integration.

We have now to determine γ so that (43) satisfies the second boundary condition (26). From (43) one derives

$$\left.\begin{aligned}\frac{2}{3}\left(\frac{dy}{dt}\right)_{t=0} = &-\frac{1}{3}\int_0^\infty e^{-\sqrt{3\lambda_0}\,t}\cdot 3y\cdot\delta\cdot dt\\ &+\frac{1}{3}\int_0^\infty e^{-\sqrt{3\lambda_0}\,t}\cdot\frac{d^2B}{dt^2}\cdot dt+\frac{1}{3\sqrt{3\lambda_0}}\cdot(3y\cdot\delta)_{t=0}\\ &-\frac{1}{3\sqrt{3\lambda_0}}\left(\frac{d^2B}{dt^2}\right)_{t=0}-\frac{1}{3\sqrt{3\lambda_0}}\cdot(3y\cdot\delta)_{t=0}\\ &+\frac{1}{3\sqrt{3\lambda_0}}\left(\frac{d^2B}{dt^2}\right)_{t=0}-\tfrac{2}{3}\sqrt{3\lambda_0}\,\gamma\end{aligned}\right\}\quad(44)$$

and

$$\left.\begin{aligned}(y)_{t=0} = &-\frac{1}{2\sqrt{3\lambda_0}}\int_0^\infty e^{-\sqrt{3\lambda_0}\,t}\cdot 3y\cdot\delta\cdot dt\\ &+\frac{1}{2\sqrt{3\lambda_0}}\int_0^\infty e^{-\sqrt{3\lambda_0}\,t}\cdot\frac{d^2B}{dt^2}\cdot dt+\gamma\,.\end{aligned}\right\}\quad(45)$$

Inserting (43) and (44) in the boundary condition (26), one gets the following equation for the determination of γ:

$$\left.\begin{aligned}&\left(-\frac{1}{3}+\frac{1}{2\sqrt{3\lambda_0}}\right)\int_0^\infty e^{-\sqrt{3\lambda_0}\,t}\cdot 3y\cdot\delta\cdot dt\\ &+\left(\frac{1}{3}-\frac{1}{2\sqrt{3\lambda_0}}\right)\int_0^\infty e^{-\sqrt{3\lambda_0}\,t}\cdot\frac{d^2B}{dt^2}\cdot dt\\ &-(1+\tfrac{2}{3}\sqrt{3\lambda_0})\gamma = a-\tfrac{2}{3}p\,.\end{aligned}\right\}\quad(46)$$

Solving this equation for γ, one finds

$$\left.\begin{aligned}\gamma = &-\frac{a-\frac{2}{3}p}{1+\frac{2}{3}\sqrt{3\lambda_0}}+\frac{1}{2\sqrt{3\lambda_0}}\,\frac{1-\frac{2}{3}\sqrt{3\lambda_0}}{1+\frac{2}{3}\sqrt{3\lambda_0}}\int_0^\infty e^{-\sqrt{3\lambda_0}\,t}\cdot 3y\cdot\delta\cdot dt\\ &-\frac{1}{2\sqrt{3\lambda_0}}\,\frac{1-\frac{2}{3}\sqrt{3\lambda_0}}{1+\frac{2}{3}\sqrt{3\lambda_0}}\int_0^\infty e^{-\sqrt{3\lambda_0}\,t}\cdot\frac{d^2B}{dt^2}\cdot dt\,.\end{aligned}\right\}\quad(47)$$

Inserting (47) in (43), one arrives at the particular solution satisfying the two boundary conditions. In order to find the quantity $(F/\pi)_{t=0}$, which is proportional to the intensity in the integrated

spectrum, one has to insert (47) in (44) or (45), and then (44) or (45) in (27). Carrying out the last-mentioned operations, one finds

$$\left.\begin{aligned}\frac{1}{2}\left(\frac{F}{\pi}\right)_{t=0} = a &- \frac{a-\frac{2}{3}p}{1+\frac{2}{3}\sqrt{3\lambda_0}} + \frac{1}{2\sqrt{3\lambda_0}}\,\frac{1-\frac{2}{3}\sqrt{3\lambda_0}}{1+\frac{2}{3}\sqrt{3\lambda_0}}\int_0^\infty e^{-\sqrt{3\lambda_0}\,t}\cdot 3y\cdot\delta\cdot dt\\ &- \frac{1}{2\sqrt{3\lambda_0}}\,\frac{1-\frac{2}{3}\sqrt{3\lambda_0}}{1+\frac{2}{3}\sqrt{3\lambda_0}}\int_0^\infty e^{-\sqrt{3\lambda_0}\,t}\cdot\frac{d^2B}{dt^2}\cdot dt\\ &- \frac{1}{2\sqrt{3\lambda_0}}\int_0^\infty e^{-\sqrt{3\lambda_0}\,t}\cdot 3y\cdot\delta\cdot dt\\ &+ \frac{1}{2\sqrt{3\lambda_0}}\int_0^\infty e^{-\sqrt{3\lambda_0}\,t}\cdot\frac{d^2B}{dt^2}\cdot dt\end{aligned}\right\} \quad (48)$$

or

$$\left.\begin{aligned}\left(\frac{F}{\pi}\right)_{t=0} = \frac{\frac{4}{3}a\sqrt{3\lambda_0}+\frac{4}{3}p}{1+\frac{2}{3}\sqrt{3\lambda_0}} &- \frac{4}{1+\frac{2}{3}\sqrt{3\lambda_0}}\int_0^\infty e^{-\sqrt{3\lambda_0}\,t}\cdot y\cdot\delta\cdot dt\\ &+ \frac{\frac{4}{3}}{1+\frac{2}{3}\sqrt{3\lambda_0}}\int_0^\infty e^{-\sqrt{3\lambda_0}\,t}\cdot\frac{d^2B}{dt^2}\cdot dt\,.\end{aligned}\right\} \quad (49)$$

Up to this point the analysis is perfectly general. It is seen that the boundary-value problem is solved when a solution y is known, accurate or approximate, which can be substituted into the first integral on the right-hand side of (49).

In the simple case discussed on page 8, that λ is constant and d^2B/dt^2 is zero, we find, on putting $\lambda = \lambda_0$, that δ is o. In that case (49) reduces to (30), as it should.

Suppose now that δ and d^2B/dt^2 are small quantities of the first order. Then (28) with $\lambda = \lambda_0$ is an approximate solution y, the error of which is of the first order. Introducing this y in (49), one consequently finds the intensity in the integrated spectrum with an error that is only of the second order.

In the same way, substituting the approximate solution (28) in (42), one gets the general solution y with an error of the second order. This is, in fact, the standard procedure for finding the perturbed general solution of (32). Similarly, the particular solution satisfying the boundary conditions could be found from (43) and (47), substituting (28) in the integrals of these equations.

If a better approximation to y than (28) is known, it can, of course,

be used in (49) to give a still better approximation to the intensity. For instance, the Bessel function solution mentioned on page 1 might be used for this purpose.

Finally, it should be mentioned that if λ is constant, so that $\delta = 0$, the correct value of the intensity can be found from (49), irrespective of the properties of the function $B(t)$. This corresponds to the fact pointed out by Milne[10] and Rosseland[8] that it is relatively simple to avoid assumptions concerning B in solving the boundary-value problem.

The dependence of the intensity in the integrated spectrum upon B is perhaps more clearly brought out when the second integral in (49) is transformed by two partial integrations. One has identically (cf. [24] and [25]):

$$\int_0^\infty e^{-\sqrt{3\lambda_0}\,t} \cdot \frac{d^2B}{dt^2} \cdot dt = -\sqrt{3\lambda_0}\,a - p + 3\lambda_0 \int_0^\infty e^{-\sqrt{3\lambda_0}\,t} \cdot B \cdot dt\,. \quad (50)$$

Inserting this identity in (49), we find

$$\left.\begin{aligned}\left(\frac{F}{\pi}\right)_{t=0} = &-\frac{4}{1+\frac{2}{3}\sqrt{3\lambda_0}} \int_0^\infty e^{-\sqrt{3\lambda_0}\,t} \cdot y \cdot \delta \cdot dt \\ &+ \frac{\frac{4}{3}\sqrt{3\lambda_0}}{1+\frac{2}{3}\sqrt{3\lambda_0}} \int_0^\infty e^{-\sqrt{3\lambda_0}\,t} \cdot B \cdot d(\sqrt{3\lambda_0}\,t)\,.\end{aligned}\right\} \quad (51)$$

This relation holds quite generally. In the special case that λ is constant, we have $\lambda = \lambda_0$ and $\delta = 0$, so that the first integral vanishes. The second integral is always proportional to a certain mean value of B. The larger the ratio η of line absorption to continuous absorption, the smaller is λ_0 and the larger is the exponent for the same optical depth τ in the continuous spectrum $[\sqrt{3\lambda_0}\,t \approx (\sqrt{3}/\sqrt{\lambda_0})\tau]$, and the higher are the layers that contribute appreciably when forming the proper mean value of B.

Substituting now the approximate solution (28) with $\lambda = \lambda_0$ in

[10] *Phil. Trans. Royal Society, London*, Ser. A, **223**, 201, 1923.

(49), one gets the following expression for the intensity in the integrated spectrum, the error of which is of the second order:

$$\left(\frac{F}{\pi}\right)_{t=0} = \frac{\frac{4}{3}a\sqrt{3\lambda_0} + \frac{4}{3}p}{1 + \frac{2}{3}\sqrt{3\lambda_0}} + \frac{4}{(1 + \frac{2}{3}\sqrt{3\lambda_0})^2}(a - \tfrac{2}{3}p)\int_0^\infty e^{-2\sqrt{3\lambda_0}t} \cdot \delta \cdot dt + \frac{\frac{4}{3}}{1 + \frac{2}{3}\sqrt{3\lambda_0}}\int_0^\infty e^{-\sqrt{3\lambda_0}t} \cdot \frac{d^2B}{dt^2} \cdot dt \,. \tag{52}$$

Similarly, (51) gives the equivalent expression

$$\left(\frac{F}{\pi}\right)_{t=0} = \frac{4}{(1 + \frac{2}{3}\sqrt{3\lambda_0})^2}(a - \tfrac{2}{3}p)\int_0^\infty e^{-2\sqrt{3\lambda_0}t} \cdot \delta \cdot dt + \frac{\frac{4}{3}\sqrt{3\lambda_0}}{1 + \frac{2}{3}\sqrt{3\lambda_0}}\int_0^\infty e^{-\sqrt{3\lambda_0}t} \cdot B \cdot d(\sqrt{3\lambda_0}t) \,. \tag{53}$$

In the form given, the equations are suited for numerical determinations of intensities within stellar absorption lines. For given values of λ and B as functions of t, one determines a and p, chooses a suitable λ_0, then finds δ as a function of t and carries out the quadratures numerically. For purposes of interpretation of the equations we shall, however, carry out a few further transformations.

IV

Let us consider for a moment the case that λ is constant and d^2B/dt^2 is equal to zero. One might then choose a λ_0 differing from λ by a quantity of the first order. The corresponding δ would be constant and of the first order. Carrying out the quadrature for δ constant, we arrive at an expression for $(F/\pi)_{t=0}$, which must agree with (30), neglecting quantities of the second order in δ. These considerations lead to the following transformations of (52). Introduce the quantities

$$q = \tfrac{2}{3}\sqrt{3\lambda} \tag{54}$$

and

$$q_0 = \tfrac{2}{3}\sqrt{3\lambda_0} \,, \tag{55}$$

and define Δq by

$$q = q_0 + \Delta q \,. \tag{56}$$

Then, neglecting terms of the second order,

$$\Delta q = \frac{2\delta}{3q_0} . \tag{57}$$

The part of (52) which is proportional to a can now be re-written as follows:

$$\left.\begin{aligned} &\frac{\frac{4}{3}a\sqrt{3\lambda_0}}{1+\frac{2}{3}\sqrt{3\lambda_0}} + \frac{4a}{(1+\frac{2}{3}\sqrt{3\lambda_0})^2}\int_0^\infty e^{-2\sqrt{3\lambda_0}\,t}\cdot\delta\cdot dt \\ &\qquad = \frac{2q_0a}{1+q_0} + \frac{2a}{(1+q_0)^2}\int_0^\infty e^{-3q_0t}\cdot\Delta q\cdot d(3q_0t) . \end{aligned}\right\} \tag{58}$$

Now,

$$\frac{d}{dq}\left(\frac{2qa}{1+q}\right) = \frac{2a}{(1+q)^2} . \tag{59}$$

Therefore one has, neglecting quantities of the second order,

$$\frac{\frac{4}{3}a\sqrt{3\lambda_0}}{1+\frac{2}{3}\sqrt{3\lambda_0}} + \frac{4a}{(1+\frac{2}{3}\sqrt{3\lambda_0})^2}\int_0^\infty e^{-2\sqrt{3\lambda_0}\,t}\cdot\delta\cdot dt = \frac{2a(q_0+\overline{\Delta q})}{1+(q_0+\overline{\Delta q})} , \tag{60}$$

where $\overline{\Delta q}$ has been defined by

$$\overline{\Delta q} = \int_0^\infty e^{-3q_0t}\cdot\Delta q\cdot d(3q_0t) . \tag{61}$$

Defining $\bar{q}$ by (cf. [56])

$$\bar{q} = q_0 + \overline{\Delta q} , \tag{62}$$

we can consequently write the part of equation (52) that is proportional to a in the form

$$\frac{2a\bar{q}}{1+\bar{q}} . \tag{63}$$

From (61) and (62) it follows that

$$\bar{q} = \int_0^\infty q\cdot e^{-3q_0t}\cdot d(3q_0t) = \tfrac{2}{3}\sqrt{3}\int_0^\infty \sqrt{\lambda}\cdot e^{-2\sqrt{3\lambda_0}\,t}\, d(2\sqrt{3\lambda_0}\,t) . \tag{64}$$

Quite similarly one derives that the part of (52) proportional to p can be written as follows:

$$\frac{\frac{4}{3}p}{1+\frac{2}{3}\sqrt{3\lambda_0}} - \frac{\frac{8}{3}p}{(1+\frac{2}{3}\sqrt{3\lambda_0})^2}\int_0^\infty e^{-2\sqrt{3\lambda_0}\,t}\cdot\delta\cdot dt = \frac{\frac{4}{3}p}{1+\bar{q}}. \quad (65)$$

Inserting the expressions thus derived in (52), we get

$$\left(\frac{F}{\pi}\right)_{t=0} = \frac{2a\bar{q}+\frac{4}{3}p}{1+\bar{q}} + \frac{\frac{4}{3}}{1+\frac{2}{3}\sqrt{3\lambda_0}}\int_0^\infty e^{-\sqrt{3\lambda_0}\,t}\cdot\frac{d^2B}{dt^2}\cdot dt\,. \quad (66)$$

According to (66), the formal difference between the case of constant and that of varying λ is that in the latter case a certain mean value of $\sqrt{\lambda}$ has to be substituted for $\sqrt{\lambda_0}$. It should be noted that it is only by introducing the mean value of a quantity proportional to the *square root* of λ (cf. [54] and [64]) that one arrives at an equation having this property.

Assuming now in (66) that d^2B/dt^2 is a small quantity of the first order, one can substitute $\bar{q}$ for $q_0 = \frac{2}{3}\sqrt{3\lambda_0}$ in the second term on the right-hand side of (66), the error being of the second order. Performing, further, two partial integrations (cf. [50]), we find

$$\left(\frac{F}{\pi}\right)_{t=0} = \frac{2a\bar{q}+\frac{4}{3}p}{1+\bar{q}} - \frac{2a\bar{q}+\frac{4}{3}p}{1+\bar{q}} + \frac{2\bar{q}}{1+\bar{q}}\int_0^\infty e^{-\frac{3}{2}\bar{q}t}\cdot B\cdot d(\tfrac{3}{2}\bar{q}t) \quad (67)$$

or[11]

$$\left(\frac{F}{\pi}\right)_{t=0} = \frac{2\bar{q}}{1+\bar{q}}\int_0^\infty e^{-\frac{3}{2}\bar{q}t}\cdot B\cdot d(\tfrac{3}{2}\bar{q}t)\,. \quad (68)$$

Introducing again λ instead of q (cf. [54] and [55]), and inserting for the sake of clarity the indices ν (cf. p. 7), the equations for calculating the intensity in the integrated spectrum are (cf. [64] and [68])

$$\overline{\sqrt{\lambda_\nu}} = \int_0^\infty \sqrt{\lambda_\nu}\cdot e^{-2\sqrt{3(\lambda_\nu)_0}\,t_\nu}\,d(2\sqrt{3(\lambda_\nu)_0}\,t_\nu)\,, \quad (69)$$

$$\overline{B_\nu} = \int_0^\infty B_\nu\cdot e^{-\sqrt{3}\,\overline{\sqrt{\lambda_\nu}}\,t_\nu}\,d(\sqrt{3}\,\overline{\sqrt{\lambda_\nu}}\,t_\nu)\,, \quad (70)$$

[11] It is interesting to compare eq. (68) with an equation given by Milne (*loc. cit.*,[10] eq. 60]), which corresponds to the special case of λ constant throughout the atmosphere. The structure of the equations is exactly the same.

and

$$\left(\frac{F_\nu}{\pi}\right)_{t_\nu=0} = \frac{\frac{4}{3}\sqrt{3}\,\overline{\sqrt{\lambda_\nu}}}{1+\frac{2}{3}\sqrt{3}\,\overline{\sqrt{\lambda_\nu}}}\,\overline{B_\nu}\,. \tag{71}$$

In the very simplest case that both λ_ν and B_ν are constant, this reduces to

$$\left(\frac{F_\nu}{\pi}\right)_{t_\nu=0} = \frac{\frac{4}{3}\sqrt{3}\sqrt{\lambda_\nu}}{1+\frac{2}{3}\sqrt{3}\sqrt{\lambda_\nu}}\,B_\nu\,, \qquad (\lambda_\nu \text{ and } B_\nu \text{ are constant}), \tag{72}$$

as it should (cf. [30], with $a = B$ and $p = 0$).

The procedure for calculating the intensity within the absorption line according to (69), (70), and (71) can be described as follows: *For* λ_ν *and* B_ν *varying with the optical depth* t_ν, *we strike a mean of the* λ_ν *values with the weighting function* $e^{-2\sqrt{3}\sqrt{(\lambda_\nu)_0}\,t_\nu}$, *then a mean of the* B_ν *values with the weighting function* $e^{-\sqrt{3}\sqrt{\lambda_\nu}t_\nu}$. *The intensity is calculated as if* λ_ν *and* B_ν *were constant throughout the atmosphere and equal to the mean values mentioned.*

V

In many practical cases sufficient accuracy is obtained by putting B_ν equal to a linear function of the optical depth τ in the *continuous* spectrum:[8]

$$B_\nu = a_\nu + b_\nu \tau\,, \tag{73}$$

where

$$\tau = \int_0^x \bar{k}\rho dx\,, \tag{74}$$

$\bar{k}$ being the Rosseland mean of the continuous absorption coefficient over the spectrum. It should be noted that when λ_ν is not constant, this may be an approximation of sufficient accuracy, while the approximation of B_ν equal to a linear function of the optical depth t_ν within the spectral line (cf. [9]) is not.

We shall consider in this section the form the equations developed for calculating the intensity within the absorption lines take when the assumption (73) is made.

From (9) and (74) it follows that

$$\frac{dt_\nu}{d\tau} = \frac{k_\nu + l_\nu}{\overline{k}} . \tag{75}$$

Defining n_ν as the ratio of k_ν and $\overline{k}$,

$$k_\nu = n_\nu \overline{k} , \tag{76}$$

we have (cf. [10])

$$\frac{dt_\nu}{d\tau} = n_\nu(1 + \eta_\nu) . \tag{77}$$

In the analysis of the continuous spectrum it will usually have been assumed that n_ν is constant throughout the atmosphere. We shall, for simplicity, make the same assumption here, though it presents no difficulty to treat the case when n_ν is variable.

From (73) and (77) it follows that

$$\frac{dB_\nu}{dt_\nu} = \frac{b_\nu}{n_\nu} \frac{1}{1 + \eta_\nu} . \tag{78}$$

Therefore,

$$B_\nu = a_\nu + \frac{b_\nu}{n_\nu} \int_0^{t_\nu} \frac{1}{1 + \eta_\nu} \, dt_\nu . \tag{79}$$

Call

$$\frac{1}{1 + \eta_\nu} = \mu_\nu , \tag{80}$$

so that

$$B_\nu = a_\nu + \frac{b_\nu}{n_\nu} \int_0^{t_\nu} \mu_\nu dt_\nu . \tag{81}$$

In the case that $\epsilon = 0$, μ_ν thus defined coincides with λ_ν. The difference between the two quantities generally will only be appreciable for large values of η_ν, i.e., near the center of strong absorption lines.

We now introduce the expression (81) for B_ν in equation (70), defining $\overline{B_\nu}$,

$$\overline{B_\nu} = a_\nu + \frac{b_\nu}{n_\nu} \int_0^{\infty} e^{-\sqrt{3}\sqrt{\lambda_\nu} t_\nu} d(\sqrt{3}\sqrt{\lambda_\nu} t_\nu) \cdot \int_0^{t_\nu} \mu_\nu \, dt_\nu . \tag{82}$$

The second term on the right-hand side of (82) is transformed by a partial integration:

$$\overline{B_\nu} = a_\nu + \frac{b_\nu}{n_\nu} \int_0^\infty e^{-\sqrt{3}\,\overline{\sqrt{\lambda_\nu}}\,t_\nu} \cdot \mu_\nu \cdot dt_\nu \,. \tag{83}$$

Defining a mean value of μ_ν by

$$\overline{\mu_\nu} = \int_0^\infty e^{-\sqrt{3}\,\overline{\sqrt{\lambda_\nu}}\,t_\nu} \cdot \mu_\nu \cdot d(\sqrt{3}\,\overline{\sqrt{\lambda_\nu}}\,t_\nu) \,, \tag{84}$$

we have

$$\overline{B_\nu} = a_\nu + \frac{b_\nu}{n_\nu}\,\overline{\mu_\nu} \cdot \frac{1}{\sqrt{3}\,\overline{\sqrt{\lambda_\nu}}} \,. \tag{85}$$

Introducing this expression for $\overline{B_\nu}$ in (71), one finally gets

$$\left(\frac{F_\nu}{\pi}\right)_{t_\nu=0} = \frac{\frac{4}{3}\sqrt{3}\,a_\nu\overline{\sqrt{\lambda_\nu}} + \frac{4}{3}\frac{b_\nu}{n_\nu}\,\overline{\mu_\nu}}{1 + \frac{2}{3}\sqrt{3}\,\overline{\sqrt{\lambda_\nu}}} \,, \qquad (B_\nu = a_\nu + b_\nu\tau) \,. \tag{86}$$

In the case considered in this section, that $B_\nu = a_\nu + b_\nu\tau$, we therefore find that *the intensity within the absorption line is calculated by striking proper averages* (*cf.* [69] *and* [84]) *over the quantities* $\lambda_\nu = (1 + \epsilon\eta_\nu)/(1 + \eta_\nu)$ *and* $\mu_\nu = 1/(1 + \eta_\nu)$, *and then introducing these into the simple formula valid when* λ_ν *and* μ_ν *are constant throughout the atmosphere.*

In calculating equivalent widths of stellar absorption lines ϵ can usually be put equal to zero. The corresponding small change of the contour near the center of the line means only a small change in the equivalent width. In that case (86) reduces to

$$\left(\frac{F_\nu}{\pi}\right)_{t_\nu=0} = \frac{\frac{4}{3}\sqrt{3}a_\nu\overline{\sqrt{\lambda_\nu}} + \frac{4}{3}\frac{b_\nu}{n_\nu}\,\overline{\lambda_\nu}}{1 + \frac{2}{3}\sqrt{3}\,\overline{\sqrt{\lambda_\nu}}} \,, \quad (B_\nu = a_\nu + b_\nu\tau \,; \quad \epsilon = 0) \,, \tag{87}$$

with $\overline{\sqrt{\lambda_\nu}}$ and $\overline{\lambda_\nu}$ given by (69) and (84).

It means neglecting quantities of the second order only, if in (69) and (84) we put

$$\sqrt{(\lambda_\nu)_0}\, t_\nu = \frac{1}{\sqrt{(\lambda_\nu)_0}}\, \tau \tag{88}$$

and

$$\overline{\sqrt{\lambda_\nu}}\, t_\nu = \frac{1}{\sqrt{(\lambda_\nu)_0}}\, \tau\,. \tag{89}$$

Therefore

$$\overline{\sqrt{\lambda_\nu}} = \int_0^\infty \sqrt{\lambda_\nu}\, e^{-\frac{2\sqrt{3}}{\sqrt{(\lambda_\nu)_0}}\tau}\, d\left(\frac{2\sqrt{3}}{\sqrt{(\lambda_\nu)_0}}\,\tau\right) \tag{90}$$

and

$$\overline{\lambda_\nu} = \int_0^\infty \lambda_\nu\, e^{-\frac{\sqrt{3}}{\sqrt{(\lambda_\nu)_0}}\tau}\, d\left(\frac{\sqrt{3}}{\sqrt{(\lambda_\nu)_0}}\,\tau\right). \tag{91}$$

In (87) one can substitute the usual expressions[8] for a_ν and b_ν obtained by expanding B_ν in a Taylor series from the surface, assuming the temperature to be given by

$$T^4 = T_0^4(1 + \tfrac{3}{2}\tau)\,, \tag{92}$$

where T_0 is the surface temperature.

The contrast

$$r_\nu = \frac{F_\nu}{F_\nu^{(\mathrm{cont})}} \tag{93}$$

between spectral line and continuous spectrum is obtained by putting $\overline{\sqrt{\lambda_\nu}}$ and $\overline{\lambda_\nu}$ in (87) equal to 1 in order to get $F_\nu^{(\mathrm{cont})}$. One thus finally gets

$$r_\nu = \frac{1 + \frac{2}{3}\sqrt{3}}{\frac{4}{3}\sqrt{3} + \frac{1}{2}\frac{x_0}{n_\nu}}\, \frac{\frac{4}{3}\sqrt{3}\,\overline{\sqrt{\lambda_\nu}} + \frac{1}{2}\frac{x_0}{n_\nu}\,\overline{\lambda_\nu}}{1 + \frac{2}{3}\sqrt{3}\,\overline{\sqrt{\lambda_\nu}}}\,, \tag{94}$$

where

$$x_0 = \frac{h\nu}{kT_0}\left(1 - e^{-\frac{h\nu}{kT_0}}\right). \tag{95}$$

For many purposes, equations (90), (91), (94), and (95) will be convenient and sufficiently accurate for calculating r_ν.

It is interesting to note the difference in the weighting functions for $\sqrt{\lambda_\nu}$ and λ_ν (cf. [90] and [91]). Going from the surface inward, the weighting function for $\sqrt{\lambda_\nu}$ falls off much more rapidly than that for λ_ν. This means that for *two* reasons the intensity near the center of an absorption line depends upon the properties of layers higher than those that determine the intensity in the wing of the line. First, as we go from the wing toward the center, $\sqrt{(\lambda_\nu)_0}$ decreases and the weighting factors for both $\sqrt{\lambda_\nu}$ and λ_ν fall off more and more rapidly with increasing τ. Second, as one approaches the center, the $\overline{\lambda_\nu}$ term in (94) becomes smaller and relatively less important compared with the $\overline{\sqrt{\lambda_\nu}}$ term. Therefore, the effective weighting function tends toward that for $\sqrt{\lambda_\nu}$ as we approach the center, and the latter weighting function is the one that falls off more rapidly.

The difference between the weighting functions just referred to is perhaps best interpreted by considering the expression (71) for the intensity within the absorption line. Quite generally, line absorption affects the intensity within the radiated spectrum in two ways. First, it cuts down the intensity as would increased continuous absorption, the effect depending upon the existence of a temperature gradient in the stellar atmosphere. Second, it causes a deviation from Kirchhoff's law, in the sense that emission is reduced, so that there is a further reduction in the radiated intensity. The first effect can be studied formally by putting $\epsilon = 1$ (cf. the equation of transfer [1]) and hence $\lambda_\nu = 1$ (cf. [11]). Considering (70) and (71), one now sees that the first effect is associated with the weighting factor that falls off relatively slowly, whereas the second effect is connected with the weighting factor that falls off rapidly.

The first effect, that analogous to the effect of large continuous absorption, cannot reduce the intensity below the Planck intensity corresponding to the surface temperature (cf. [70] and [71]). Therefore, when near the center of a strong line the line absorption is already great, a change in the line absorption means relatively little as far as the first effect is concerned. This corresponds to the de-

creasing importance of the $\overline{\lambda_\nu}$ term in (97) as one approaches the center of the absorption line.

Finally, it should be mentioned that the first effect is naturally the more important the greater the change of the Planck intensity B_ν with optical depth τ, and therefore is more important the larger the ratio $h\nu/kT_0$ (cf. the increase of the limb darkening with decreasing wave-length). Corresponding to this, x_0 occurs as a factor of the $\overline{\lambda_\nu}$ term in (94). The factor $1/n_\nu$ in the same term can be interpreted in a similar way.

VI

The case of the extreme wings of absorption lines studied by Unsöld is a special case of that considered in the present paper. For in this case η_ν is a small quantity of the first order, and hence λ_ν differs from a constant, namely unity, only by a small quantity of the first order throughout the atmosphere.

In this section we shall specialize the equations obtained in the previous sections to the case that n_ν is small. The comparison with Unsöld's result is of interest, because Unsöld did not make use of the Eddington approximations in treating the infinite system of differential equations (1) but considered the corresponding Schwarzschild integral equation.

We shall limit ourselves to the most important case when $\epsilon = 0$ and $B_\nu = a_\nu + b_\nu\tau$. We can then determine r_ν from (90), (91), and (94), putting $\lambda_\nu = 1 - \eta_\nu$ and $(\lambda_\nu)_0 = 1$. Thus, one finds

$$\left.\begin{aligned} 1 - r_\nu = {} & \frac{2 - \frac{1}{2}\frac{x_0}{n}}{(1 + \frac{2}{3}\sqrt{3})\left(\frac{2}{3}\sqrt{3} + \frac{1}{4}\frac{x_0}{n}\right)} \int_0^\infty e^{-2\sqrt{3}\tau} \cdot \eta_\nu \cdot d\tau \\ & + \frac{\frac{1}{4}\sqrt{3}\frac{x_0}{n}}{\frac{2}{3}\sqrt{3} + \frac{1}{4}\frac{x_0}{n}} \int_0^\infty e^{-\sqrt{3}\tau} \cdot \eta_\nu \cdot d\tau \,. \end{aligned}\right\} \quad (96)$$

Writing Unsöld's formula in the form

$$\left.\begin{aligned} 1 - r_\nu = \frac{1}{1 + \frac{1}{4}\frac{x_0}{n}} \int_0^\infty \left[Ei_2^2(\tau) - \frac{3}{8}\frac{x_0}{n} Ei_2(\tau) Ei_3(\tau) \right] \cdot \eta_\nu \cdot d\tau \\ + \frac{1}{1 + \frac{1}{4}\frac{x_0}{n}} \int_0^\infty \frac{3}{4}\frac{x_0}{n} Ei_3(\tau) \cdot \eta_\nu \cdot d\tau , \end{aligned}\right\} \quad (97)$$

it is easy to see the correspondence of the various terms. The exponential integrals correspond to $e^{-\sqrt{3}\tau}$ and the square or the product of the exponential integrals corresponds to $e^{-2\sqrt{3}\tau}$. A similar correspondence was noted by Minnaert in the investigation mentioned on page 2. In this connection it is interesting to note that in the theory of the continuous spectrum of a gray body, Eddington's approximation leads to an integral expression for the flux in terms of the Planck intensity, which differs from the Schwarzschild-Milne expression[8] only by the substitution of $e^{-\sqrt{3}\tau}$ for $Ei_2(\tau)$.

Numerical values of the weighting function G for η_ν according to (96) and (97) are given in Table 1 for x_0/n equal to 2, 4, and 6, respectively. It is seen that the differences between the functions are small.

TABLE 1*

$\frac{x_0}{n}=2$			$\frac{x_0}{n}=4$			$\frac{x_0}{n}=6$		
τ	G Acc. (96)	G Acc. (97)	τ	G Acc. (96)	G Acc. (97)	τ	G Acc. (96)	G Acc. (97)
0	0.80	0.92	0	0.80	0.88	0	0.80	0.85
0.1	.64	.61	0.1	.68	.66	0.1	.70	.69
0.2	.51	.47	0.2	.57	.54	0.2	.60	.58
0.5	.27	.26	0.5	.34	.33	0.5	.38	.38
1.0	.10	.12	1.0	.14	.16	1.0	.17	.19
1.5	.040	.058	1.5	.060	.085	1.5	.072	.10
2.0	.017	.039	2.0	.025	.045	2.0	.030	.054
3.0	0.0029	0.009	3.0	0.0045	0.013	3.0	0.0054	0.016

* Weight function for the extreme wing: $1-r_\nu = \int_0^\infty G \cdot \eta_\nu \cdot d\tau$.

VII

As was mentioned on page 1, Eddington has treated the case when $1/(1+\eta_\nu)$ is a linear function of the optical depth τ,

$$\frac{1}{1+\eta_\nu} = a + \beta\tau\,, \tag{98}$$

with

$$B_\nu = a_\nu + b_\nu\tau\,. \tag{99}$$

We shall limit ourselves again to the case that $\epsilon = 0$. Also we shall consider the case only that $x_0/n = 4$, so that $b_\nu = \frac{3}{5}a_\nu$. Then the expression for r_ν is[1] (cf. also Woolley[2])

$$r_\nu = \frac{a - \dfrac{2+\beta}{3}\sqrt{3a}\cdot\dfrac{K_0'(\sqrt{12a/\beta^2})}{K_0(\sqrt{12a/\beta^2})}}{1 - \frac{2}{3}\sqrt{3a}\cdot\dfrac{K_0'(\sqrt{12a/\beta^2})}{K_0(\sqrt{12a/\beta^2})}}\,. \tag{100}$$

Here[12] K_0 is a Bessel function of order zero and $K_0' = -K_1$ is the derivative of this function. Tables of these functions are given in Watson's *Bessel Functions* (pp. 698 and 737) and also in Jahnke-Emde's *Tables of Functions* (2d rev. ed., p. 286). (In the notation of Jahnke-Emde, they are proportional to $iH_0^{(1)}(i\sqrt{12a/\beta^2})$ and $-H_1^{(1)}(i\sqrt{12a/\beta^2})$, the functions $H_0^{(1)}$ and $H_1^{(1)}$ being Hankel's functions of the third kind, of orders 0 and 1.)

For $\beta = 0$, equation (100) reduces to (94) with $x_0/n = 4$ and with λ_ν constant throughout the atmosphere. The case $\lambda_\nu = 1/(1+\eta_\nu)$ given by (98), with β small, can be treated with the aid of both (94) and (100). We shall now consider this case and shall show that the results agree. This means that we specialize (94) for the case when the variation of λ, assumed small but otherwise arbitrary, is linear, and specialize (100) for the case when the variation of λ, assumed linear but otherwise unrestricted, is small.

[12] Eddington considers in detail only the case when β is positive. In this case eq. (100) holds true. Thus the following derivation of (103) is true for β positive. For β small it is very easy to see that in the case of negative β the Bessel functions I_0 and I_1 have to be substituted for K_0 and K_1 in (100). Further, in this case I_1/I_0 is, apart from terms of the second order, equal to the reciprocal of K_1/K_0. It follows that (103) holds true for negative values of β also.

When β is small, the argument of the Bessel functions is large. Then, as was pointed out by Eddington, we have

$$-\frac{K_0'(\sqrt{12a/\beta^2})}{K_0(\sqrt{12a/\beta^2})} = \frac{1+\frac{3}{8\sqrt{12a/\beta^2}}}{1-\frac{1}{8\sqrt{12a/\beta^2}}} \qquad \left(\sqrt{\frac{12a}{\beta^2}} \gg 1\right). \quad (101)$$

In the limiting case considered, we may write this as

$$-\frac{K_0'(\sqrt{12a/\beta^2})}{K_0(\sqrt{12a/\beta^2})} = 1+\frac{1}{4}\sqrt{\frac{\beta^2}{3a}}. \quad (102)$$

Introducing this expression in (100) and neglecting quantities of the second order and higher, we find

$$r_\nu = \frac{\frac{2}{3}\sqrt{3a}\left(1+\frac{1}{4}\frac{\beta}{\sqrt{3a}}\right)+a+\frac{1}{3}\beta\sqrt{3a}}{1+\frac{2}{3}\sqrt{3a}\left(1+\frac{1}{4}\frac{\beta}{\sqrt{3a}}\right)}. \quad (103)$$

On the other hand, on introducing (98), which, neglecting quantities of the second order and higher, is equivalent to

$$\lambda_\nu = a+\beta l_\nu \quad (104)$$

in (90) and (91), we find

$$\overline{\sqrt{\lambda_\nu}} = \sqrt{a}\left(1+\frac{1}{4}\frac{\beta}{\sqrt{3a}}\right) \quad (105)$$

and

$$\overline{\lambda_\nu} = a+\tfrac{1}{3}\beta\sqrt{3a}. \quad (106)$$

Inserting this expression in (94), we obtain, for $x_0/n = 4$,

$$r_\nu = \frac{\frac{2}{3}\sqrt{3a}\left(1+\frac{1}{4}\frac{\beta}{\sqrt{3a}}\right)+a+\frac{1}{3}\beta\sqrt{3a}}{1+\frac{2}{3}\sqrt{3a}\left(1+\frac{1}{4}\frac{\beta}{\sqrt{3a}}\right)}, \quad (107)$$

which is identical with (103).

It is interesting to note that (105) can be written in the form

$$\overline{\sqrt{\lambda_\nu}} = \sqrt{a + \beta \cdot \frac{\sqrt{a}}{2\sqrt{3}}}, \tag{108}$$

which is equal to the square root of the value of λ_ν for $\tau = \sqrt{a}/2\sqrt{3}$. Similarly $\overline{\lambda_\nu}$, according to (106), is equal to the value of λ_ν for $\tau = \sqrt{a}/\sqrt{3}$.

It follows that *in the case of a small linear variation of* λ_ν *with* τ, *the proper mean values to use in* (94) *are: for* $\overline{\sqrt{\lambda_\nu}}$, *the square root of the value of* λ_ν *at* $\tau = \sqrt{(\lambda_\nu)_0}/2\sqrt{3}$; *and for* $\overline{\lambda_\nu}$, *the value of* λ_ν *at* $\tau = \sqrt{(\lambda_\nu)_0}/\sqrt{3}$.

TABLE 2*

λ_ν	$\tau_1 = \frac{\sqrt{(\lambda_\nu)_0}}{\sqrt{3}}$	$\tau_2 = \frac{\sqrt{(\lambda_\nu)_0}}{2\sqrt{3}}$	$\overline{\lambda_\nu}$	$\overline{\sqrt{\lambda_\nu}}$	r_ν Acc. (94)	r_ν Exact Value*
0.954–0.142 τ	0.56	0.28	0.88	0.96	0.94	0.94
.823– .320 τ	.52	.26	.65	.86	.82	.82
.650– .460 τ	.47	.23	.44	.74	.70	.70
0.377–0.370 τ	0.36	0.18	0.25	0.56	0.54	0.55

*Woolley's values have been slightly revised, using I_1/I_0 instead of K_1/K_0 because β is negative (cf. above).

The discussion on page 21 shows that in this case the representative point moves from $\sqrt{(\lambda_\nu)_0}/\sqrt{3}$ toward $\sqrt{(\lambda_\nu)_0}/2\sqrt{3}$ as we pass from the wing of the line toward the center, there being thus two causes for the shift toward higher layers, namely, the effect just mentioned, and the effect of the decrease of $\sqrt{(\lambda_\nu)_0}$, which quantity is roughly equal to r_ν.

Table 2 illustrates the use of the rule just stated. The examples are taken from an investigation by Woolley[2] and refer to the case of the *Ca* lines in the solar spectrum.

In all these examples there is agreement practically within two-figure accuracy.

It is interesting to determine the accuracy of r_ν values computed from (90), (91), and (94) in cases of rather large linear variations of λ_ν, making use of (100). Table 3 gives two typical examples. In spite of the very considerable variation of η_ν with depth, the results

are only slightly in error. This is connected with the fact that λ_ν has the limits 0 and 1.

TABLE 3

a	$\sqrt{\frac{12a}{\beta^2}}$	β	$\overline{\lambda_\nu}$	$\overline{\sqrt{\lambda_\nu}}$	r_ν Acc. (94)	r_ν Exact Value	η_ν at $\tau=0$	η_ν at $\tau=0.5$
0.01	1	0.35	0.03	0.14	0.17	0.18	99	4.5
0.1	1	1.10	0.30	0.45	0.54	0.60	9	0.54

The relative change of λ_ν from the surface to the representative point $\tau = \sqrt{(\lambda_\nu)_0}/2\sqrt{3}$ is a measure of the variation of λ_ν in the relevant part of the atmosphere:

$$\text{Relative change} = \frac{1}{a} \cdot \beta \frac{\sqrt{a}}{2\sqrt{3}} = \sqrt{\frac{\beta^2}{12a}} . \qquad (109)$$

Comparing with (100), we see that this quantity is the reciprocal of the argument of the Bessel function in the expression for r_ν. Thus, when the relative change is small, the argument is large and the simplified expression (101) is valid.

Quite generally one gets a good estimate of the accuracy of r_ν values obtained with the aid of (90), (91), and (94) by calculating r_ν first with $(\lambda_\nu)_0$ equal to the value of λ_ν on the surface, and then with $(\lambda_\nu)_0$ equal to $(\overline{\sqrt{\lambda_\nu}})^2$. As was stated in the introduction, the accuracy proves to be sufficient in a number of cases of practical importance.

YERKES OBSERVATORY
May 18, 1937

REGIONAL STUDY OF INTERSTELLAR SODIUM*

PAUL W. MERRILL

ABSTRACT

Introduction.—The main circumstances which underlie an investigation of interstellar lines are briefly discussed.

Line intensity and distance.—Data for double stars (Table 1) bear out the expectation that interstellar lines should behave alike in the spectra of the components of a pair. The relationship between distance and intensity of the D lines was examined in 23 small groups of stars scattered along the Milky Way from longitude 310° through 0° to 190°. In several groups the more distant stars exhibit little increase in line intensity. Possible causes of this effect are discussed. Normal places from the 23 areas, when brought together (Fig. 2), show that regional differences, while probably present, are not extremely great. The mean relationship between intensity, $y = 0.5(D2 + D1)$ and x = distance corrected for space absorption, is represented to 2000 parsecs by the equation

$$y = 0.001440\, x^{0.860}\,.$$

The distance-intensity relationship in seven large regions (Figs. 3 and 4), chosen with regard to the null points of galactic rotation, indicates that the standard galactic rotation plays a relatively minor role in producing the observed intensities of detached D lines. Little evidence of an increase of density of sodium vapor toward the galactic center appears in the region observed. Stars in areas with strong reddening do not behave abnormally.

Line intensity and displacement.—Longitudes 311° through 0° to 212° were divided into 14 regions, for each of which a correlation diagram between residual radial velocity and intensity is exhibited in Figures 5 and 6. In spite of considerable scatter, the influence of galactic rotation is plainly marked in the observed motions.

INTRODUCTION

Numerous investigations have demonstrated a statistical increase in the intensities of detached lines with the distances of the stars in whose spectra the lines appear, and this relationship has been used to find the distances of early-type stars and of novae. While the method appears to be fairly successful, its reliability for individual objects remains to be determined. For this reason, as well as to increase our general knowledge of the properties of interstellar gas, a detailed investigation of the relationship between distance and line intensity is desirable.

The intensity of an interstellar line, say D2 of sodium, in the spectrum of any star depends not only on the total number of sodium

* *Contributions from the Mount Wilson Observatory, Carnegie Institution of Washington*, No. 569.

atoms (in the ground state) along the line of sight but also on their motions. Data on displacements should therefore be included in a general study of interstellar lines. Direction, however, as well as distance, must be considered because there is no guaranty that densities and velocities have a spherically symmetrical distribution about the sun; and effects varying in some systematic way with direction, as well as others due to spatial irregularities in density or motion, may be present.

Studies of galactic rotation suggest that, for a given distance, intensities of interstellar lines may be some function of

$$\sin 2(l - 331^\circ),$$

where l is the galactic longitude of the light path, 331° that of the center of rotation.[1] In addition, since distant stars in high galactic latitudes probably lie outside the gaseous stratum along the plane of the galaxy, the intensities in such stars should be related to the cosecant of the latitude. This latitude effect appears to be important, however, in relatively few of the stars on the Mount Wilson program, which means simply that most of the brighter B-type stars lie within the boundaries of the gaseous stratum. The emphasis in the present investigation is therefore placed on the behavior of interstellar lines with respect to *longitude*. Distant stars in high latitudes should be discussed separately.

Irregularities may be caused by clouds of interstellar gas having a partly random distribution, perhaps analogous to that of the dark dust clouds that obstruct our view of the Milky Way; or by local stream motions comparable with those of relatively small groups of stars; or by differences in kinetic motions of atoms in various portions of space.

The observational investigation of these problems is not altogether simple. The ideal set of data would include intensities and displacements of interstellar lines in the spectra of a large number of stars uniformly distributed throughout the galaxy. Practical considerations, however, greatly restrict the number of suitable stars. In the first place, a serious limitation arises from the small distances

[1] A. S. Eddington, *M.N.*, **95**, 11, 1934.

of most of the brighter stars relative to the dimensions of the galaxy. Among objects brighter than apparent magnitude 7.0, only the scarce c stars have distances greater than 2000 parsecs. Moreover, stars whose own spectral lines prevent reliable measurements of the interstellar lines must be excluded. This requirement eliminates practically all stars later than B3 for observations of detached H and K, and those later than A0 for the D lines, although somewhat later types may be of service in special circumstances. In the spectra of the distant c stars, for example, useful measurements of detached sodium lines can be made in types as late as A2.

A practical difficulty in the discussion of the data is introduced by the fact that the distances of individual early-type stars are not known with accuracy. Distances derived from the differences between the apparent magnitudes and the assumed absolute magnitudes serve well for groups of stars but are not wholly reliable for individual objects.

LINE INTENSITY AND DISTANCE

A convenient first test of the behavior of interstellar lines is afforded by observations of double stars. The components of a given pair are at practically the same distance from the observer, while the two light-paths are separated by very small angles. Corresponding interstellar lines in the spectra of the components would therefore be expected to have equal intensity, and all interstellar lines should have the same displacement. With possible minor exceptions, these expectations are borne out by the measurements recorded in Table 1, for which the differences between corresponding values are not in excess of errors of measurement. The results for calcium depend on measures published by the Dominion Astrophysical Observatory and on additional data obtained by Mr. R. F. Sanford and the writer at Mount Wilson, while those from sodium are wholly from observations at Mount Wilson. In certain pairs the velocities from the D lines are algebraically larger than those from H and K. This tendency, previously noticed in a larger collection of data,[2] may be a regional effect.

As already remarked, the main purpose of the present article is

[2] *Mt. W. Contr.*, No. 564; *Ap. J.*, **85**, 73, 1937.

the comparison of intensities and displacements of detached sodium lines in the spectra of stars in various galactic longitudes. The intensities were determined by Mr. O. C. Wilson and Miss Cora G. Burwell from spectrograms taken by the writer with a plane-grating spectrograph at the Cassegrain focus of the 100-inch telescope. To make the results homogeneous, that part of the process where per-

TABLE 1

DETACHED LINES IN SPECTRA OF DOUBLE STARS

STAR	HD	ADS	SEP.	MAG.	TYPE	INTENSITY (EA)		VELOCITY (KM/SEC)	
						D2	D1	*Ca*	*Na*
1 Cam.....	28446 Br	3274	10".3	5.4	B1n	0.36	0.34	− 3.0	− 0.9
	Ft	.....	.....	6.2	Bo	.36	.36	+ 4.4	+ 0.1
λ Ori.....	36861	4179	4.4	3.7	O8	.42	.24	+13.3	+19.9
	36862	.....	.....	5.6	B1	.40	.23	+15.3	+22.1
θ^1 Ori c.....	37022	.....	135	5.4	O7	.26	.16	+20.7	+22.0
θ^2 Ori.....	37041	4188	52.6	5.2	O9	.32	.17	+13.1	+22.2
	37042	.....	.....	6.5	B1	.26	.12	+11.2	+15
ζ Ori.....	37742	4263	2.6	2.0	Bon	.27	.17	+14.0	+18.0
	37743	.....	.....	4.2	B3n	.28	.16	.....	+17
β Sco.....	144217	9913	13.7	2.9	B1	.20	.12	−13.6	−12.8
	144218	.....	.....	5.1	B2	.18	.10	.....	−13
ρ Oph.....	147933	10049	3.4	5.2	B3n	.20	.15	.....	− 7.9
	147934	.....	.....	5.9	B3n	.26	.14	.....	− 9
+35°3930...	190429 Br	13312	2.0	7.2	O5n	.....	.....	−10.9	− 6
	Ft	.....	.....	7.8	O9n	.....	.....	−12.9	− 5
8 Lac.....	214168	16095	22.4	5.8	B3ne	.26	.18	−11.3	−14.9
	214167	.....	.....	6.6	B2	0.24	0.16	−12.3	−13.8

sonal equation might enter was done entirely by Mr. Wilson. Most of the displacement measurements were made by Miss Burwell. The results for individual stars, together with a description of the methods employed, will be given in another *Contribution*.

To ascertain whether the relationship between distance and intensity is subject to marked regional effects, 23 fairly small groups of stars were selected for study. These groups are scattered irregu-

larly along the Milky Way from longitude 310° through 0° to 190°; most of them are rather near the galactic plane, only 5 having centers with latitudes exceeding 6°. The distances were computed from the formula

$$\log D = 0.2(m - M) + 1 ,$$

where the apparent magnitude, m, was taken from the *Henry Draper Catalogue*, and the absolute magnitude, M, from Table 2, which represents a smoothed mean of the fairly consistent values adopted by several recent investigators.

TABLE 2

ASSUMED ABSOLUTE MAGNITUDES

Type	Lines Diffuse or Winged	Others
O5–O9	−3.4	−3.4
B0	−3.1	3.3
B1	−2.7	3.0
B2	−2.2	2.7
B3	−1.5	2.2
B5	−0.4	1.2
B8	+0.1	0.4
B9	+0.4	0.2
cB0–cA4	.....	−5.0

For each of the 23 groups a correlation diagram was made between distance and the arithmetical mean of the measured intensities of D2 and D1. Figure 1 shows sample diagrams for the following regions: h and χ clusters in Perseus, longitude 102°; χ Aurigae, 139°; Trifid Nebula, 337°.

In several of the curves, the portion corresponding to the greater distances is nearly flat. In the χ Aurigae region, for example, the intensities show but little increase beyond 800 parsecs. Possible causes of such an effect are:

a) *Obscuration.*—If an absorbing medium is present, the calculated distances of the more distant stars will be too great relative to the nearer ones, thus flattening the curve. For a uniform absorption of 0.35 visual magnitudes per kiloparsec, the displacement of the curve is not very marked for stars nearer than 1500 parsecs. Accord-

ing to Stebbins and Huffer,[3] stars in the region of χ Aurigae are subject to considerable reddening, the average color excess of those plotted in Figure 1 being about 0.2 mag. (Stebbins' C_1 scale). If the change of the visual magnitude by interstellar absorption is nu-

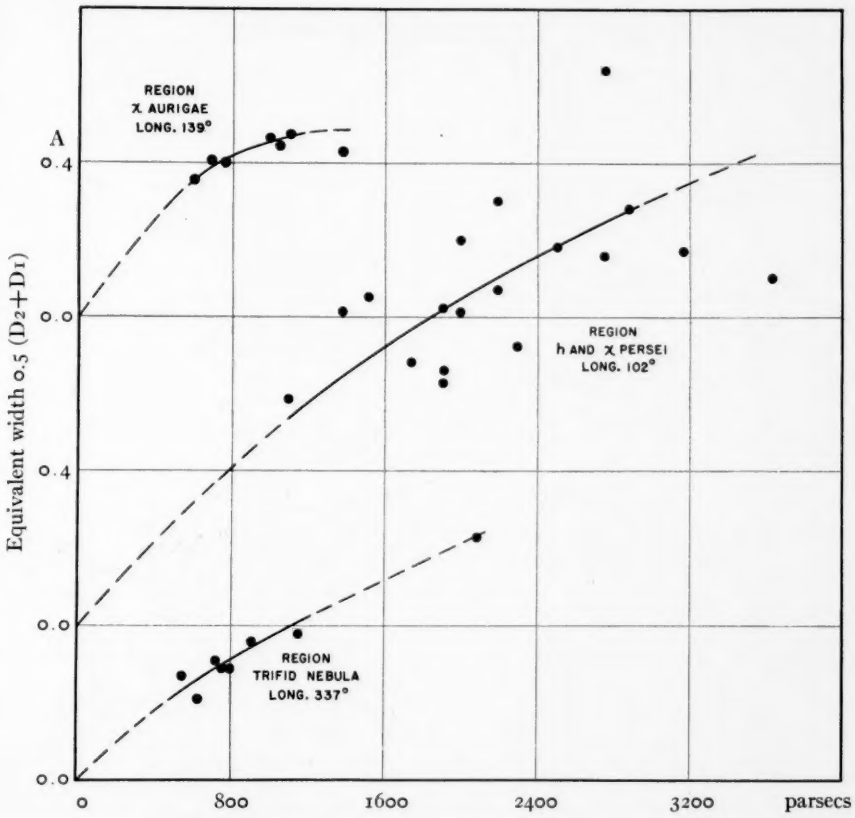

FIG. 1.—Relationship between distance and D-line intensity for individual stars in three regions.

merically equal to the accompanying color excess, as certain photometric investigations indicate, the shape of the observed curve connecting distance and D-line intensity would not be greatly altered by the correction for absorption. It seems improbable, therefore, that the flattening is caused wholly by homogeneous absorption.

[3] *Pub. Washburn Obs. Univ. Wisconsin*, **15**, 217, 1934.

b) The *curve of growth* of line intensity with number of atoms may, under certain circumstances, have a flat portion. Discussion of this point is reserved for another *Contribution*.

TABLE 3

INTENSITIES OF INTERSTELLAR SODIUM LINES IN VARIOUS REGIONS

Long.	Lat.	No. of Stars	Distance (Parsecs)	Int. EA 0.5 (D2+D1)
23°	− 4°	4	600	0.23
40	+ 1	11	1800	0.74
46	+ 1	4	1100	0.55
55	0	7	300	0.15
			1200	0.60
49	− 8	3	150	0.13
65	−17	3	600	0.24
69	+ 5	7	900	0.41
84	− 1	11	700	0.51
			1700	0.77
			2600	1.02
91	0	7	3600	0.84
102	− 3	18	1400	0.65
			2200	0.91
			3200	1.15
107	+ 2	7	1200	0.64
119	+ 1	5	800	0.40
129	−13	4	400	0.20
139	0	7	700	0.38
			1100	0.46
156	+ 2	9	500	0.30
			1700	0.48
164	−12	6	400	0.25
176	−17	9	600	0.22
173	+ 1	8	800	0.45
193	+ 1	6	800	0.30
315	0	6	600	0.35
321	+19	8	200	0.17
337	− 2	8	600	0.25
			1100	0.39
358	+11	4	550	0.37

c) *Dispersion in the absolute magnitudes* for a given type, or errors in the assumed relative magnitudes of various types, would cause stars actually at the same distance to be assigned a considerable range in distance, and the curve might thus be given a fictitious flattening. In other words, the regression-curve of intensity against distance may be less steep than the true relationship.

d) *Irregularities in density of sodium vapor.*—If a number of stars, situated in a relatively tenuous region of space, were seen through a sodium cloud of high density, the intensities would not progress with distance, and the plotted curve would be flat. This possibility should be given serious consideration.

Since in most of the 23 regions the observations do not define clearly the way in which line intensity increases with distance, a

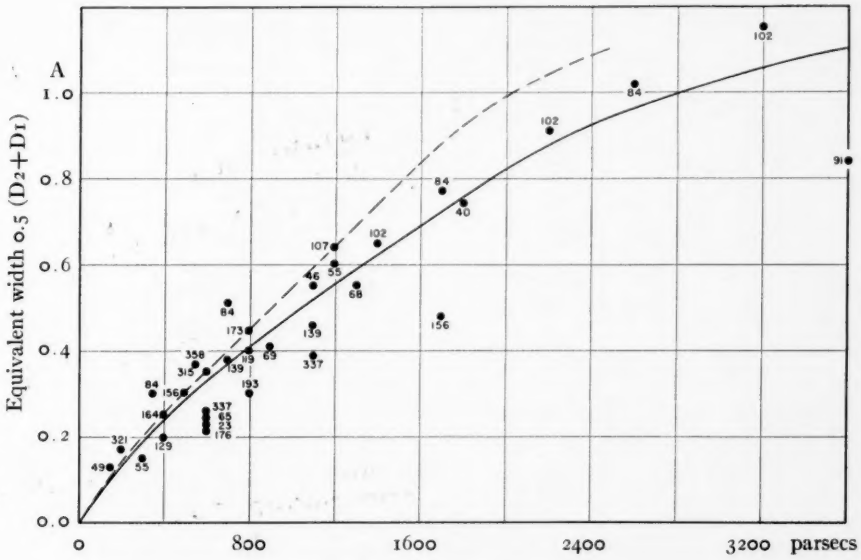

FIG. 2.—Relationship between distance and D-line intensity for mean values derived from 23 small regions. The galactic longitude corresponding to each point is given. The continuous line is the estimated mean curve as observed; the dashed line, that corrected for space absorption of 0.35 mag. per kiloparsec.

single normal place was formed for each whose co-ordinates are practically the means of those of the individual stars. Where the progression of intensity with distance is clearly exhibited, however, two or three pairs of values were determined. All these normal places are listed in Table 3 and plotted in Figure 2.

The correlation between distance and intensity is sufficient to show that regional differences, while probably present, are not extremely great. A single mean curve, such as that represented by the

continuous line, used for determining the distances of stars near the galactic plane, should give results of the right order of magnitude, although for a few areas better values may perhaps be obtained from the original regional curves.

The dashed line shows the position of the curve when corrected for a space absorption of 0.35 mag. per kiloparsec. According to this curve, the intensity increases nearly, but not quite, in proportion to the distance. Up to 2000 parsecs a good representation is given by the equation

$$y = 0.001440x^{0.860},$$

x = distance in parsecs,

y = intensity, $0.5\,(D2 + D1)$, in equivalent angstroms.

Since the 23 small areas yield reasonably consistent results for the distance-intensity relationship, all the stars observed were next grouped according to longitude in seven larger regions chosen with regard to the maxima and the null points of galactic rotation. Three regions, each extending over 20° of longitude, are centered on the null points observable from Mount Wilson, namely, those at 331°, 61°, and 151°; two regions 70° wide are centered on the maximum points, 16° and 106°; while the terminal regions, 307°–320° and 162°–212°, complete the list. Plots of the correlation between distance and D-line intensity are shown in Figures 3 and 4.

Because the D lines are intrinsically very narrow, high total intensities can be produced by a moderate number of atoms only if some external effect causes the absorption to be spread over a range of wave-length greater than the normal. Such changes in wave-length may be caused by the influence of near-by particles on the absorbing atom, but this effect is probably negligible at the low densities of interstellar space. Gross electric or magnetic fields can scarcely be postulated. The only other known cause of widening is the Doppler effect arising from the relative motions of atoms and observer. It thus appears that differential motions along the line of sight are of essential importance in producing the observed intensities of interstellar lines.

If the predominating motions are those corresponding to general

galactic rotation of a planetary type, the interstellar lines should, for a given distance, be less intense in stars near the nodes or null points at 331°, 61°, 151°, and 241° than at intermediate longitudes. For dis-

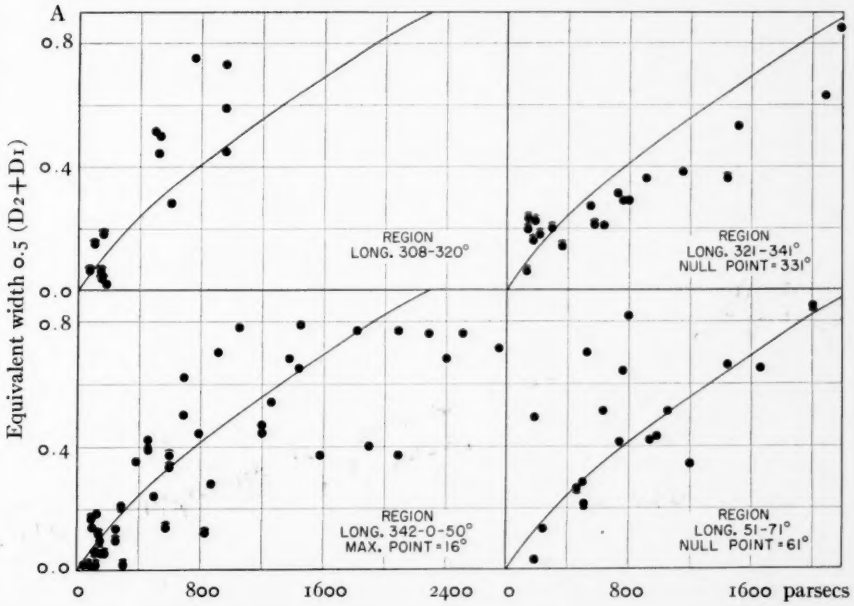

FIG. 3.—Relationship between distance and D-line intensity for individual stars grouped according to galactic longitude. An arc *above* a plotted point indicates that the star is 10° or more north of the galactic equator; *below*, 10° or more south. The mean curve (observed) from Figure 2 is placed on each diagram for reference.

Region 321°–341°.—The point at the upper right-hand corner of the diagram corresponds to HD 160529, cA4eα. The sodium lines appear double, the probable explanation being that the component toward the red is interstellar, while that toward the violet, which is less intense, is caused by stellar absorption displaced as in P Cygni. Since the wings of the components overlap, some uncertainty exists as to the intensity of the interstellar line. The plotted value probably represents an upper limit, the true intensity being perhaps 20 per cent less.

Region 342°–0°–50°.—The point at $x = 2090$, $y = 0.37$, corresponds to HD 190066, cBo. If it is an ordinary Bo star instead of a c star, its calculated distance would be only 960 parsecs. The points at $x = 1580$, $y = 0.37$, corresponding to HD 193077, Oc, and at $x = 1900$, $y = 0.40$, HD 191566, B2, have low weight. HD 227836 yields a point beyond the limits of the diagram at $x = 5250$, $y = 1.43$.

tances up to 600 parsecs, two or three small areas near null points yield slightly low intensities (Fig. 2), but the data have low weight and the plots in Figures 3 and 4 make the effect appear uncertain.

At greater distances, where the effects of rotation should manifest themselves more strongly, areas at 337° and 156° (toward the galac-

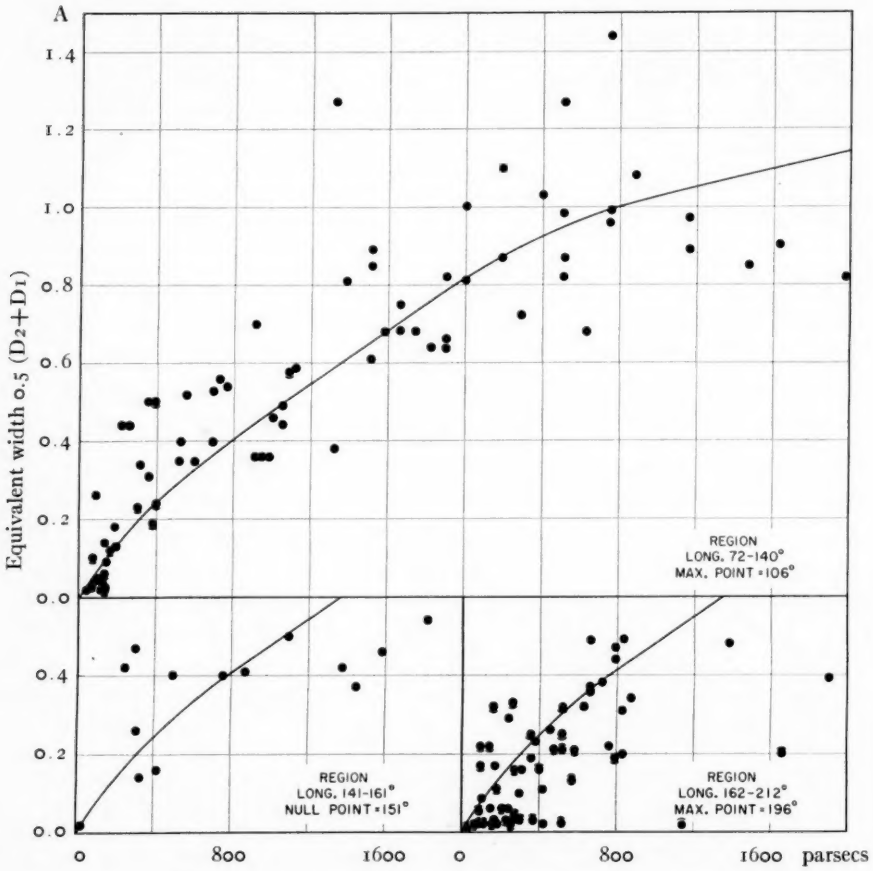

FIG. 4.—Relationship between distance and D-line intensity for individual stars grouped according to galactic longitude. An arc *above* a plotted point indicates that the star is 10° or more north of the galactic equator; *below*, 10° or more south. The mean curve (observed) from Figure 2 is placed on each diagram for reference.

Region 72°–140°.—The point at $x = 1320$, $y = 1.27$, corresponds to HD 223385 (Boss 6111), cA2ea, which may be at a greater distance than that assigned to it. HD 4717 yields a point beyond the limits of the diagram at $x = 5750$, $y = 0.98$.

Region 162°–212°.—The point at $x = 1900$, $y = 0.39$, corresponds to HD 46106, Bo (Victoria). The calculated distance for type B8 (Harvard) is 830 parsecs.

tic center and in the opposite direction) exhibit low intensities (Fig. 2), while an area at 55° (near the intermediate null point) does

not. Figures 3 and 4, based on slightly more extensive data, display the same behavior.

These results appear to indicate that the standard galactic rotation plays a relatively minor role in producing the observed intensities of detached D lines. This conclusion does not mean that interstellar matter fails to take part in galactic rotation or that the expected widening of the lines is nonexistent. The interpretation is rather that the effect is badly blurred by interstellar motions of other kinds.

A curious irregularity in which galactic rotation can scarcely play any part is the low intensity of the lines in the region of longitude 91° compared with those in regions 84° and 102°. Another interesting feature is the very low intensity found in certain stars at high galactic latitudes, in the region of longitudes 162° to 212°. This indicates either marked local irregularities or a surprisingly thin galactic stratum of sodium vapor.

There is little evidence of a general increase of density of sodium vapor toward the galactic center; but the distances to which our observations extend are, of course, small compared with the galactic radius. Moreover, it is probable that the intense lines in the more distant stars of our program would not be very sensitive to differences in interstellar density.

Points corresponding to areas in which Stebbins and Huffer have noted strong reddening[2] are not distinguished by large residuals in the distance-intensity relationship. Intensity does show a positive correlation with color, as found by E. G. Williams for the K line;[4] but this relationship, if arising statistically from the fact that both intensity and color increase with distance, does not necessarily indicate a physical dependence.

A general discussion of the distance-intensity relationship is planned for another *Contribution*.

NOTES ON TWO STARS IN NEBULAE

1. *HD 164492 in the Trifid Nebula, M 20, NGC 6514.*—The mean intensity of the D lines in the spectrum of this star in the southern lobe of the Trifid nebula is 0.16 equivalent angstroms, a value de-

[4] *Mt. W. Contr.*, No. 487; *Ap. J.*, **79**, 280, 1934.

pending on one spectrogram of fair quality. The distance read from the curve in Figure 1 is 380 parsecs, which may be taken also as a determination of the distance of the nebula. With this distance and the assumed absolute magnitude of -3.4 for spectral type O7, the apparent visual magnitude should be 4.5. The value in the *Henry Draper Catalogue* is 6.9, indicating an obscuration of 2.4 magnitudes. This result is not considered highly accurate but is given as an illustration of an interesting method.

2. *HD 164794 in M 8, NGC 6523.*—For this star (which is *not* the nuclear star) the intensity 0.5 (D2 + D1) = 0.31 EA; distance 800 parsecs; type O5; M, -3.4. From these data the calculated apparent magnitude is 6.1, which agrees within errors with the HD value, 5.9. M 8 lies within a degree and a half of the Trifid Nebula.

LINE INTENSITY AND DISPLACEMENT

Doppler effects that are symmetrically distributed about the normal position of the line center will increase the total line intensity without producing any displacement of the line as a whole. This would be true of effects due to kinetic motions or to other types of random motion whose projections on the line of sight have similar distributions in both positive and negative directions. It would not be true of motions such as differential galactic rotation whose projections are wholly or predominantly of one sign; these motions give rise to displacements having a systematic relationship to intensity.

A direct comparison of observed intensities and displacements at various longitudes is therefore in order. For this purpose the longitudes from 311° to 212° were divided into 14 regions, for each of which a correlation diagram for residual radial velocity and total intensity is exhibited in Figures 5 and 6. The residual velocity was computed by correcting the observed velocity for solar motion of 20 km/sec toward R.A. 18^h0^m, Dec. +30°.

It is instructive to compare the diagrams in sequence of longitude, bearing in mind that effects of galactic rotation should vanish at the null points, 331°, 61°, and 151°, and should have positive maxima at 16° and 196° and a negative maximum at 106°. Actually for regions

which include null points there is little progression of displacement with increasing intensity; for regions near the maxima, the increas-

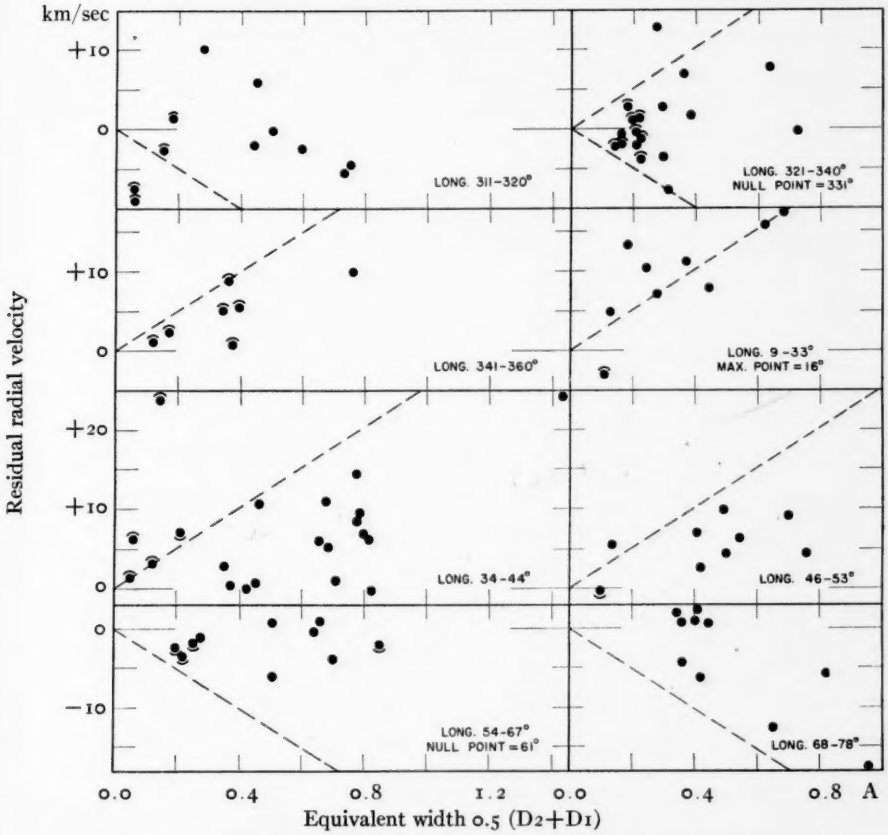

FIG. 5.—Relationship between residual radial velocity and intensity of the D lines for individual stars grouped according to galactic longitude. An arc *above* a plotted point indicates that the star is 10° or more north of the galactic equator; *below*, 10° or more south. The dashed line on each diagram marks the locus at which displacement equals one-half the equivalent width.

Region 34°–44°.—Many of the stars included in this area are faint, and the data have low weight. Nevertheless, the plot is considered representative. The very divergent point $x = 0.14$, $y = +24$, corresponds to HD 178849, B3, mag. 6.6. The data, derived from one good spectrogram, need confirmation.

ing displacements are well marked and of the proper sign, although often with considerable scatter; while for intermediate regions the progression with intensity is less rapid. Between the null points 331°

and 61° the displacements are preponderantly positive, while between 61° and 151° they are negative. The general conclusion is that

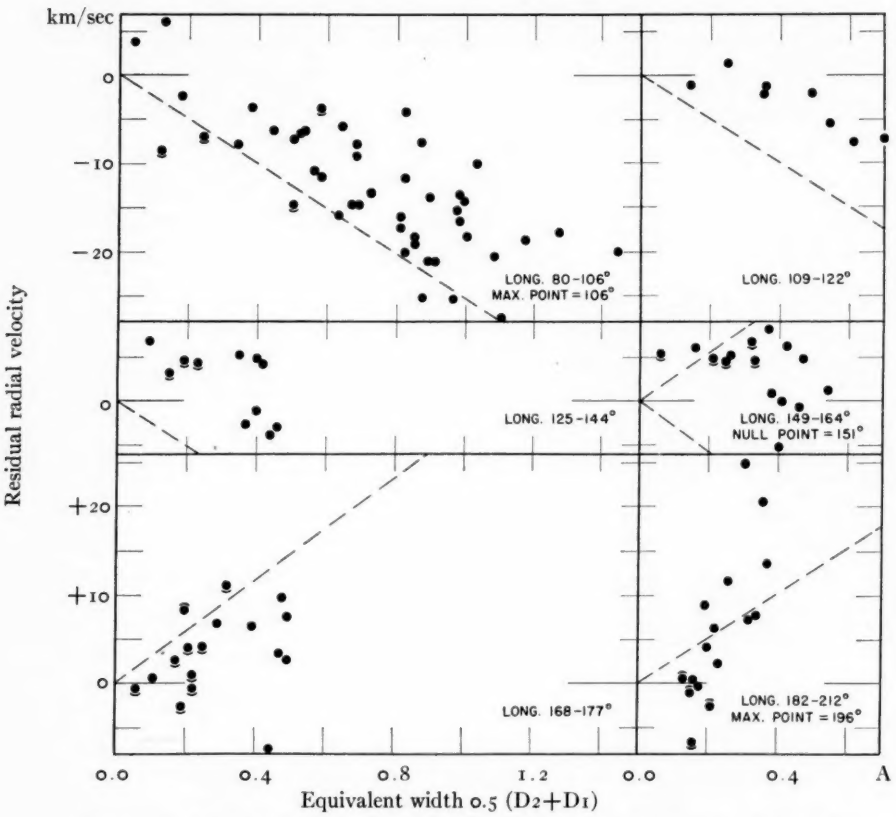

FIG. 6.—Relationship between residual radial velocity and intensity of the D lines for individual stars grouped according to galactic longitude. An arc *above* a plotted point indicates that the star is 10° or more north of the galactic equator; *below*, 10° or more south. The dashed line on each diagram marks the locus at which displacement equals one-half the equivalent width.

Region 168°–177°.—The divergent point at the lower right corresponds to HD 46300, cAo. The data appear reliable.

Region 182°–212°.—The highest point corresponds to HD 50896, Ob; the data have medium weight. The point next below corresponds to HD 52382, B2; the data have medium weight, but H and K yield a velocity lower by 9 km/sec.

the influence of galactic rotation is plainly manifest in these intensity-displacement diagrams.

For lines whose chief cause of widening is galactic rotation, the

measured displacement should equal one-half the actual width and should equal or exceed one-half the equivalent width, depending on whether or not complete saturation occurs. In no event should the displacement be less than one-half the equivalent width.

For convenient reference the locus of points for which the displacement equals one-half the equivalent width is indicated on each diagram by a dashed line. On only one diagram, longitudes from 9° to 33°, does this line provide a passable representation of the plotted points. On the others, nearly all the points correspond to displacements numerically less than half the equivalent widths. This fact confirms the previous finding that some phenomenon other than rotation must play an important part in producing the observed intensities. Quite similar was Beals's conclusion[5] "that in many cases some mechanism other than galactic rotation exercises an important influence in the formation of the line profile."

A few displacements numerically *greater* than half the equivalent widths occur, notably in the region 182°–212°, where the displacements exhibit a large scatter although the range of intensity is small. The data appear to indicate considerable irregularity in the motions of interstellar sodium vapor.

CARNEGIE INSTITUTION OF WASHINGTON
MOUNT WILSON OBSERVATORY
April 1937

[5] *M.N.*, **96**, 668, 1936.

ANALYSIS OF THE INTENSITIES OF THE INTERSTELLAR D LINES*

O. C. WILSON AND PAUL W. MERRILL

ABSTRACT

Previous investigations of interstellar lines are briefly reviewed.

The interstellar D-line intensities measured at Mount Wilson in the spectra of over 200 early-type stars are critically discussed with the object of deducing the distribution and motions of the sodium atoms in space. If the atoms are assumed to have no relative motions other than those due to temperature, the D-line intensities should follow a normal curve of growth. This assumption is shown to be incorrect because (1) the curve derived from the measured intensities does not have the proper shape and (2) it leads to very improbable distances for the stars with strong lines as compared to those with weak lines.

The introduction of galactic rotation gives a good representation of the mean decrease of the doublet ratio D2/D1 from 2.0 to 1.2 with increasing intensity. A more detailed examination proves conclusively, however, that the rotational velocity gradient cannot be responsible for the widths of the lines because, for a given distance, the line intensities and the doublet ratio are essentially the same for all galactic longitudes.

The observations can be accounted for by making the hypothesis that interstellar sodium occurs in discrete aggregations or clouds, which, while participating in the general galactic rotation, have in addition considerable random motions. This assumption requires no dependence upon the galactic longitude and succeeds in explaining how the D lines can strengthen almost linearly with the distance, while the ratio of D2 to D1 is only 1.2. By fitting computed curves to the observational data, the following numerical results are obtained: an upper limit to the temperature is 44,000°; the density of sodium atoms in the ground state is approximately 10^{-31} gm/cc; the linear dimensions of the clouds, in the galactic plane, are of the order of 700 parsecs; and the spread of the random cloud velocities need not exceed 15 or 20 km/sec.

SUMMARY OF PREVIOUS INVESTIGATIONS

Preceding work on interstellar line intensities may, for the purpose of a brief review, be conveniently classified as either theoretical or observational. The exact historical order is partially disregarded in the following summary, which begins with the theoretical aspect of the problem.

The first analysis along modern lines of the conditions prevailing in interstellar space was made by Eddington in his 1926 Bakerian lecture.[1] In this work Eddington used rather general physical arguments to arrive at estimates of the density and temperature of interstellar calcium and sodium, and it is noteworthy that his results did not depend upon accurate knowledge of the intensities of the inter-

* *Contributions from the Mount Wilson Observatory, Carnegie Institution of Washington*, No. 570.

[1] *Proc. Roy Soc.*, A, 111, 424, 1926.

stellar lines of these elements. Measurements of intensities had not, in fact, been made at the time; and only very rough estimates were available as an approximate check on the validity of the computations.

Gerasimovič and Struve[2] in 1929 utilized eye estimates of interstellar line intensities by Struve,[3] in conjunction with probable stellar distances, to derive a reasonable value for the density of ionized calcium in space. Their determination was based upon the assumption that the strength of a line depends only on the atomic absorption coefficient and the number of atoms in the line of sight.

The fact that the intensity of an absorption line is a function of the relative atomic velocities, as well as of the atomic constants and total number of atoms, was made clear by the work of Schütz in 1930.[4, 5] Unsöld, Struve, and Elvey[6] first applied these ideas to the problem of interstellar lines. They recognized that the theory of galactic rotation, as developed by Oort and others, would provide a linear velocity gradient along all lines of sight in the galactic plane except those pointing toward and away from the galactic center and at right angles thereto. If the interstellar matter participated in the rotation, the resultant differential velocities should be taken into account in computing the intensities of interstellar absorption lines. Investigation showed that the doublet ratio, K/H, could theoretically have any value in the range from 1 to 2, depending upon the distance and position of the star in whose spectrum the lines occurred. The amount of observational material included in the investigation was insufficient to provide a satisfactory comparison with the theoretical results.

More recently Eddington[7] also has adopted the idea that galactic rotation may be chiefly responsible for the widths and total absorptions of interstellar lines. He combined a linear velocity gradient with the usual atomic absorption coefficient and computed the intensities of the resultant lines. His analysis, which treats the density of the interstellar gas as a variable parameter, indicates that after the density has attained a value sufficiently great to produce a

[2] *Ap. J.*, **69**, 7, 1929.
[3] *Ibid.*, **67**, 353, 1928.
[4] *Zs. f. Ap.*, **1**, 300, 1930.
[5] Struve and Elvey, *Ap. J.*, **79**, 409, 1934.
[6] *Zs. f. Ap.*, **1**, 314, 1930.
[7] *M.N.*, **95**, 2, 1934.

saturated line, the density may then be increased about five hundred fold before the line shows a further increase in total absorption. Eddington considers this result to be the explanation of the hitherto anomalous fact that the *Na* I and *Ca* II lines are observed to be of approximately equal strength, while his previous purely theoretical calculations had shown that the ionized calcium atoms in space should be about three hundred times as numerous as those of neutral sodium. By considerations of this nature and by comparison with measured line intensities, Eddington was led to estimates of the densities of interstellar calcium and sodium which, owing partly to insufficient observational data, cannot be considered as completely satisfactory. Among other results of this stimulating paper, there is one which is very easy to test observationally. This is the fairly obvious statement that, if for a saturated line the width and displacement are both due to a linear velocity gradient along the line of sight, the radial velocity cannot exceed half the equivalent width expressed in velocity units.

Struve[3] was the first to make a systematic attack on the problem from the observational side. He made eye estimates of the intensities of the interstellar *Ca* II lines in the spectra of a large number of early-type stars. Although his individual values were undoubtedly of low weight, owing to the inhomogeneity of his material and the inherent uncertainties of such work, they were of great statistical importance. He found that the intensities of the lines increased with the distances of the stars in whose spectra they were observed. This fact has been amply confirmed by later work, although there is evidence that the precise correlation between intensity and distance found by Struve is probably not correct.

The extensive and well-known researches of Plaskett and Pearce[8] had as their main objective the determination of the constants of galactic rotation from measures of the displacements of the stellar and interstellar lines in the spectra of many early-type stars. These authors made careful eye estimates of the intensities of numerous interstellar *Ca* II lines, by comparison with a set of standard artificial lines, the chief purpose being to arrange the stars into groups on the

[8] *Pub. Dominion Ap. Obs.*, **5**, 167, 1933.

basis of the strength of the K line. The intensities derived in this manner are probably representative of the highest accuracy that has been attained by visual comparison. Nevertheless, the superiority of photometric measurement of line strength over the best previous results is clearly brought out by E. G. Williams' comparison of his own measures with the Victoria values.[9] He found a considerably larger scatter on plotting the two sets of data against each other than would be anticipated from the size of his probable errors alone. Evidently the greatly increased labor of measuring interstellar line intensities by the usual photometric methods is entirely justified, particularly where accurate determinations of the relative strengths of the two members of a doublet are required.

Williams was concerned chiefly with determining the relationship of interstellar K intensity to color excess; and his results do not, for the most part, have a direct bearing on the present investigation. It is noteworthy, however, that he encountered considerable difficulty in obtaining reliable values of the doublet intensity ratio, K/H, owing to the blending of the interstellar H line with stellar $H\epsilon$. We have seen that accurate knowledge of this ratio is very desirable for comparison with theoretical predictions, and the much greater freedom of the sodium D lines from blends with stellar lines is a strong argument in favor of employing them in an extensive investigation.

In his most recent paper Beals[10] has collected and discussed his published observational material on both calcium and sodium and has arrived at certain important results. He finds, on plotting radial velocities of interstellar lines against their intensities, only a weak correlation at best, and concludes that Eddington's simple picture of line formation cannot be adequate. He suggests irregular group motions in the interstellar cloud as the main widening agent, at least for the near-by stars, and in support of this idea finds that high-dispersion spectrograms of three bright B-type stars show the K lines to consist of two components, neither of which, judged by velocity or appearance, is at all likely to be of stellar origin. He investigates also the doublet ratios, K/H and D2/D1, and finds good evidence that in both cases the ratio attains the value 2 for weak lines and de-

[9] *Mt. W. Contr.*, No. 487; *Ap. J.*, **79**, 280, 1934. [10] *M.N.*, **96**, 661, 1936.

creases as the lines become stronger. His data are probably not complete enough to determine accurately the variation of the ratio with line strength, since there appears to be considerable scatter.

DISCUSSION OF MOUNT WILSON DATA

The need for further measures of interstellar line intensities has been made clear by the foregoing summary of previous work in this

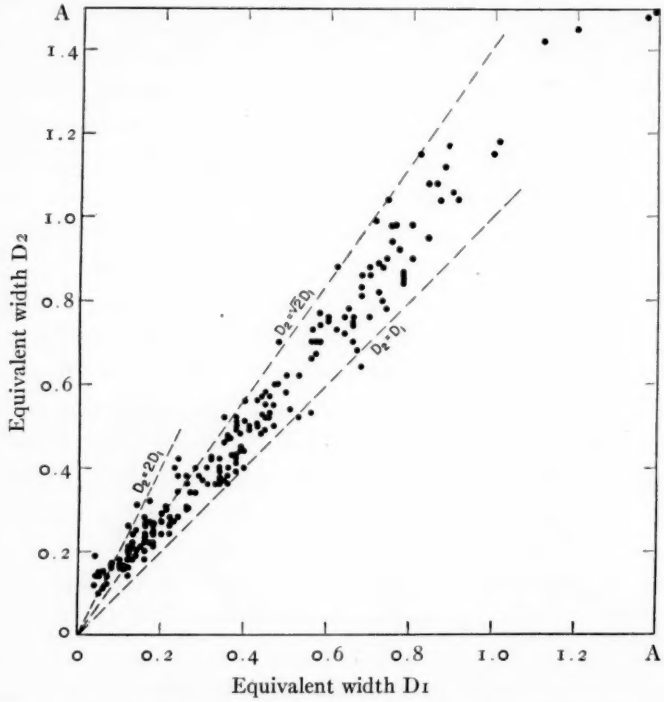

FIG. 1.—Relationship between equivalent widths, D1 and D2

field, and the advantages to be derived from an extensive study of the sodium D lines have been pointed out. We have therefore undertaken the measurement of the intensities of the interstellar D lines in the spectra of over 200 stars, well distributed over the range of galactic longitude observable from Mount Wilson. Our measures, together with such relevant matters as discussions of the photometric technique and general accuracy, will be presented fully in another *Contribution*.[11] In the present paper the data are analyzed

[11] *Mt. W. Contr.*, No. 576; in press.

in an attempt to deduce the temperature and density of sodium in interstellar space and the mechanism of interstellar line formation. The analysis consists of a comparison of the observational data with the results of computations based upon various assumptions as to the motions and distribution of the interstellar gas, the simplest hypothesis being considered first, and more complicated ones introduced as the need for them arises.

In Figure 1 the total absorption of D1 is plotted against that of D2 for each star.[12] This diagram illustrates the general consistency

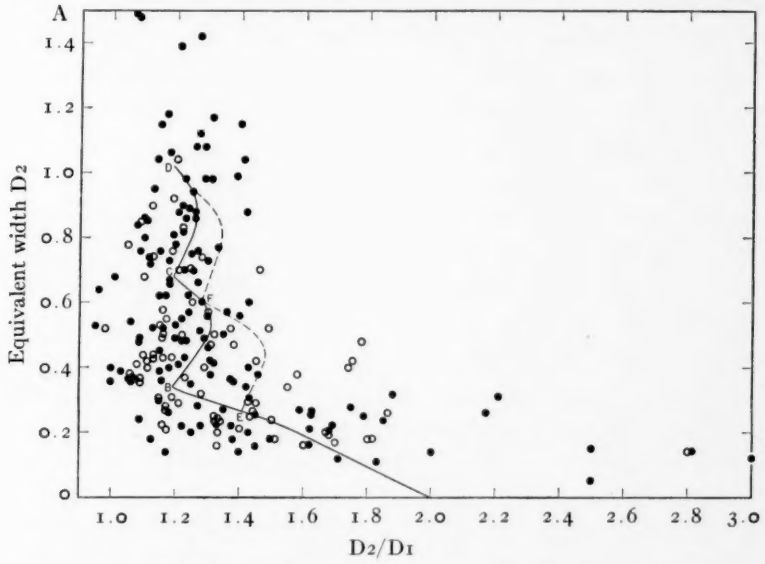

FIG. 2.—The doublet ratio, D2/D1, as a function of the intensity of D2. Circles correspond to stars near the null directions of galactic rotation.

of the measures and shows clearly that the ratio of D2 to D1 tends to be decidedly larger for the weaker lines than for the stronger ones. This interesting feature of the data is best exhibited by plotting the doublet ratio, D2/D1, against D2, as has been done in Figure 2. The curves drawn in Figure 2 will be referred to in a later section; for the present, attention is directed to the distribution of the plotted points. It is evident that, for the weakest lines, the doublet ratio is

[12] Hereafter the symbols D1 and D2 will frequently be used to signify the total absorptions of the lines as well as to refer to them in the more general sense. The meaning in any case will be clear from the context.

about 2; and, as the lines increase in strength, the ratio rapidly diminishes to about 1.2 and remains constant throughout the range of intensity covered by the observations. Beals's data are in essential agreement with these results.

The correlation of high ratio with low intensity suggests the possible blending of interstellar D2 with some other weak line. This point was forcibly brought to our attention by the fact that several stars with weak D lines were found to yield doublet ratios definitely in excess of the theoretical upper limit, 2. The anomalous ratios in these spectra were traced to a blending with D2 of the stellar *C* II pair at λ 5889.97 and λ 5891.65. The presence of these *C* II lines can apparently be inferred from the behavior of the other well-known *C* II lines at λ 4267 and λ 3919. If the latter lines can be seen easily, the doublet ratio should probably not be used unless the equivalent width of D2 exceeds 0.15 A. If D2 is greater than 0.15 A, the contribution of the *C* II lines, if present, will probably not be sufficient to produce a serious distortion of the doublet ratio. This criterion has eliminated several stars from consideration. Figure 2 includes only those stars in which we feel that the ratio is reasonably free from the influence of the stellar *C* II lines.[13]

The appearance of Figure 2 suggests an attempt to explain the doublet ratios by means of a normal curve of growth. The first step is to construct a curve of growth from the measured intensities. If we assume a homogeneous distribution of atomic velocities throughout space, the construction of the curve from the measured intensities would be a very simple matter provided the number of atoms in the line of sight to each star were known. But knowledge of the total number of atoms to any star requires knowing its distance, as well as the density of interstellar sodium; and, since we hope to determine these data from our measures, we do not wish to assume them.

First consider the physical conditions under which a normal curve of growth would be anticipated. These are typified by a laboratory experiment in which a tube contains atoms whose only motions are those due to the temperature, *T*, assumed constant throughout the

[13] We are indebted to Dr. J. A. Pearce, of the Dominion Astrophysical Observatory for data on the violet lines of *C* II in a number of spectra.

tube. If, in such an experiment, the number of effective atoms, Nf, can be varied and the corresponding equivalent widths, W, measured, then the curve resulting when log Nf is plotted against log W is the curve of growth for the given line at the specified value of T. Such curves are characterized by the fact that they represent relations of the form $W \propto (Nf)^a$, where the exponent a can range from 1 to nearly 0. Curves of growth computed for sodium are shown by the dashed lines in Figure 3. The straight line on the right represents

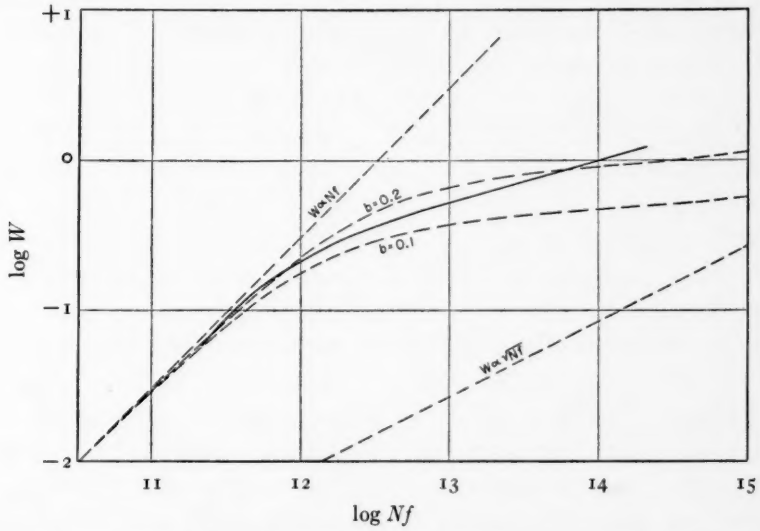

FIG. 3.—Curves of growth for the D lines. The continuous curve is constructed from the measured equivalent widths. The dashed curves are theoretical.

the case where the atoms are quiescent and the absorption lines are produced by pure radiation damping. This line corresponds to $a = \frac{1}{2}$. In general, for a given T, the EW's will start on the left-hand line, where $a = 1$, rise to a point determined by T, and then will follow a curve such as those shown, ultimately joining the square-root branch on the right. The important case where W is not a function of Nf alone, but of the distance as well, will be discussed later.

Suppose now that we have measures of the total absorptions of a doublet, such as the D lines, for a series of values of the number of

atoms, N. Let the successive values of N be so close together that, if W_1^i and W_2^i are the EW's of the ith pair, we have

$$W_1^i < W_1^{i+1} < W_2^i .$$

Any pair of values corresponds to effective numbers of atoms in the ratio 1:2, since this is the ratio of the f values for the D lines. Hence, if $\log W_1^i$ and $\log W_2^i$ are plotted against $\log N$ and $\log N + \Delta \log N$, respectively, where N is arbitrary and $\Delta \log N = \log 2 = 0.30$, the straight line joining these two points will have a slope which is equal to that of the curve of growth at some point between W_1^i and W_2^i. Successive values of $\log W_1$ and $\log W_2$ are then plotted against the same values of $\log N$, and each pair of points is joined by a straight line. Thus we have a series of line segments of varying inclination, lying one above the other and each having a slope equal to that of the curve of growth at some point. Next, the second of these segments is moved horizontally to the right until it touches the first; then the third until it touches the second; etc. Finally, if a smooth curve is drawn such that all the segments are tangent to it, we should have a good approximation to the true curve of growth. This method was tested by reading pairs of points from a computed curve of growth and using them in the foregoing manner to reconstruct the original curve. The agreement between the two curves was quite good, and the method outlined appears satisfactory.

This scheme was applied to the measured EW's of interstellar lines. All the stars were arranged in order of increasing D1, and means of D1 and D2 were taken in groups of ten, overlapping five each time. These mean values of D1 and D2 satisfied the condition noted above and were used to construct the curve of growth for the interstellar sodium lines. Finally, this curve was superposed on the theoretical ones and shifted horizontally to obtain the most generally satisfactory fit. The result is shown by the solid curve in Figure 3. Evidently the observed curve corresponds to a value of the parameter b in the neighborhood of 0.1 or 0.2, where, in the notation of Struve and Elvey,[5] b is defined by $b = \lambda_0 v_0/c$, with v_0 equal to the most probable velocity of the atoms.

By fitting the observed curve to the theoretical curves, we have supplied it with a true $\log N$ scale. Thus, if the lines were formed

under conditions which yield a normal curve of growth, Figure 3 would give the number of atoms active in producing any given observed line. The assumption of uniform sodium density then leads immediately to the relative distances of the stars. Assuming the legitimacy of this process, we note from the figure that there are about three hundred times as many atoms involved in the production of our strongest lines as in the weakest. Since there is good reason to believe that the weakest lines correspond to stellar distances of at least 100 parsecs, the stars with intense lines should be 30,000 parsecs distant, whereas their actual distances are probably only two or three thousand parsecs. This difficulty could be avoided, of course, by postulating nonuniform density; but, when it is considered in conjunction with the fact that the observed and theoretical curves definitely disagree in shape, the proper conclusion appears to be that interstellar line intensities are not represented by a normal curve of growth. Accordingly, the solution shown in Figure 3 is rejected.

Since the hypothesis of uniform density, together with that of pure temperature motion or small-scale turbulence, appears incapable of giving a satisfactory solution, motions *dependent on the distance*, as suggested by the theory of galactic rotation, may next be considered. The appearance of Figure 2 suggests the following tentative ideas. For the near-by stars the temperature or other small-scale motions of the atoms are the determining factor in producing the absorption lines, while for greater distances the effect of rotation will predominate. Hence the proper manner of introducing rotation, without sacrificing the possibility of deducing both the temperature and density of the sodium, appears to be the following:

Consider an element dl of any line of sight having a cross-section 1 sq cm. The optical thickness of this element for wave-length λ is given by[14]

$$d\tau_\lambda = \frac{\sqrt{\pi}e^2\lambda_0^2 nf}{mc^2 b} e^{-\left(\frac{\lambda_0-\lambda}{b}\right)^2} dl\,, \qquad (1)$$

where e, m, c, and λ_0 have their usual meanings, n is the number of active atoms per cubic centimeter, f the oscillator strength, and

$$b = \frac{\lambda_0 v_0}{c} = \frac{\lambda_0}{c}\sqrt{\frac{2kT}{m}}$$

[14] A. Unsöld, *Mt. W. Contr.*, No. 377; *Ap. J.*, **69**, 209, 1929.

on the assumption of a Maxwellian velocity distribution corresponding to temperature T. We assume n and b constant along the line of sight. If the radial velocity of the element is taken to be proportional to its distance, we may write

$$d\tau_\lambda = ce^{-\left(\frac{\lambda_0-\lambda}{b}\right)^2} dl = c'e^{-\left(\frac{\lambda_0-\lambda}{b}\right)^2} d\lambda_0 ,$$

whence,

$$\tau_\lambda = c' \int_{\lambda_1}^{\lambda_2} e^{-\left(\frac{\lambda_0-\lambda}{b}\right)^2} d\lambda_0 ,$$

where λ_1 and λ_2 are the values of λ_0 at the two ends of the line of sight. Setting $(\lambda_0 - \lambda)/b = x$, we have

$$\tau_\lambda = bc' \int_{\frac{\lambda_1-\lambda}{b}}^{\frac{\lambda_2-\lambda}{b}} e^{-x^2} dx .$$

Finally, convenient units are introduced, and the expression for τ becomes

$$\tau_{\Delta\lambda} = \frac{2.42 \times 10^{10} nf}{V} \left[\phi\left(\frac{0.98 \times 10^{-5} Vl}{b} + \frac{\Delta\lambda}{b} \right) + \phi\left(\frac{0.98 \times 10^{-5} Vl}{b} - \frac{\Delta\lambda}{b} \right) \right] . \qquad (2)$$

In equation (2) the various symbols mean:

n = number of active atoms per cubic centimeter.
V = velocity gradient along the line of sight in kilometers per second per kiloparsec.
$b = \frac{\lambda_0 v_0}{c} = \frac{\lambda_0}{c}\sqrt{\frac{2kT}{m}}$.
l = length of light-path in parsecs.
$\Delta\lambda$ = wave-length distance in angstroms to the line center.
ϕ = probability integral.

This expression for τ is quite complicated and does not yield a simple result for the EW as does that derived by Eddington, but it has the advantage of taking accurate account of temperature mo-

tions as well as galactic rotation. To apply equation (1) the EW is given, as usual, by

$$W = \int (1 - r) d\lambda , \tag{3}$$

with

$$r = \frac{I}{I_0} = e^{-\tau} . \tag{4}$$

The method of computing line intensities from equations (2), (3), and (4) deserves some comment. Originally the contours derived from (2) and (4) were plotted and integrated with a planimeter. This is a time-consuming process when the number of lines is fairly great, and a much shorter method was found to be the following: Let r_c be the value of r at the center of the line, i.e., for $\Delta\lambda = 0$. Then for any line we may always write

$$W = 2(1 - r_c)\Delta\lambda_m ,$$

where $\Delta\lambda_m$ is the half-width at some point within the line. For the kind of lines given by (2) and (4) it turns out that the correct value of $\Delta\lambda_m$ is the $\Delta\lambda$ at $r = (1 + r_c)/2$, i.e., at the point halfway from the continuous background to the bottom of the line. Values of W obtained in this manner have been compared with those derived by planimeter measures over the entire range of intensity needed for this investigation and always agree within a per cent or two. Incidentally, this method is applicable also to the case where τ is given by (1) and is shorter in practice than the series expansions used by Struve and Elvey.[5]

There now remains the step of comparing the observed and computed line intensities in such a way as to determine as many as possible of the unknown parameters entering into equation (2). This comparison might be effected in various ways. We have adopted the following procedure for reasons which will presently become clear.

A little thought will show that, unless additional data are given, measures of line intensity alone can scarcely determine the velocity gradient V. This quantity is most logically found from velocity measures, and we have therefore adopted the value $V = 17$ km/sec/kiloparsec in the direction of a maximum point of the rotational effect.

This is the value assumed by Eddington in his discussion and is very close to the final result of Plaskett and Pearce. In order to use all our stars statistically, we must take the appropriate mean value of the gradient, which is $2/\pi$ times that at a maximum, or 10.8 km/sec/kiloparsec. V is now set equal to 10.8 in equation (2), and the total absorptions of D1 and D2 are computed for a set of standard distances ranging from 100 to 6000 parsecs and for various com-

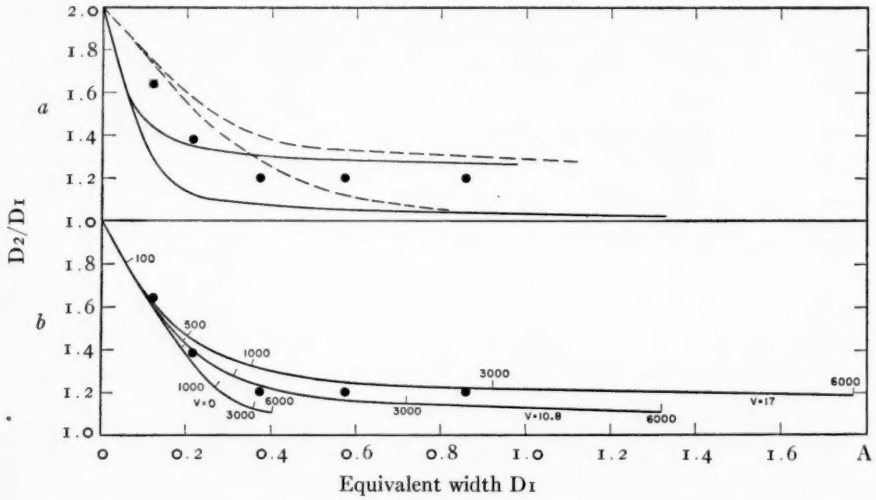

FIG. 4.—(*a*) Illustration of the method of determining n and b by comparing the results of computation with the observations. Dots are observed normal points. For the continuous curves, $b=0.05$; for the dashed curves, 0.15. The upper curve of each pair is for $n=0.95\times10^{-9}$; the lower one for $n=3.8\times10^{-9}$.

(*b*) Representation of observed intensities (and ratios) by the accepted values, $n=2.0\times10^{-9}$ atoms per cubic centimeter, $b=0.11$ A. Distances in parsecs are indicated on the curves.

binations of the two parameters n and b. From these computed values a series of curves of D2/D1 against D1 are plotted, and n and b are adjusted for the best possible fit with the corresponding observed curve. This method proves to be more sensitive in practice than might be judged from the foregoing description.

The process is illustrated in Figure 4*a*. The dots are normal points representing the observed relation for the sodium lines. The two solid curves are for $b = 0.05$, and the broken ones for $b = 0.15$.

The uppermost curve of each pair corresponds to $n = 0.95 \times 10^{-9}$, and the lower one to $n = 3.8 \times 10^{-9}$ atoms per cubic centimeter. The fit of the observed with the computed curves depends chiefly upon n for large values of D1 and chiefly upon b for small values, thus permitting semi-independent estimates to be made of both quantities. Further computation resulted in the curves of Figure 4*b*. The values of the parameters entering here are $n = 2.0 \times 10^{-9}$ and $b = 0.11$. The three curves are, from top to bottom, for values of V equal, respectively, to 17.0, 10.8, and 0 km/sec/kiloparsec, corresponding to conditions at a maximum point, an average point, and a null point. The observations should fit the upper curve somewhat better than the middle one for the stronger lines, since it happens that we have observed more of these stars near maximum points than near null points. So far, the results of this analysis seem satisfactory, and the derived numerical values of the constants are reasonable. The temperature corresponding to $b = 0.11$ A is 44,000°, rather higher than is usually assumed; but this value may, of course, include some small-scale turbulence, in which case the true temperature would be less than the foregoing value. The density of neutral sodium comes out to be 7.6×10^{-32} gm/cc, in quite close agreement with Eddington's estimate.

We have thought it of sufficient general interest to carry through these computations based on the galactic rotation hypothesis, although a simpler approach to the problem[10, 15] has already thrown considerable doubt on the validity of the assumption that rotation is the main cause of the widening of interstellar lines. Thus far, only the statistical aspect of the problem has been considered, and we must now investigate in detail whether or not the dependence of line intensity on galactic longitude is in agreement with the predictions of rotation theory.

This dependence on galactic longitude could be examined in a variety of ways. The method chosen is based on the desire to use the derived constants, n and b, for the determination of more accurate distances of individual stars from measures of intensity of interstellar sodium lines. Evidently it is now possible to compute from

[15] *Mt. Wilson Contr.*, No. 569; *Ap. J.*, **86**, 28, 1937.

equations (2) to (4) a series of curves relating intensity and distance at various galactic longitudes. Distances obtained in this way may then be compared with those derived by the "spectroscopic" method. The latter values may, of course, involve systematic errors; but such errors should not be functions of galactic longitude. Hence, if these two sets of distances are found to bear different relations to each other for different longitudes, the fault must lie, almost certainly, with equation (2) and the underlying theory.

One set of distances was computed in the usual way from the apparent magnitudes and assumed absolute magnitudes.[16] Another set was determined by the measured line strengths, and the curves computed by means of equations (2) to (4). The stars were divided into three groups for which Δl, the longitude difference between the star and the nearest null point, lay between 0° and 11°, 12° and 23°, 24° and 45°, respectively. The longitude of the galactic center was taken to be 331°. The two values of the distance were plotted against each other for every star, with the results shown in Figure 5*a*, *b*, *c*, where abscissae are distances based on line intensity and rotation theory, and ordinates are distances derived from the spectral types and apparent magnitudes. Obviously, the relation between the two sets of distances is very decidedly a function of the galactic longitude of the stars considered. For those stars not near rotational null points, the distances computed from observed line intensity are in reasonable agreement with the other set. On the other hand, for the stars nearest the nulls, where the rotational velocity gradient is small, much greater distances must be assumed in order to yield intensities equal to those observed. These facts may be put into other words, as follows: If galactic rotation plays the chief role in the formation of the interstellar sodium lines, then, near the null points, where the rotational effect is small, the lines should be weaker, for a given distance, than near the maxima. Observationally this is not found to be true, for the lines have much the same strength, for a given distance, at all longitudes. Clearly, some potent widening effect other than rotation must be sought.

On the entirely groundless assumption that the rotational velocity

[16] For details see *Mt. W. Contr.*, No. 569; *Ap. J.*, **86**, 28, 1937. Especial care was taken to avoid errors in spectral type.

gradient $V = 17$ km/sec/kiloparsec applies to stars at *all* longitudes, we find the result shown in Figure 5*d*, which, while having no signifi-

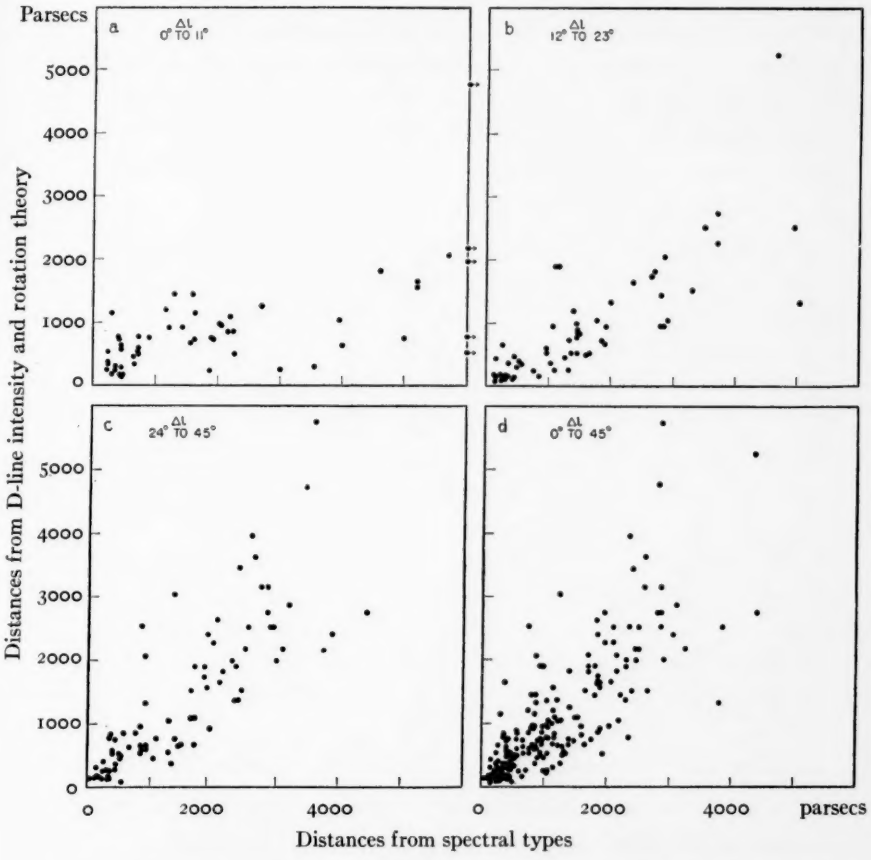

FIG. 5.—Comparison of stellar distances derived from measured D-line intensity and rotation theory (ordinates) with those deduced from spectral types and apparent magnitude (abscissae). Δl is the longitude difference, regardless of sign, between a star and the nearest null point of galactic rotation. In the lower right-hand diagram the velocity gradient, 17 km/sec/kiloparsec, is assumed to apply to all stars regardless of galactic longitude.

cance on the basis of rotation theory, is likely to be of considerable importance in determining the velocity distribution of the interstellar sodium.

Thus we find, as did Beals, that rotation is inadequate as the

source of the strength of interstellar lines. However, one more set of diagrams proves interesting in this connection. In Figure 6 are plotted residual interstellar radial velocities against total absorptions in kilometers per second, the grouping of stars being the same as that of Figure 5.[17] Evidently, for those stars nearest the null points a correlation between these quantities could be found only with the exercise of considerable imagination. For the intermediate group the situation is not much better, except possibly for a half-

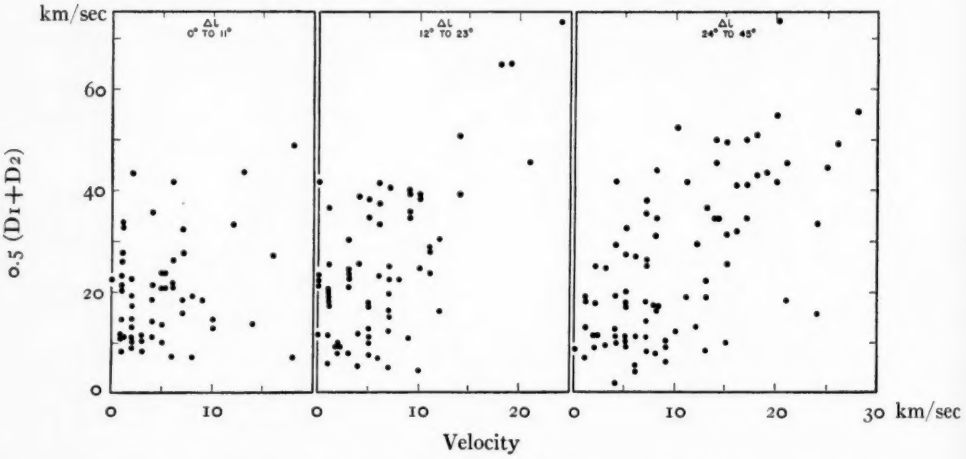

FIG. 6.—Residual radial velocities from the D lines compared with the mean equivalent widths in km/sec, for groups of stars used in Fig. 5.

dozen or so of the stars with strongest lines. But for the stars in the vicinity of the maxima of rotational effect, a correlation is undoubtedly present. In all three diagrams a very great scatter is evident. Lines having two or three times their maximum allowable strength, on the basis of rotation, as judged by their measured velocities, are numerous. The measures of both velocity and intensity are sufficiently accurate to insure that this scatter is real for the most part.

At this point it is well to bring together the facts we have ascertained and to indicate the requirements of a successful theory. We have found:

[17] The data are plotted in greater detail in *Mt. W. Contr.*, No. 569, Figs. 5 and 6; *Ap. J.*, **86**, 41, 42, 1937.

1. The doublet ratio D2/D1 is approximately 2 for our weakest lines, thereafter decreasing and maintaining the value 1.2 for the stronger lines.

2. The attempt to explain the observations on the basis of homogeneous conditions in interstellar space is considered unsuccessful because (*a*) the shape of the observational curve differs from the theoretical by a larger amount than we feel is to be attributed to observational error, and, (*b*) on this hypothesis many stars must be placed at improbably great distances.

3. By introducing galactic rotation a good quantitative explanation of the variation in the doublet ratio is obtained, and reasonable values for the temperature and density of the interstellar sodium can be deduced by using the measured intensities statistically.

4. The simple rotational picture becomes untenable, however, when the behavior of line strength as a function of galactic longitude is investigated. For a given distance, the lines are not markedly weaker near the null points than near the maxima. Moreover, the ratio D2/D1 shows no dependence on galactic longitude. This fact is illustrated in Figure 2, where the stars are divided into two groups, depending on whether they lie closer to a null point or to a maximum point.

5. The presence of the rotational effect is, however, indicated by the fact that the correlation between velocity and intensity is much better for stars near the maxima than for those near the nulls (Fig. 6). Apart from this, the great scatter in Figure 6 is evidence that some powerful widening agent besides rotation is at work.

A further attack on the problem, which seems to have proved successful, will now be presented. As a preliminary step, attention is directed to some of the diagrams in the regional study of the sodium lines by one of the authors.[15] Figure 1 of that paper shows, for the stars in certain small areas of the sky, the mean D-line intensity plotted against distance. The distances used in these figures are those derived from the spectral types and apparent magnitudes. In practically all cases the intensities increase with the distances; but, while the rate of increase is definitely not the same for all regions, the scatter of the points for a given area from the mean relation for that area is generally fairly small. Combination of the results for

twenty-three areas leads to Figure 2 of the regional paper, in which the mean curve has been corrected for an assumed space absorption of 0.35 mag. per kiloparsec. The figure shows that, in the mean, the intensities of the interstellar sodium lines increase very nearly proportionally to the distances of the stars in whose spectra they are observed.

The mean sodium-line intensities are plotted against the corrected distances for all stars within 10° of the null points in Figure 7 of the

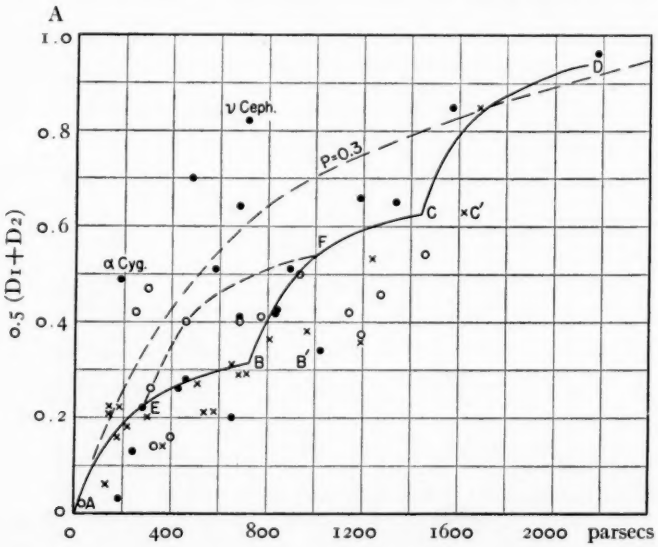

FIG. 7.—Mean D-line intensity plotted against distance for stars within 10° of the rotational null points. Crosses represent stars near longitude 331°, circles those near 151°, and dots those near 61°. The curves are explained in the text.

present paper. Although effects of galactic rotation should be very small, the intensities nevertheless are again nearly proportional to the distances. The stars at the three observed null points have been given distinguishing symbols, and it appears that the relationship of intensity to distance is not quite the same at the three nulls. The stars near galactic longitude 331°, for instance, seem to lie somewhat lower in the diagram than those near longitude 61°. Such a difference could be accounted for by postulating somewhat heavier local obscuration at 331° than at 61°. The group of stars with strong lines

at distances less than 800 parsecs is somewhat more troublesome. Two of them, α Cygni and ν Cephei, indicated in the figure, are of type cA2, and there is evidence that such stars are intrinsically brighter than was assumed in assigning them distances. Hence these two stars are perhaps plotted too far to the left. The point between them corresponds to HD 203025, a nebulous star whose sodium lines so greatly exceed the K line in strength as to indicate almost certainly that the D lines are abnormally strong. The remaining stars in this group seem to be normal.

These sources of error appear, however, not to explain all the scatter in Figure 7. In order to bring a number of the plotted points into agreement with the mean, it must be assumed that either the intensities or the distances, or both, are incorrect by rather large factors, of the order of 2 in some instances. The authors believe it to be almost certain that a considerable part of this scatter is real, since the analogous diagrams for small regions previously referred to indicate the purely observational scatter to be considerably less.

We may now set forth the facts which must be met by any successful explanation. These are:

1. The decrease in doublet ratio from 2.0 for weak lines to 1.2 for stronger lines (Fig. 2).

2. The almost linear increase of intensity with distance in the null directions without accompanying bodily displacements of the lines.[18]

3. The scatter of the observations as shown in Figure 7.

4. The observed displacements of the lines, which in general are in good agreement with the predictions of the rotation hypothesis.

If it is agreed that the widening and displacement of interstellar lines are manifestations of Doppler effect, the only reasonable hypothesis satisfying the requirements is that the interstellar gas exists in discrete masses, or clouds, and that these clouds, while partaking of the general galactic rotation, have additional relative motions.

The usefulness of the notion of discrete clouds having a spread of velocities is made apparent by considerations like the following. Suppose that a star is observed at such a distance that its light has traversed one cloud. The interstellar sodium lines in its spectrum

[18] The displacements are plotted against longitude by Plaskett and Pearce; see footnote 8. Measurements of interstellar sodium lines yield essentially similar results.

will have intensities, D_1 and D_2, and a ratio, D_2/D_1, which will depend upon the dimensions of the cloud and the density and temperature of the sodium within it. Now the light of a second star at about twice the distance of the first may be considered to pass through two clouds, whose radial velocities differ sufficiently to prevent blending of the two sets of lines.[19] Consequently, the interstellar lines in the spectrum of the second star will have about twice the intensity of those in the first, but the doublet ratio will be the same for both stars. As still more distant stars are observed, a point will be reached ultimately where overlapping of the individual cloud lines becomes prevalent, and from there on the intensities increase less rapidly, approximating the behavior of the flat portion of a normal curve of growth having a parameter P determined by the average velocity of the clouds.

The preceding example should help to clarify the following more general discussion. The cloud hypothesis makes four parameters available for adjustment. These are: n, the average number of ground-state sodium atoms per cubic centimeter within the clouds; b, the "temperature" parameter expressing the average kinetic motions of the atoms; P, the corresponding quantity expressing the spread of the cloud velocities; l_o, the average length of a line of sight within a cloud. The problem is to choose such values of these quantities that the line intensities computed from them most nearly agree in behavior with the observed values. In other words, the observational data shown by the plotted points in Figures 2 and 7 must be fitted as accurately as possible by computed curves, and the achievement of a satisfactory fit fixes the values of the parameters. The process is thus quite analogous to that already employed in this paper in the attempt to satisfy the observations by simple rotation theory, and is, essentially, a method of trial and error.

The authors are greatly indebted to Dr. R. Minkowski for suggesting and carrying out the computations necessary for a compari-

[19] It turns out in practice that a difference in wave-length of about 0.1 A, corresponding to a velocity difference between the clouds of about 5 km/sec, is sufficient to prevent serious overlapping of the lines. Such a small difference is, however, not enough to separate the lines with the relatively small dispersion used in this investigation, and consequently the interstellar lines appear single on our spectrograms.

son of the hypothesis with the observations. His solution, which was greatly facilitated by the use of tables published by Ladenburg and Levy,[20] is exhibited by the curves shown in Figures 2 and 7.

The first step is to reproduce that portion of the ratio-curve in which the doublet ratio decreases from 2 to 1.2, and this amounts to choosing values of b and of the average total number of atoms traversed by the line of sight in the cloud nearest the observer. In Figure 2, the solid curve between points A and B, which has been taken from a curve of growth with $b = 0.11$, is considered to be in satisfactory agreement with the observations. Turning now to Figure 7, we find that the same curve of growth gives the solid curve between A and B for the relationship between mean D intensity and distance. The point B is seen to lie at a distance of 720 parsecs. Hence, dividing the average total number of atoms in the line of sight in the first cloud by the number of centimeters in 720 parsecs yields the value of n.

After passing points B in the diagrams, the average line of sight is assumed to enter a second cloud having the same physical characteristics as the first one, but differing sufficiently from the latter in radial velocity to prevent overlapping of the two sets of absorption lines. Thus, adding the intensities of the second set of lines carries the two curves from points B to points C. Similarly, a third cloud takes the curves to points D, beyond which a scarcity of observations renders further calculation futile.

The argument as presented above corresponds to the idealized case where the clouds, all identical, are penetrated centrally one after the other by the line of sight. A little thought will show that, when the more likely case of only partial penetration of some of the clouds is considered, the theory demands a considerable scatter in diagrams like Figures 2 and 7. Suppose, for instance, that we are somewhere within a cloud and that in some direction we find its boundary at a distance of only 250 parsecs, corresponding to the point designated E in the figures. After passing this point, the second cloud is entered, and the variation of intensity with distance will follow the dashed curves from E to F. Similarly, gaps between the

[20] *Zs. f. Phys.*, **65**, 189, 1930.

clouds will produce scatter. If, for instance, there were a space of 200 parsecs between the first and second clouds, the curve should pass through the points $ABB'C'$ in Figure 7 rather than as drawn. Thus it is clear that the present hypothesis is not only capable of accounting for the scatter in such a diagram but, in fact, actually requires that scatter exist.

The numerical values of the parameters used for the calculation of the curves in the diagrams are of great interest. It has already been stated that b was taken equal to 0.11 A and that the average length of a line of sight through a cloud turned out to be 720 parsecs. The corresponding value of n is 2.9×10^{-9} atoms per cubic centimeter. The observations suffice to determine only an approximate lower limit to the value of P, the parameter which expresses the distribution of cloud velocities. A glance at Figure 7 shows the basis for this statement. The dashed curve in the figure labeled $P = 0.3$ is computed from a curve of growth with the parameter P equal to 0.3 A. Clearly, as the number of clouds in the line of sight increases, a point will be reached where overlapping of the individual cloud lines will become prevalent, and from there on the rate of growth of intensity with distance will be slower and will, in fact, approximate more and more closely to that computed from a curve of growth having the parameter P corresponding to the distribution of cloud velocities. The smaller the value of P, the smaller will be the distance at which this effect sets in. Evidently, from Figure 7, P cannot be taken as much less than 0.3 without giving a disagreement with the observations. The true value of P could be found only by observing stars at sufficiently great distances to fix the point at which the rate of growth of the lines with distance begins to deviate appreciably from that for the nearer stars.

There is, of course, some latitude in the values of constants determined by a method of the kind employed here, but it proves to be surprisingly small. In fact, it is found that n must lie between 2.9×10^{-9} and 3.6×10^{-9}, and b between 0.11 and 0.09 A in order not to spoil the fit with either of the observed curves. It will be recalled that simple rotation theory yielded the values $n = 2.0 \times 10^{-9}$ and $b = 0.11$ A, in remarkably close agreement with the present ones. The two values of b should agree closely, since they are de-

termined in essentially the same manner; and so we adopt $b = 0.11$ as the best value obtainable from our data. The values of n are easily reconciled since, in the rotation solution, it was assumed that $b = 0.11$ applied at all distances. It is now clear that for the more distant stars allowance should have been made for the distribution of cloud velocities. When two Maxwellian velocity distributions having the parameters b and P are combined, the resultant is a Maxwellian distribution with the parameter $\beta = \sqrt{b^2 + P^2}$. With $b = 0.11$ and $P = 0.3$, $\beta \sim 0.3$. If this value is used in place of 0.11 and n is set equal to 2.9×10^{-9}, a repetition of the rotational calculation yields the doublet ratio 1.22 for the more distant stars, in good agreement with the observations.

It remains now to discuss a few additional points concerning the combination of the rotational and cloud hypotheses. There are two distinct ways in which the clouds may conceivably participate in the general galactic rotation. The first case is that in which the whole cloud moves with the velocity of its center of gravity. In this event it is clear that toward a maximum, rotation would not play any role in producing the equivalent widths of the absorption lines, at least out as far as the extreme distances in Figure 7. Successive cloud lines would, of course, be gradually shifted in one direction, thus causing a displacement of the resultant line as a whole. A linear velocity gradient would not, however, tend to increase overlapping of the individual lines. On the contrary, it would, at sufficient distances, have the effect of retarding the onset of overlapping; and hence, toward the maxima, a linear relationship between intensity and distance should continue to hold at greater distances than in the null directions. Our observations do not extend to sufficiently distant stars to show this effect, if it exists. It would appear, then, that if the clouds move as units with the velocities of their centers of gravity, it was at least partly a fortuitous circumstance that caused the application of simple rotation theory to yield an approximately correct value of n.

The other possibility is that the rotational gradient is effective within the individual clouds. In this case the cloud lines are widened and caused to overlap, and our previous solution, with the appropriate value of β, would have physical significance. Of course, if

differential rotation takes place within the clouds, there is the logical difficulty of accounting for their continued existence; but as a purely observational matter, the present data do not seem capable of deciding between the two possibilities.

One important consequence of the correctness of the hypothesis advanced here would be that Eddington's explanation of the equality of the interstellar calcium and sodium lines could no longer be considered valid. The reason is that, to account for the doublet ratio for weak lines, we have found it necessary to make use of that portion of the curve of growth in which the intensity varies directly with the number of atoms. Hence, if the ionized calcium atoms were three hundred times as numerous as those of neutral sodium, the expectation would be that for near-by stars the H and K lines should be considerably stronger than the D lines. Conversely, since the observations indicate approximate equality, the conclusion is that the numbers of the two kinds of atoms are roughly the same.

To summarize briefly, we have found that the intensities and displacements of the interstellar sodium lines can be explained by the assumption that the sodium occurs in large clouds having average linear dimensions of the order of 700 parsecs. The clouds participate in galactic rotation and in addition have a velocity distribution of their own whose spread need not exceed a value of the order of 15 or 20 km/sec. The temperature of the gas within the clouds cannot be specified exactly since any small-scale turbulence will necessarily be included. An upper limit to the temperature is about 44,000°, corresponding to $b = 0.11$ A. The best value of the average number of neutral sodium atoms per cubic centimeter is of the order of 3×10^{-9}, corresponding to a density of about 10^{-31} gm/cc.

The outstanding task in the interpretation of interstellar sodium lines is to reconcile the low ratio of D_2 to D_1, 1.2 (except for very weak lines), with the nearly linear increase of intensity with length of light-path. The observed doublet ratio testifies that, if the number of atoms is doubled by matching each atom with a similar additional atom, the line intensity is increased by 20 per cent; on the other hand, if the number of atoms is doubled by extending the light-path twice as far into space, the line intensity is nearly doubled.

The properties of sodium gas cannot therefore be identical at all points in interstellar space. Motions corresponding to the standard concept of galactic rotation do not suffice to solve the enigma. The only reasonable solution which has occurred to us is that of discrete clouds of sodium vapor, although on account of the complexity of the problem we are scarcely disposed to argue that other possibilities are entirely precluded. Such discrete clouds perhaps form the gaseous counterpart to the well-known dust clouds of obscuring matter along the Milky Way. The origin and stability of these clouds may furnish interesting questions for discussion.

CARNEGIE INSTITUTION OF WASHINGTON
MOUNT WILSON OBSERVATORY
May 1937

PHYSICAL PROCESSES IN GASEOUS NEBULAE

II. THEORY OF THE BALMER DECREMENT

DONALD H. MENZEL AND JAMES G. BAKER

ABSTRACT

An exact algebraic solution of the equations given in the first paper of this series is carried out for the statistical equilibrium of an assembly of hydrogenic atoms. The exciting radiation is assumed to come only from beyond the limit of the Lyman series. Hence discrete states are filled only by capture from the continuum and by cascade from higher discrete states. The electrons are assumed to have a Maxwellian velocity distribution. The formula is given in terms of a quantity b_n, the ratio between the actual population of state n and the population under conditions of thermodynamic equilibrium. An asymptotic expression is given for b_n in the case of large quantum number, from which it is shown that b_n approaches unity as n becomes infinite. Numerical solutions are deferred until the next paper.

The problem of the theoretical decrement of the Balmer series has been attacked by several investigators, notably Plaskett,[1] Carroll,[2] and Cillié.[3] General equations for the statistical equilibrium of an assembly not in thermodynamic equilibrium were first given by Rosseland.[4] For each atomic state one writes down the condition that the number of transitions from that state, by all possible processes, is equal to the number of transitions to that state, per unit time. Equilibrium is thus insured. Atoms possess, however, an infinite number of states, and an accurate solution of the problem requires the treatment of an infinite number of simultaneous linear equations.

To simplify the problem, Plaskett and Carroll have assumed that the atom possesses but seven discrete levels, the eighth denoting ionization. The effect of the remaining levels was entirely neglected. For the atomic emission probabilities they used the values of the Einstein A's as given by Slack[5] and of the capture probabilities as given by Gaunt.[6] Cillié[7] has recently employed the more extensive data on the emission probabilities, as given by Menzel and Pekeris,[8] to extend his original calculations to fourteen states.

[1] *Harvard Circ.*, No. 335, 1928.
[2] *M.N.*, **90**, 588, 1930.
[3] *Ibid.*, **92**, 820, 1932.
[4] *Ap. J.*, **63**, 218, 1926.
[5] *Phys. Rev.*, **31**, 527, 1928.
[6] *Phil. Trans.*, A, **229**, 163, 1930.
[7] *M.N.*, **96**, 771, 1936.
[8] *M.N.*, **96**, 77, 1935.

One further simplifying assumption, justified to some extent by physical reasoning, is made. In the problem of the planetary nebula the argument is that the Lyman line radiation from the nuclear star is so depleted by the star's atmosphere and the lower nebular layers that the only radiation available for atomic excitation lies beyond the limit of the Lyman series.

For the present we shall accept the conditions of the preceding paragraph. It is instructive to carry out the accurate solution of the equations in this particular case. The general procedure followed by the earlier investigators is, however, open to question. The numerical solutions are none too satisfactory, because of the approximations involved. One has the feeling that more attention should be paid to the neglected transitions. Continuity of the energy levels through the higher terms and on into the continuum is an essential feature of every atom. Furthermore, the use of the exact values of the Einstein A's is incompatible with the use of the Kramer-Gaunt approximation to the emission in the continuum, since such procedure involves a discontinuity at the series limit. A further and serious objection is that this method gives no information about the intensities of high series members.

The exact equations for the statistical equilibrium have been given in the first paper[9] of this series, hereinafter referred to as "I." An atom in quantum state n may make spontaneous transitions to lower discrete states n', or, under the influence of radiation, to either higher discrete states n'' or higher continuous states κ. Let $F_{nn'}$ denote the number of transitions n to n' per unit volume per second. Then the condition of equilibrium (I, equation 31) requires that

$$\left.\begin{aligned}\sum_{n''=n+1}^{\infty} F_{n''n} + \int_{\nu_n}^{\infty} F_{\kappa n}\,d\nu + \sum_{n'=1}^{n-1} F_{n'n} = \sum_{n''=n+1}^{\infty} F_{nn''} \\ + \int_{\nu_n}^{\infty} F_{n\kappa}\,d\nu + \sum_{n'=1}^{n-1} F_{nn'}\,.\end{aligned}\right\} \quad (1)$$

Under the assumed conditions, there is no radiational excitation from any quantum state but the first; and, since the effect of Lyman

[9] Menzel, *Ap. J.*, **85**, 330, 1937.

line radiation is neglected, the only excitation of the 1-quantum atoms is to the continuum. Hence, for each state other than the first we have an equation of the form

$$\sum_{n''=n+1}^{\infty} F_{n''n} + \int_{\nu_n}^{\infty} F_{\kappa n} d\nu = \sum_{n'=1}^{n-1} F_{nn'} . \tag{2}$$

Substituting from I, equations (10) and (25), we find that

$$N_i N_e \frac{KZ^4}{T_e^{3/2}} \left\{ \sum_{n''=n+1}^{\infty} b_{n''} e^{X_{n''}} g_{n''n} u_{n''n} + \bar{g} S_n - b_n e^{X_n} t_n \right\} = 0 , \tag{3}$$

where

$$u_{n''n} = \frac{2n^2}{n''(n''^2 - n^2)} ,$$

$$S_n = e^{X_n}[-E_i(-X_n)] ,$$

$$t_n = \sum_{1}^{n-1} - u_{n'n} ,$$

$$X_n = \frac{hRZ^2}{n^2 kT_e} = \frac{1.5703 \times 10^5}{n^2 T_e} ,$$

for hydrogen.

In the foregoing equations N_i and N_e are, respectively, the number of ions and electrons per unit volume; T_e is the electron temperature; g, the Kramer-Gaunt factor for the transition in question; and b_n, a factor that denotes the departure of the assembly from thermodynamic equilibrium at temperature T_e. It is defined by the relation (I, 4)

$$N_n = b_n N_i N_e \frac{h^3}{(2\pi mkT_e)^{3/2}} n^2 e^{X_n} . \tag{4}$$

For thermodynamic equilibrium, $b_n = 1$.

$$K = \frac{h^3}{(2\pi mk)^{3/2}} \frac{8\pi^2 e^2 R^2}{mc^3} \frac{2^4}{3\sqrt{3\pi}} . \tag{5}$$

To duplicate Cillié's solution we have merely to substitute the accurate g values for the first fourteen equations, cut off all the summations at $n''=14$, set $\bar{g}$ (the averaged g for the bound-free transitions) equal to unity, and, neglecting all higher equations, solve simultaneously for the various b_n's. We prefer to start from the opposite end and obtain the b_n's for the higher levels first.

A consistent procedure is to set, as a first approximation, g equal to unity throughout. The second of the two summations is easily evaluated for large values of n:

$$\left.\begin{aligned} l_n &= \sum_{n'=1}^{n-1} \frac{2n^2}{n'(n^2-n'^2)} = \sum_{n'=1}^{n-1} \left(\frac{2}{n'} + \frac{1}{n-n'} - \frac{1}{n+n'}\right) \\ &= 3\sum_{n'=1}^{n-1} \frac{1}{n'} - \sum_{n'=1}^{n-1} \frac{1}{n+n'} \end{aligned}\right\} \tag{6}$$

$$= \left[3ln\, n + 3\gamma - ln\, 2 - \frac{3}{4n} - \frac{5}{16n^2} - \ldots.\right] \tag{7}$$

$$\sim 3ln\, n + 1.04\,. \tag{8}$$

For n as small as 10 the bracket in (7) is correct to five significant figures. In deriving these formulae we have noted the identity

$$\sum_{1}^{n-1} \frac{1}{n'} = \sum_{1}^{n-1} \frac{1}{n-n'} \tag{9}$$

and also the well-known expression for the sum to a terms of the harmonic series

$$\sum_{1}^{a} \frac{1}{a} = ln\, a + \gamma + \frac{1}{2a} - \frac{1}{12a^2} + \ldots., \tag{10}$$

where γ is Euler's constant, 0.577..... Various functional expansions of an obvious nature have also been used.

For the middle term of equation (3), certain relationships may be derived.

For all values of X_n different from zero,

$$S_n = e^{X_n}[-E_i(-X_n)] = e^{X_n}\left[-\gamma - lnX_n + \frac{X_n}{1\cdot 1!} - \frac{X_n^2}{2\cdot 2!} + \frac{X_n^3}{3\cdot 3!} - \ldots.\right]. \quad (11)$$

For $X_n >> 1$, it is convenient to employ the following asymptotic expansion:

$$S_n = e^{X_n}[-E_i(-X_n)] = \frac{1}{X_n}\left[1 - \frac{1!}{X_n} + \frac{2!}{X_n^2} - \ldots.\right]. \quad (12)$$

Equation (12) is needed only for the lowest quantum states.

Thus, the only troublesome term in equation (3) is the first. The difficulty arises from the occurrence of the factor $b_{n''}$ under the summation sign. Before proceeding to the exact solution of the equation, we shall employ an approximation, which indicates clearly the physical nature of b_n. From the character of the summation we note that the principal contribution to its value comes from n'' terms bordering on n. If, therefore, $b_{n''}$ is a slowly changing function of n'', we may remove it from the summation sign in order to obtain the first approximation.

The first term may be written as follows:

$$b_n \sum_{n''=n+1}^{\infty} \frac{2e^{X_{n''}}}{\left(\frac{1}{n^2} - \frac{1}{n''^2}\right)n''^3} \sim b_n \int_{n+1}^{\infty} \frac{e^{X_{n''}}}{\left(\frac{1}{n^2} - \frac{1}{n''^2}\right)} \frac{2dn''}{n''^3}, \quad (13)$$

since, when n'' is large, we may approximate the sum by an integral. If we change variables by

$$\left.\begin{aligned} \frac{hRZ^2}{kT}\left(\frac{1}{n^2} - \frac{1}{n''^2}\right) &= X_n - X_{n''} = y, \\ \frac{2hRZ^2}{kT}\frac{dn''}{n''^3} &= dy, \end{aligned}\right\} \quad (14)$$

the summation becomes, by equation (11),

$$\left.\begin{aligned} &= b_n e^{X_n} \int_{X_n - X_{n+1}}^{X_n} \frac{e^{-y}}{y}\, dy = b_n e^{X_n}[-E_i(-X_n + X_{n+1}) + E_i(-X_n)] \\ &\sim b_n e^{X_n}\left[ln\ n - ln\ 2 - X_n + \frac{3}{2n} - \frac{7}{8n^2} \ldots .\right]. \end{aligned}\right\} \quad (15)$$

When the limiting formulae (8), (11), and (15) are substituted back into equation (3) and the common factors are canceled, we may solve for b_n and find

$$b_n \sim \frac{2\ ln\ n - \gamma - lnX_1 + X_n + \ldots .}{2\ ln\ n + 3\gamma - \frac{9}{4n} + \frac{9}{16n^2} + X_n - \ldots .} . \quad (16)$$

As $n \to \infty$, $b_n \to 1$. This limiting value of unity is in accord with our physical intuition, which leads us to expect a continuity between states of negative and positive energy near the ionization limit of the atom.[10] Since our calculations are based on the assumption that the electrons possess a Maxwellian velocity distribution, the value of b, appropriate to the continuum where thermodynamic equilibrium obtains, is unity. The approximate value of (16) can be employed, however, only for the uppermost states.

Equation (3) may be written as an infinite set of simultaneous equations involving an infinite number of unknowns. One may write down symbolically the infinite determinants for the general case and expand by minors. Since equation (3) does not contain n' directly, the solution for any b_n is of precisely the same form. Accordingly, the equations as written for the solution of b_n begin with the nth equation and not with $n = 2$, although the answer is the same. This fact simplifies the solution considerably. The determinant of the coefficients of the unknowns has the value $\prod_n^\infty t_i$. Since $t_i > 1$, this expression is, of course, infinite in value. The determinants in the numerator, however, contain the same minors from some point on, and hence, the ratios reduce to infinite series.

[10] The limiting form of b_n was given by Menzel and Cillié, *Ap. J.*, **85**, 88, 1937.

An expansion of the terms and a recombination of the cyclical subscripts reduce to the exact solution

$$b_n = \frac{S_n + V_n}{e^{X_n} t_n}, \tag{17}$$

where

$$\left.\begin{aligned} V_n = \sum_{n+1}^{\infty} \frac{S_i u_{in}}{t_i} + \sum_{n+1}^{\infty} \sum_{j+1}^{\infty} \frac{S_i u_{ij} u_{jn}}{t_i t_j} \\ + \sum_{n+1}^{\infty} \sum_{\kappa+1}^{\infty} \sum_{j+1}^{\infty} \frac{S_i u_{ij} u_{j\kappa} u_{\kappa n}}{t_i t_j t_\kappa} + \cdots\cdots \end{aligned}\right\} \tag{18}$$

It is evident that these summations converge individually, for

$$\frac{S_i}{t_i} \to \tfrac{2}{3} \qquad \text{as} \qquad i \to \infty$$

and

$$\sum_{n+1}^{\infty} \frac{S_i}{t_i} u_{in} < \tfrac{2}{3} \sum_{n+1}^{\infty} u_{in} < \tfrac{2}{3} \ln n .$$

Indeed, since

$$b_n \underset{n\to\infty}{\to} 1 , \qquad V_n \underset{n\to\infty}{\to} \ln n + \text{const.}$$

An examination of equation (3) shows that formula (17) may be derived directly by the method of successive approximations. This procedure is by far the shortest. The fact that these two entirely different methods yield precisely the same formula for b_n is interesting in itself. What is so obvious here, however, will not be so at all for the more complicated solutions to come. Accordingly, we have employed the determinant method to indicate how the future refinements will go.

We are now enabled to determine precisely the numerical values of b_n. The solution (17) is of the final form for the nebular problem, since, upon introducing the Gaunt factor and collision and radiation terms from I, we need only to redefine the functions given above.

The next paper will contain useful tables of the important functions of the preceding equations and, in particular, will contain a tabulation of the values of b_n over a wide range of temperature and of quantum number, on the basis of the straight capture spectrum of hydrogenic atoms. A comparison with observations and results of other investigators will also be included.

HARVARD COLLEGE OBSERVATORY
May 14, 1937

THE OPACITY IN THE INTERIOR OF A STAR

S. CHANDRASEKHAR

ABSTRACT

In this paper two integral theorems on the radiative equilibrium of a gaseous star are proved.

I

In two recent papers[1] the author has proved some general theorems on the equilibrium of a star. These theorems are of some importance in the theory of stellar structures, in so far as they provide inequalities for the physical variables, e.g., central pressure, mean pressure, central radiation pressure $(1 - \beta_c)$, etc., which should be valid under very general circumstances. The method consists in obtaining inequalities for the physical variables which are direct consequences of the equation of hydrostatic equilibrium:

$$\frac{dP}{dr} = -\frac{GM(r)}{r^2}\rho\,. \tag{1}$$

In obtaining inequalities based on equation (1), one generally restricts one's self to such equilibrium configurations as are characterized by the mean density $\bar{\rho}(r)$, inside r decreasing outward. Further, in obtaining inequalities for the mean temperature a further restriction, namely, that $(1 - \beta)$ decreases outward, is introduced (cf. II, Theorem 7).

In this paper we shall obtain certain inequalities for equilibrium configurations in *radiative equilibrium*. We shall then have an additional differential equation for the radiation pressure $p_r(= \frac{1}{3}aT^4)$, namely,

$$\frac{dp_r}{dr} = -\frac{\kappa L(r)}{4\pi cr^2}\rho\,, \tag{2}$$

where κ is the opacity coefficient, c is the velocity of light, and $L(r)$ is the amount of energy crossing the spherical surface of radius r.

The numbering of the theorems is continued from II, and references to the equations of that paper are inclosed in square brackets.

[1] *M.N.*, **96**, 644, 1935; *Ap. J.*, **85**, 372, 1937. These papers will be referred to as "I" and "II," respectively.

II

In the following, L, M, and R refer to the luminosity, the mass, and the radius of a star; and the auxiliary variable η is defined by

$$\eta = \frac{L(r)}{M(r)} \Big/ \frac{L}{M} . \tag{3}$$

THEOREM 8.—*In a wholly gaseous configuration in radiative equilibrium, in which the mean density* $\bar{\rho}(r)$ *inside* r *decreases outward, we have*

$$L \leqslant \frac{4\pi cGM(1 - \beta^*)}{\overline{\kappa\eta}} , \tag{4}$$

where $(1 - \beta^*)$ *has the same meaning as in Theorem 2 and* $\overline{\kappa\eta}$ *is defined by*

$$P_c \overline{\kappa\eta} = \int_R^0 \kappa\eta dP . \tag{5}$$

Part of the analysis leading up to this theorem is originally due to B. Strömgren.[2]

Proof: The equation of radiative equilibrium (2) can be written as

$$dp_r = -\frac{\kappa}{4\pi^2 c} \frac{L(r)dM(r)}{r^4} . \tag{6}$$

Since

$$dP = -\frac{G}{4\pi} \frac{M(r)dM(r)}{r^4} , \tag{7}$$

we have, using equation (3), that

$$dp_r = \frac{L}{4\pi cGM} \kappa\eta dP . \tag{8}$$

Integrating equation (8) and using the boundary condition that $p_r = 0$ at $r = R$, we have

$$p_r = \frac{L}{4\pi cGM} \int_R^r \kappa\eta dP . \tag{9}$$

[2] *Handbuch der Astrophysik*, **8**, 159, 1936.

The foregoing equation has been given before by Strömgren. From equation (9) we can easily show that *if* $\kappa\eta$ *decreases outward,* $(1 - \beta)$ *would also decrease outward.* Extending the integral from 0 to R and using the definition (5) for the average value for $\kappa\eta$, we clearly have that

$$1 - \beta_c = \frac{L}{4\pi cGM}\,\overline{\kappa\eta}\,, \tag{10}$$

or

$$L = \frac{4\pi cGM(1 - \beta_c)}{\overline{\kappa\eta}}\,. \tag{11}$$

Since we have assumed that the mean density decreases outward, we can apply Theorem 2, which states that

$$1 - \beta_c \leq 1 - \beta^*\,, \tag{12}$$

where β^* satisfies a certain quartic equation (equation [3]) and is determined by the mass M, uniquely. Combining equations (11) and (12), we have

$$L \leqslant \frac{4\pi cGM(1 - \beta^*)}{\overline{\kappa\eta}}\,, \tag{13}$$

which proves the theorem.

III

THEOREM 9.—*In a wholly gaseous configuration in which the mean density* $\bar{\rho}(r)$ *inside* r *and the rate of generation of energy* ϵ *decrease outward, we have*

$$\bar{\kappa} \leqslant \frac{4\pi cGM(1 - \beta^*)}{L}\,, \tag{14}$$

where $\bar{\kappa}$ *is the mean opacity coefficient defined by*

$$P_c\bar{\kappa} = \int_R^0 \kappa dP\,, \tag{15}$$

and the equality sign in equation (14) is possible only when ϵ *is constant.*

Proof: This is an immediate consequence of Theorem 8. For, if ϵ decreases outward, η must also decrease outward, and consequently the *minimum* value of η is unity. Hence

$$\overline{\kappa\eta} \geqslant \bar{\kappa}\,, \tag{16}$$

the equality sign in equation (16) being possible only when $\eta =$ constant $= 1$, i.e., when ϵ is constant. By Theorem 8

$$\overline{\kappa\eta} \leqslant \frac{4\pi cGM(1-\beta^*)}{L}\,. \tag{17}$$

Combining equations (16) and (17), we have the required result.

IV

We will apply equation (14) to certain practical cases of interest. Numerically, equation (14) reduces to

$$\bar{\kappa} \leqslant 1.318 \times 10^4 \frac{M}{\odot} \cdot \frac{L_\odot}{L}(1-\beta^*)\,, \tag{18}$$

where $L_\odot$ refers to the luminosity of the sun.

For Capella we have $M = 4.18\odot$ and $L = 126\ L_\odot$. Assuming $\mu = 1$, the solution of the quartic equation for β^* yields $1 - \beta^* = 0.22$. Hence

$$\bar{\kappa}_{\text{Capella}} < 96.1\ gm^{-1}\ cm^2\,. \tag{19}$$

In the same way for the sun, we find ($\mu = 1$, $1 - \beta^* = 0.03$)

$$\bar{\kappa}_\odot < 395\ gm^{-1}\ cm^2\,. \tag{20}$$

V

There is one interesting application of equation (14) to stellar models in which the opacity coefficient κ is assumed to be constant. For equation (14) can then be written as

$$L \leqslant L^* = \frac{4\pi cGM(1-\beta^*)}{\kappa}\,. \tag{21}$$

Equation (21) has to be interpreted in the following sense: If $L > L^*$, then the configuration *must* be characterized by the oc-

currence of negative density gradients (i.e., $\bar{\rho}(r)$ increases outward in some finite regions of the interior), no matter what the law of energy generation is, provided only the rate of generation of energy ϵ decreases outward. On the other hand, if $L < L^*$, it does not *necessarily* follow that the configuration is characterized by positive density gradients throughout its interior. But if $L < L^*$ we can always find a "mild"-enough law for the rate of generation of energy such that the configuration is characterized by a positive density gradient throughout its interior. Further, it should be noticed that if

$$L > L_1 = \frac{4\pi cGM}{\kappa}, \tag{22}$$

then no equilibrium configuration is possible.[3] The inequality (22) is interpreted by the statement that if $L > L_1$ then the configuration would "blow up." We now see that this tendency to "blow up" must set in at lower values for the luminosity, in the event of negative density gradients in its interior. Negative density gradients must certainly exist for configurations with $L > L^*$. Depending on the concentration of the energy sources toward the center, the negative density gradients will set in for some $L < L^*$.

VI

Corollary to Theorem 9.—If, in addition to the conditions of Theorem 9, κ is assumed to increase outward, then

$$\kappa_c \leqslant \frac{4\pi cGM(1 - \beta^*)}{L}, \tag{23}$$

where κ_c is the opacity at the center. This is, of course, obvious.

If we assume any definite law for opacity, then equation (23) can be converted into an inequality for the central temperature, for a star of known mass and luminosity. Thus, if we assumed that

$$\kappa = \kappa_1 \frac{\rho}{T^{3+S}}, \qquad (S > 0), \tag{24}$$

[3] E. A. Milne, *M.N.*, **91**, 4, 1930. See esp. pp. 12, 13, and 53 of this paper.

then κ would *increase* outward if $(1 - \beta)$, and T would *decrease* outward; for we can write equation (24) as

$$\kappa = \kappa_1 \frac{\mu H}{k} \frac{a}{3} \frac{\beta}{1 - \beta} T^{-s}. \tag{25}$$

Hence, by Theorem 2,

$$\kappa_c \geqslant \kappa_1 \frac{\mu H}{k} \frac{a}{3} \frac{\beta^*}{1 - \beta^*} T_c^{-s}. \tag{26}$$

Combining this with (23), we have

$$T_c^s \geqslant \frac{L\kappa_1}{4\pi cGM} \frac{\mu H}{k} \frac{a}{3} \frac{\beta^*}{(1 - \beta^*)^2}. \tag{27}$$

The foregoing inequality giving the minimum central temperature for a star of known M and L is generally not as good as the minimum central temperature set by Theorem 7 for a star of known M and R.

APPENDIX

We have seen that $(1 - \beta^*)$, giving the maximum possible $(1 - \beta_c)$ in a wholly gaseous configuration in which the mean density $\bar{\rho}(r)$, inside r, is assumed to decrease outward, plays an important role in Theorems 7, 8, and 9. It is therefore convenient to have a table giving M for different values of $(1 - \beta^*)$. Table I should be sufficient for most purposes.

TABLE 1

SOLUTIONS OF THE EQUATION

$$M = \left(\frac{6}{\pi}\right)^{1/2} \left[\left(\frac{k}{\mu H}\right)^4 \frac{3}{a} \frac{1 - \beta^*}{\beta^{*4}}\right]^{1/2} \frac{1}{G^{3/2}}$$

$1-\beta^*$	$\left(\frac{M}{\odot}\right)\mu^2$	$1-\beta^*$	$\left(\frac{M}{\odot}\right)\mu^2$
0.025	0.908	0.5	15.432
.05	1.352	0.6	26.41
.1	2.130	0.7	50.72
.2	3.812	0.8	122.0
.3	6.099	0.9	517.6
0.4	9.585	1.0	.....

YERKES OBSERVATORY
June 8, 1937

THE ANNUAL VARIATION IN THE INTENSITY OF THE ZODIACAL LIGHT*

C. T. ELVEY

ABSTRACT

The series of visual observations of the zodiacal light made by the Japanese observers has been reduced to a uniform system of intensities with the aid of photoelectric observations of the standard comparison areas in the Milky Way. Corrections were applied for differences in the zenith distance of the zodiacal light and the comparison field.

Annual variations are shown to exist for both the evening and the morning zodiacal lights. The maximum for the evening light is near the middle of January, and that for the morning light is near the end of the preceding October.

The suggestion is made that the enhancement of the zodiacal light at certain seasons of the year may be due to scattering by meteoric material associated with cometary orbits.

In a recent survey of the light from the night sky with a recording photoelectric photometer, Elvey and Roach[1] obtained the intensities of the zodiacal light over the sky. The observations were grouped roughly in accordance with the seasons, and it was shown that there is a seasonal variation in the intensity of the zodiacal light during the period covered by the observations, namely, November, 1934, to July, 1935. The maximum of intensity of the morning and evening zodiacal light occurred, in general, at the times of the best visibility of these phenomena. To account for the displacement of the maximum of the morning light with respect to that of the evening light it was suggested that there may be a condensation in the scattering medium, which is in conjunction with the sun in the late winter.

Since the above-mentioned photometric observations are somewhat limited in number and time, they are probably affected by variations in the intensity of the zodiacal light which are irregular in character and which may or may not be due to differences in the transparency of the atmosphere. For this reason it seems advisable to investigate the large mass of visual observations for possible seasonal variations, even though they do not have the accuracy of photometric data. An excellent series of observations were obtained by the Zodiacal Light Section of the Society of Astronomical Friends

* *Contributions from the McDonald Observatory, University of Texas*, No. 4.

[1] *Ap. J.*, **85**, 213, 1937.

of Kyoto, Japan, which later became the Oriental Astronomical Society. These observers, numbering as many as twenty or more, have been making systematic observations of the position and outline of the zodiacal light as well as of its color and brightness and of such other miscellaneous observations as pulsations in brightness and variations in outline.

We are concerned only with the estimates of the brightness of the zodiacal light, which we have compared with selected regions of the Milky Way. The Japanese reports do not give details of the positions of the zodiacal light observed and that of the comparison field; however, approximate values can be obtained from the statement that the maximum of the zodiacal light was observed. Japanese Central Standard Time is given for each observation. From these data we see that the observations have been taken over a considerable range in relative zenith distance between the zodiacal light and the comparison field, which in many cases gives systematic effects. For example, a given comparison field, such as that in Lacerta and Cepheus, was used over a period of two or three months in succession. The zodiacal light remains at nearly the same zenith distance throughout the series, but the comparison field changes month by month, thus introducing into the observations an effect which may be seasonal.

Before discussing further the calibration of the observations or the corrections to be applied, we should look, perhaps, at the quantities which are measured by the eye. The eye measures the intensity of an object relative to the intensity of the background. In the case of the comparison fields this is the integrated light of the faint stars of the Milky Way, plus the scattered light, plus the galactic light, while the background illumination consists of the faint stars, the auroral light, and the general amount of zodiacal light over that region, as well as the scattered light from all these sources. The light which originates outside the atmosphere will be affected by extinction, which is a function of the secant of the zenith distance up to values of about 70°, when some other function of the zenith distance must be used, such as that derived by Bemporad.[2] The light originating in the earth's atmosphere increases in intensity with zenith

[2] *Handbuch d. Astrophysik*, **2**, 184, 1929.

distance, except for very large values, when the extinction becomes powerful enough to cause a reversal and, consequently, a maximum of intensity at about 80° zenith distance. Since the comparison field, located in the Milky Way, is outside the atmosphere and consequently decreases in intensity with zenith distance by extinction, while the background is composed mainly of light originating in the atmosphere which increases with zenith distance, it is readily seen that extinction and variation of the background combine to cause a decrease in the contrast between the Milky Way field and the background.

In the case of the zodiacal light the observations are made at the point of maximum intensity. This point, except in rather adverse

TABLE 1

Comparison Field	Intensity in Numbers of Stars of the Tenth Magnitude per Square Degree
Auriga	100
Cygnus	300
Lacerta-Cepheus	300
Monoceros	200
Ophiuchus	200

weather conditions, should be near the same zenith distance, on the average. The position is dependent upon the extinction and background illumination; and since we do not have data as to the altitude at which the zodiacal light was observed, I have estimated it as 20° (zenith distance 70°).

In order to convert the estimates of the intensity of the zodiacal light into true intensities, it is necessary to know the intensities of the comparison fields. These should be determined with a visual photometer; but since such measures are not available to me, I have used measures made with a photoelectric photometer. For a study of a variation in the zodiacal light the use of photoelectric intensities is satisfactory, unless there are differences in color between the various comparison fields. The intensities of the comparison fields are the averages over the Milky Way in the designated positions and are listed in Table 1 to the nearest 25 units.

All estimates of the intensity of the zodiacal light for the years 1928–1935, inclusive, published in the Kyoto *Bulletins*,[3] were reduced to intensities by means of the foregoing calibrations. It was soon evident that there were curious discrepancies within the observations over a short period of time—say during one month. These are related to the comparison field employed by the observer. In cases of large differences it was found that one comparison field was usually at the same zenith distance as the zodiacal light, while the other was at a small zenith distance, thus indicating that extinction and background illumination had an important effect on the observations.

It is necessary to know the amount of the sky background at each point of observation and also the value of the extinction, in order to reduce the observations to a uniform system of intensities. In the absence of such data for the place of observation, we can only try to estimate a reasonable value for the two quantities from our experiences at other places. The series of photoelectric observations made by Elvey and Roach[1] was used for this purpose, and it was found that the average extinction was 0.25 mag. at the zenith. This is for the blue end of the spectrum. Of course, the extinction would be smaller in the visual region. On the other hand, our observations were made at an elevation of about 2000 meters, and the Japanese observations of the zodiacal light were made close to sea-level, hence the extinction would have to be increased. The foregoing value of 0.25 mag. has been assumed for the extinction to be used in correcting the zodiacal light observations. This is quite close to the extinction constant, 0.23 mag., used in the mean extinction tables for visual light at Potsdam,[4] at 100 meters elevation, and to the value of 0.195 mag. in Bemporad's[2] extinction table for sea-level. A table of differential extinction corrections can be readily computed, either in magnitudes or as a factor, to correct the observed intensities. The differential extinction corrections are listed in columns 2 and 3 of Table 2.

A correction for the variation in the background intensity with

[3] *Bull. Kwasan Obs.*, Nos. 142, 164, 166, 168, 179, 190, 208, 212, 252, 255, 273, 275, 299, 325 (1928–36).

[4] *Handbuch d. Astrophysik*, **2**, 264, 1929.

zenith distance was taken also from the observations with the photoelectric photometer. The average intensity of the auroral light plus

TABLE 2

Zenith Distance	Correction for Extinction		Correction for Auroral Light Plus Scattered Light for Area in Auriga		Total Correction (Factor)
	Mag.	Factor	Mag.	Factor	
0°	+0.47	1.54	+0.22	1.22	1.89
10	+ .47	1.54	+ .20	1.20	1.85
20	+ .45	1.51	+ .17	1.17	1.77
25	+ .44	1.50	+ .16	1.16	1.74
30	+ .43	1.49	+ .15	1.15	1.71
35	+ .42	1.47	+ .13	1.13	1.66
40	+ .40	1.45	+ .11	1.11	1.60
45	+ .37	1.41	+ .08	1.08	1.51
50	+ .33	1.36	+ .07	1.06	1.45
55	+ .28	1.30	+ .05	1.05	1.36
60	+ .22	1.22	+ .03	1.03	1.26
65	+ .13	1.13	+ .02	1.02	1.15
70	.00	1.00	.00	1.00	1.00
75	− .24	0.80	− .03	0.97	0.78
80°	−0.68	0.53	+0.03	1.03	0.55

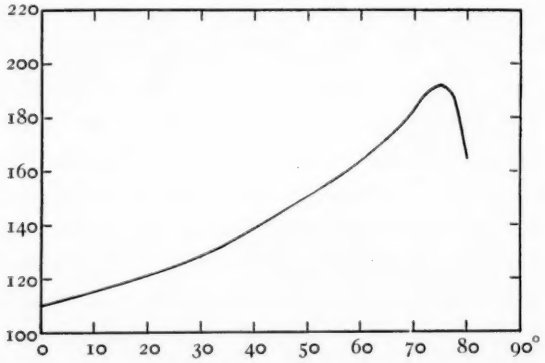

Fig. 1.—The average variation of auroral light plus scattered light, with zenith distance.

scattered light, as observed at the McDonald Observatory, was used, and its variation with zenith distance is shown in Figure 1. The intensities are expressed in numbers of tenth-magnitude stars per

square degree. Since this observed curve would have to be corrected to apply to visual light at sea-level, and since we do not know the amount of the correction, these data have been assumed. Some of the changes for the variation in elevation would result in an increase of the intensities, while others would decrease them, thus justifying the use of the foregoing data as they stand.

By assuming the curve in Figure 1 as representing the variation of the sky background with zenith distance, we can compute the apparent variation in intensity of a constant amount of illumination superimposed on the sky background. For purposes of illustration an intensity of 100 has been added to the background, and the amount by which it is brighter than the background has been computed in magnitudes. This was converted into the factor for correcting the observed intensities, and these data are tabulated in columns 4 and 5 of Table 2. The total correcting factor is given in column 6, this being the correction for the comparison field in Auriga.

It is seen that these correcting factors are large. It is, therefore, important that observations be made of points in the zodiacal light whose zenith distances are the same as those of the comparison field in the Milky Way. If the visual observers will take such precautions, this will add very materially to the value of their estimates of the intensity of the zodiacal light.

The observations of the zodiacal light were not corrected individually for the differences in zenith distance but were first averaged for a given month. The average zenith distance of the comparison field[5] for the month was readily obtained, and the correction was then applied to the mean intensity for the month. The accuracy of the method and of the visual estimates hardly warrants the greater amount of work required in reducing each observation separately.

The results are shown in Figure 2 in the form of curves. There were no obvious periodic variations in the observations, other than the annual variation; hence the data were arranged into annual curves for the evening and the morning zodiacal light. The total number of observations for each month is indicated by the size of the plotted point. The observations are plotted for the middle of the

[5] Usually only one comparison field was used over a period of one month. Otherwise it is necessary to make corrections for each comparison field of a different intensity.

month. A continuous heavy curve has been drawn for all the means containing twenty-five or more observations. During the summer, when the ecliptic is low in the southern sky, there are very few observations and the means have low weight.

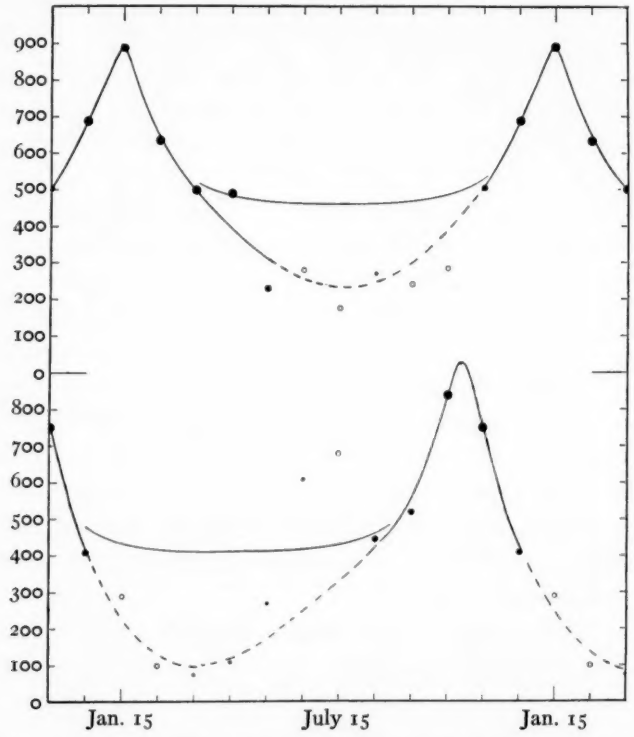

FIG. 2.—The annual variation of the zodiacal light. The upper curve is for the evening observations, and the lower for the morning observations. The size of each dot represents the number of observations forming the mean, the large dots being for more than one hundred observations and the small circles for less than five.

In both the evening and the morning zodiacal light there is a rather sharp maximum, the one for the evening light falling very near the middle of January and the one for the morning light near the end of the preceding October. There is a broad minimum extending through the season when it is difficult to observe the zodiacal light, namely, from May to October for the evening light, and from January to June for the morning light.

The time of maximum intensity of the morning zodiacal light agrees satisfactorily with that found by Elvey and Roach from their photoelectric observations. The maximum intensity of the evening zodiacal light does not agree: the photoelectric observations placed it in April, instead of in January. It is probable that because of the small number of photoelectric observations the true seasonal variation was masked by rather large irregular variations in the intensity of the zodiacal light.

No mention has been made of a correction for a variation in the elongation of the observed point in the zodiacal light through the year. When the observations are made with the ecliptic in its most favorable position, the point is much closer to the sun than in its less favorable positions. We can obtain an estimate of the difference in longitude of the point observed and the sun by taking the average of the times of the observations and the assumed zenith distance of the observed point. For the observations in the more favorable position of the ecliptic the differential longitude is between 40° and 45°. For the summer observations, or the times when the ecliptic is inclined toward the horizon, the differential longitude is estimated at about 70°. By referring to the isophotes of the zodiacal light determined by Elvey and Roach,[1] it is estimated that a factor of 2 or 2.5 must be applied to the observations of the zodiacal light made during the unfavorable season in order to reduce them to the same units as the observations taken when the ecliptic is nearly perpendicular to the horizon. In Figure 2 the probable intensity of the zodiacal light is indicated by the faint continuous line.

Attention should be called to one discordant point in the morning zodiacal light. The observations for July indicate a large value for the intensity of the zodiacal light during that month. The plotted point is an average of the observations for only two years; in addition, all of the observations for one year were taken under bad observing conditions. The observations for the other year, however, are apparently good. It will be rather difficult to decide from observations taken only at latitudes greater than 30° north whether the foregoing discordant point is real. We do not have available photometric observations of the zodiacal light taken from the southern hemisphere, but there are some sketches of the zodiacal cones made

by R. B. Bousfield[6] at Stanthorpe, Australia, which indicate that during July the morning zodiacal light reaches large intensities.

The observations of the intensity of the zodiacal light, after due consideration has been given to the accuracy of the observations and to the corrections which had to be applied to reduce the intensities to a homogeneous system, indicate rather definitely that the

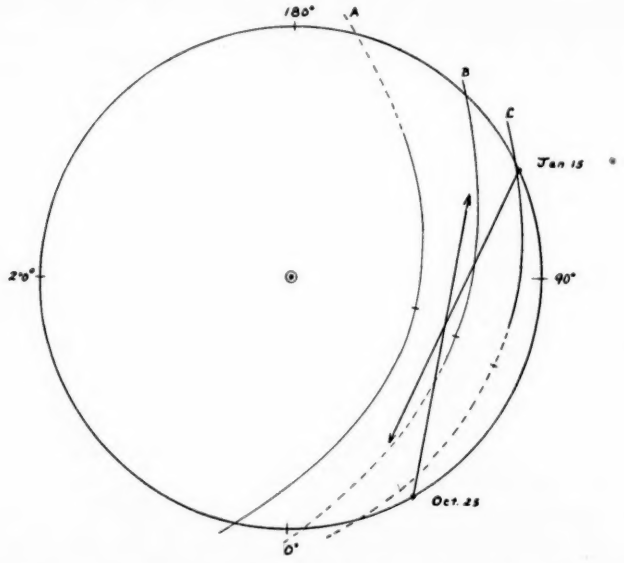

FIG. 3.—Positions of the earth in its orbit at the times of maximum intensity of the zodiacal light, with the directions toward the points of observation, in elongations of 40°. The enhancement of the zodiacal light may be a result of meteoric material moving in a cometary orbit. Three possible orbits are shown: *A*, Daniel's Comet; *B*, Comet 1813 I; and *C*, Comet 1819 IV.

annual variation noted is real. However, no interpretation of the annual variation of the zodiacal light can be definitely made without an investigation of the distribution of its intensity over the celestial sphere in conjunction with the theories of scattering of light by particles. Besides the photometric observations giving the distribution of intensities, a study of the color of the zodiacal light will give additional information concerning the size of the particles producing the scattering of sunlight.

[6] *M.N.*, **94**, 824, 1934.

For the present we can say that the observed maxima represent a greater density of the scattering particles in the directions of the observations, namely, at an elongation of 40° west of the sun for the morning light and 40° east of the sun for the evening light. This is represented graphically in Figure 3, which shows the positions of the earth on the two dates of maximum intensity of the zodiacal light and the directions of the observed points. Data are not available for other points, and a limit for the cloud of particles cannot be given. However, the fact that the maxima are rather sharp indicates that the cloud of particles is not very extensive.

The maxima are present each year and at the same time; it is, of course, very improbable that there is a stationary cloud of particles at the indicated position, in longitude 77° and at 0.65 astronomical units from the sun. The observed effect could perhaps be produced by a meteor swarm seen lengthwise along a considerable part of its orbit. However, none of the observed orbits of meteor swarms fits our data. There remains the remote possibility that one of the known comets has produced a meteor swarm in the required position. An examination of Crommelin's *Comet Catalog* shows three comets that would come under consideration. The orbits of these comets are shown in Figure 3. Daniel's comet, 1907 IV, is probably too close to the sun. The next orbit belongs to Comet 1813 I, and the outer one is for Comet 1819 IV. It is, of course, not possible to prove this connection with the zodiacal light, and the association with cometary orbits can only be tentatively suggested. Those indicated are either parabolic or have very long periods, and it is doubtful whether such comets could shed sufficient meteoric material to form a continuous swarm of particles around the orbits.

McDonald Observatory
April 26, 1937

AN EMISSION NEBULA NEAR σ SCORPII*

OTTO STRUVE

ABSTRACT

With the use of a photographic emulsion sensitized for $H\alpha$, diffuse galactic nebulae have been classified into three groups, depending upon the relative intensity of the red image to the violet image. This method is used to determine the character of nebular spectra. A nebula near σ Scorpii is found to be of the emission type. The red image does not, however, coincide exactly with the violet image. A part of the latter is therefore attributed to pure reflection. The spectrum of the star is B1.

Photographs of the nebulous region in Scorpius and Ophiuchus, obtained last year with the 94-mm Schmidt camera, revealed[1] that the bright nebulae surrounding the B-type stars 22 Scorpii (B3), ρ Ophiuchi (B5), $-24°12684$ (B3), σ Scorpii (B1), and ν Scorpii (B3) are strong in violet light. This was interpreted to mean that the nebulae were at least as blue as, and possibly slightly bluer than, the illuminating stars. However, this interpretation stands or falls with the assumption that the spectra of the nebulae are continuous.

The spectra of the nebulae near ν Scorpii, 22 Scorpii, and ρ Ophiuchi have actually been observed as continuous.[2] The nebula near σ Scorpii, however, has not been observed, and Hubble has merely inferred from the spectral type of the star, B1, that the spectrum of the nebula is probably continuous.

This nebula is so faint, and the star near it so bright, that it is exceedingly difficult to obtain a spectrogram which would definitely settle the question. However, following a suggestion by Keenan,[3] Elvey and I successfully used red-sensitive plates with red filters to isolate the $H\alpha$-radiation.[4] Emission nebulae are very strong when photographed on such plates.

This method has now been materially improved by the use of a new emulsion furnished by the Eastman Kodak Research Labora-

* *Contributions from the McDonald Observatory, University of Texas*, No. 5.

[1] *Ap. J.*, **84**, 219, 1936.

[2] Hubble, *ibid.*, **56**, 405, 1922.

[3] *Ibid.*, **84**, 604, 1936.

[4] *Pub. A.A.S.*, **9**, 23, 1936; *Ap. J.*, **85**, 252, 1937.

PLATE I

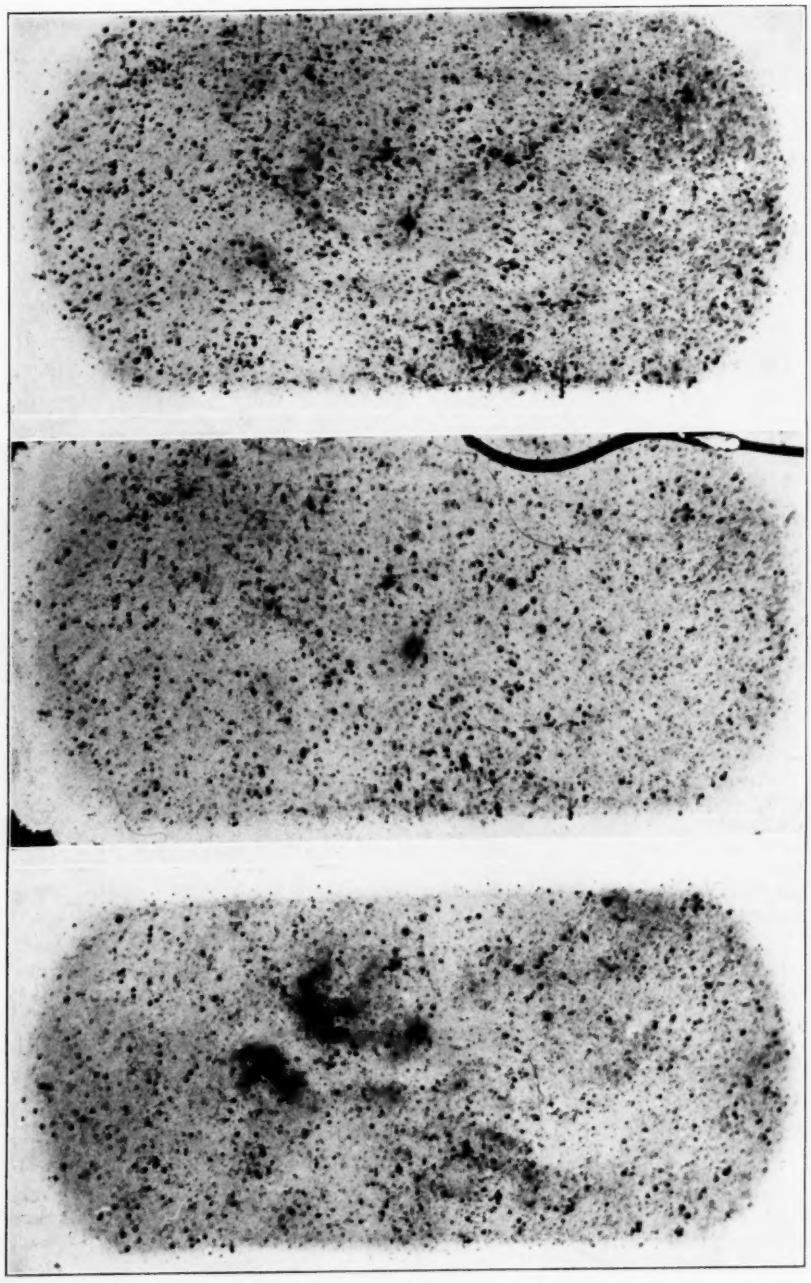

NEBULAE NEAR γ CYGNI
(Enlarged 5.4 times)

UNIV. OF MICH.

tory. This emulsion[5] is especially sensitive to the spectral region on both sides of *Hα*. It is much slower than emulsion IC for yellow light but surpasses it at *Hα*. The contrast is very good.

Plate I shows the region near γ Cygni. Exposure (*a*) was obtained on an Eastman Process emulsion, without filter. This represents the nebulae in violet light, since the Process emulsion is sensitive only to about λ 4800. Exposure (*b*) was taken on emulsion IG with a yellow filter, and exposure (*c*) on the *Hα* emulsion with a red filter (Wratten 29 F). This combination cuts off sharply at λ 6000 on the violet side and just beyond *Hα* on the red. It therefore transmits effectively only a relatively small amount of continuous radiation from the night sky, while any existing nebular emission in *Hα* is transmitted freely. Accordingly, the contrast between an emission nebula and the sky is enhanced.

The nebulae near γ Cygni are well shown on the violet exposure. They are almost completely absent in yellow light, but they are exceedingly strong in *Hα*. This confirms our previous result[6] that these nebulae are of the emission type. The emission which completely surrounds γ Cygni (near the center of the plate), being strongest east of the star, shows rather conclusively that γ Cygni, type F8p, is responsible for the nebular emission. Also of great interest is the faint film of nebulosity which covers the entire western half of the plate and which is obviously also due to emission. This sheet of nebulosity covers a considerable portion of the eastern and northeastern part of the great Cygnus cloud—a region which is rich in B- and O-type stars.[7]

Plate II shows two photographs of the region near σ Scorpii. α Scorpii with its red nebula is on the left. The *Hα* emulsion was used in both cases, and the filter was Wratten 29 F. The blue nebula near 22 Scorpii is completely absent, in spite of the great contrast of the emulsion. The slightly redder nebulosity near −24°12684 is barely visible.

Quite unexpected is the presence of a large unsymmetrical nebula near σ Scorpii. Violet-sensitive plates show a large, fairly symmetri-

[5] Emulsion Spl. Exptl. H-alpha, No. 63147 (Eastman Kodak Company, Rochester, New York).

[6] *Ap. J.*, **85**, 252, 1937.

[7] *A.N.*, **231**, 17, 192.

cal nebula. Barnard's photographs[8] show it slightly stronger on the east than on the west, and considerably stronger on the north than on the south. Ross's photographs and those taken with the Schmidt camera[1] confirm this appearance. On the *Hα* plate the nebula is fairly strong. However, it is almost entirely concentrated in one quadrant—from the north to the west, with a slight extension toward southwest but with only the barest trace east of the star.

It is safe to infer that the nebula shown on the *Hα* emulsion has an emission spectrum; it is also certain that only a part of the light observed on the violet-sensitive plates can be identified with the emission nebula. The rest must be of the reflection type. Why only the western portion of the nebula emits *Hα* cannot be answered. The densest part of the dark nebula illuminated by σ Scorpii lies northeast of the star. There is an arm of obscuring nebulosity on the west. The star density is greatest south and southeast of σ Scorpii.

The spectral type of σ Scorpii is B1. The lines are fairly sharp, and there is not much uncertainty in assigning the proper class. The hydrogen lines are rather weak, suggesting an early subdivision of class B, but the *Si* IV lines λ 4089 and λ 4116 are not strong enough to make it earlier than B1 and not weak enough to make it B2. The existence of a mixed spectrum in connection with a B1 star is not very unusual: Hubble lists at least one other case.[9] The unusual thing about the emission nebula near σ Scorpii is the fact that it does not coincide with the violet reflection nebula.

A number of other nebulae have been observed with red-sensitive plates in order to establish the character of their spectra. The results for all nebulae are summarized in Table 1. The last column contains a classification of the nebular image in red light. The designations I, II, and III are relative to the image obtained on a violet-sensitive plate of high contrast. Comparisons were made either with Process plates of the same region taken with the Schmidt camera or with the photographs in the atlases by Barnard and by Ross. Experience has shown that on the small scale of the Schmidt camera a Process plate reveals approximately the same amount of detail as is shown on the photographs of either atlas. Class I indicates that

[8] *Atlas*, Pl. 13.

[9] *Ap. J.*, **56**, 184, 1922. Star Bond 734 in NGC 1982, type B1p.

PLATE II

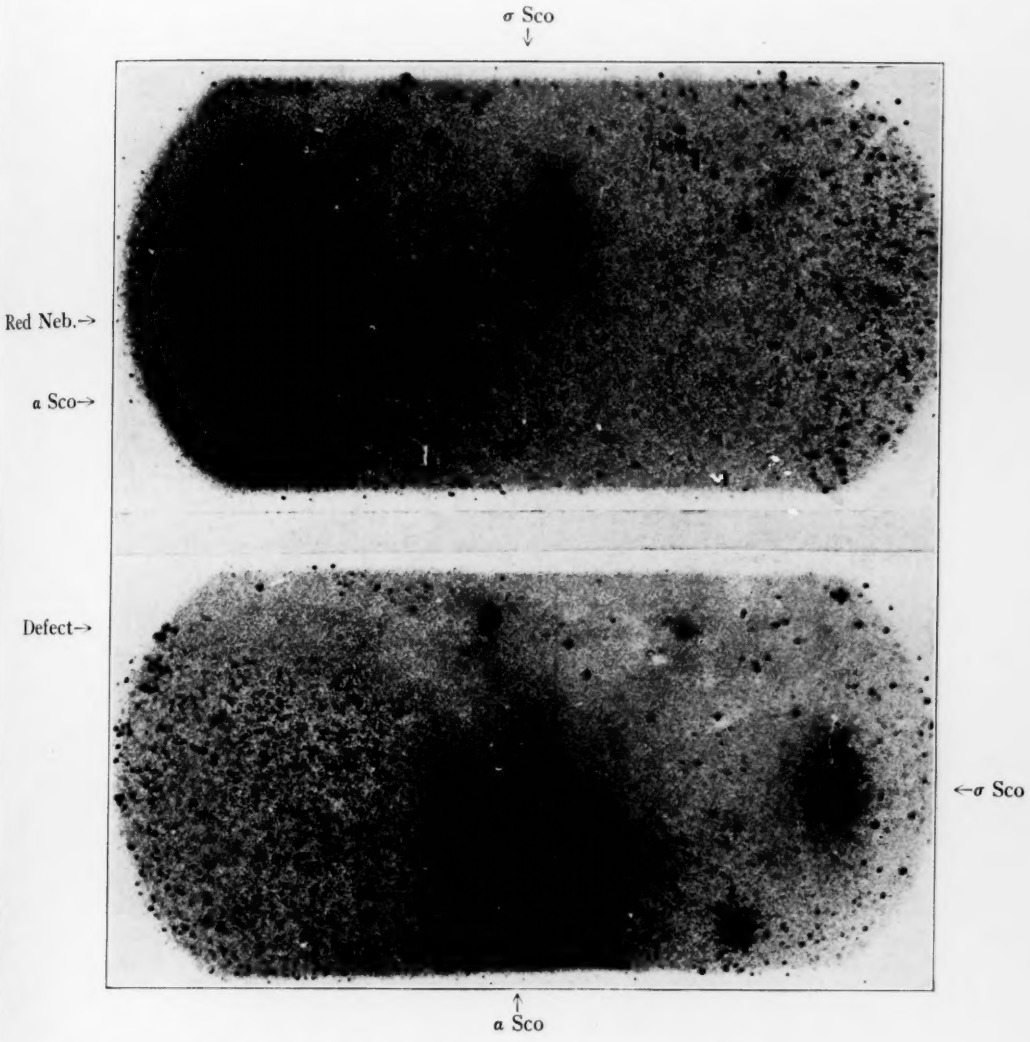

EMISSION NEBULA NEAR σ SCORPII PHOTOGRAPHED ON *Hα* EMULSION
(Enlarged 5.9 times)

UNIV. OF MICH.

TABLE 1

NEBULAE OBSERVED IN RED LIGHT*

No.	Nebula	Exciting Star	Sp. of Star	Sp. of Nebula	Class	Remarks
1	IC 59	γ Cas	Bop	E	II or III	1
2	IC 63	γ Cas	Bop	E	II	2
3	Pleiades	Merope	B5	C	III	3
4	Pleiades	Maia	B5	C	III	3
5	NGC 1499	ξ Per	Oe5	E	I	4
6	IC 2118	Rigel	B8p	C	III	5
7	NGC 2068	+0°1177	B5	C	III	.....
8	Orion	.....	.....	.....	III	6
9	IC 434	σ Ori ζ Ori	Bo Bo	E	I	7
10	NGC 2023	−2°1345	B2	C	II	8
11	NGC 2024	ζ Ori	Bo	E	I	9
12	λ Ori	λ Ori	Oe5	.....	III	10
13	Barnard 223	+8°933	B2	.....	III	.....
14	NGC 2175	+20°1284	Oe5	.....	I	9
15	NGC 2237	Cluster	Oe5	E	I	11
16	IC 446	.....	B1	C	III	.....
17	NGC 2245	+10°1159	B1p	C	III	12
18	S Mon	S Mon	Oe5	.....	II	13
19	Large nebula	S Mon	Oe5	.....	II	14
20	π Sco	π Sco	B2	C	III	.....
21	1 Sco	1 Sco	B3	.....	III	.....
22	2A Sco	2A Sco	B3	.....	III	.....
23	σ Sco	σ Sco	B3	C	I and III	15
24	IC 4604	ρ Oph	B3	C	III	16
25	−24°12684	−24°12684	B3	.....	III	16
26	IC 4605	22 Sco	B3	C	III	16
27	α Sco	α Sco	Mo	.....	I	17
28	+41°3687	γ Cyg ?	F8p	.....	I	.....
29	+40°4103	γ Cyg ?	F8p	.....	I	18
30	+39°4186	γ Cyg ?	F8p	.....	I	.....
31	+39°4206	γ Cyg ?	F8p	.....	I	.....
32	Large nebula	γ Cyg ?	F8p	.....	I	19
33	NGC 7000	α Cyg	A3p	C+E	I	20
34	Near 56 and 57 Cyg	α Cyg	A3p	.....	I	20
35	ξ Cyg	ξ Cyg	K5	.....	II	21

* Class I: the red images are stronger than the violet images. Class II: the red images are equal to the violet images. Class III: the red images are weaker than the violet images. The spectra of the nebulae are from Hubble (*Ap. J.*, **56**, 1922).

REMARKS

1. North of γ Cas.
2. East of γ Cas.
3. The nebula near Maia appears to be slightly bluer than that near Merope.

4. This nebula is not as strong in *Hα* as would be expected from the violet image.

5. Large nebula northwest of Rigel.

6. Outer nebulosity of Orion, northeast of NGC 2068.

7. Bay nebula, south of ζ Orionis. Not quite as strong in red light as NGC 2024. The extreme southern extension of this nebula seems to be relatively weaker in red light than the more intense northern portion.

8. This nebula is unexpectedly red for the spectral class of its star.

9. Very strong in *Hα*.

10. The *Hα* plate is underexposed; and since the violet image is weak, the color class may not be correct.

11. The *Hα* exposure is very strong; it shows greater extent and more detail than Ross's *Atlas*, No. 35, or Lick Pub., **11**, Pl. 27.

12. The designation is according to Barnard (*Pub. Lick Obs.*, **11**, Pl. 28, 1913). Hubble designates this nebula IC 447 (*Ap. J.*, **56**, 405, 1922) and reserves the designation NGC 2245 for a cometary nebula near by (*ibid.*, **44**, 195, 1916).

13. For a nebula stimulated by an Oe5 star the *Hα* image is surprisingly weak. It is too strong, however, to be attributed wholly to reflection.

14. This is the faint diffuse nebulosity extending a degree or more northeast and east of S Mon.

15. The eastern part of this nebula is of class III; the northwestern part is of class I.

16. IC 4605 is bluest, and the nebula around $-24°12684$ is slightly less blue. IC 4604 is intermediate.

17. Red reflection nebula near Antares. The strength of the yellow image proves that the nebula is not of the emission type.

18. The nebula contains the B2p star $+40°4103$; but the uniform surface brightness of the nebula, exhibiting no concentration toward this star, suggests that the excitation does not originate in it.

19. This is the faint nebulous sheet extending toward the southwest from γ Cyg. It covers a part of the cluster of B stars in the Cygnus cloud.

20. The nebula between 56 and 57 Cyg is relatively stronger in *Hα* than NGC 7000 (the North America nebula).

21. The red star ξ Cyg is surrounded by a faint wisp of nebulosity which is strongest northeast of the star. It is probably of the reflection type.

the *Hα* image is appreciably stronger than the violet image; II stands for approximately equal images; III is used to designate nebulae which are much weaker in red light than in violet light. Some of the red images used for this investigation were taken on emulsion IC with a red filter.

Since many of the nebulae in Table 1 have known spectra, we can roughly calibrate our classification. Emission nebulae are almost always I or II. The difference between these two classes is appreciable. Thus, the nebula near 15 S Monocerotis is relatively much weaker in red light than NGC 2237. Pure reflection nebulae illuminated by

stars of early spectral type are always of class III. Those illuminated by very red stars may be of class I or class II.

The method described here has two advantages over the spectrographic method: it can be used for very faint nebulae, and it permits us to study the entire nebula—not only its brightest portion. Its principal disadvantage lies in the fact that it does not permit us to determine for each nebula the fraction of light concentrated in emission lines and in the continuous spectrum. For example, we do not know whether the difference between emission nebulae of classes I and II is caused by a difference in the relative intensities of the emission lines or by different amounts of continuous spectrum superposed over the emission lines.

I am indebted to Dr. C. T. Elvey and to Dr. P. Rudnick for valuable assistance in making the observations.

YERKES OBSERVATORY
AND
MCDONALD OBSERVATORY
May 19, 1937

NOTES

NOTE ON A POSSIBLE EFFECT OF THE RECENT INCREASE IN BRIGHTNESS OF γ CASSIOPEIAE

ABSTRACT

Attention is called to possible effects of the recent increase in brightness of γ Cassiopeiae on the brightness of the two near-by diffuse nebulosities.

The rise in brightness of the Be star γ Cassiopeiae in the latter part of 1936 may prove to be of additional interest because of pos-

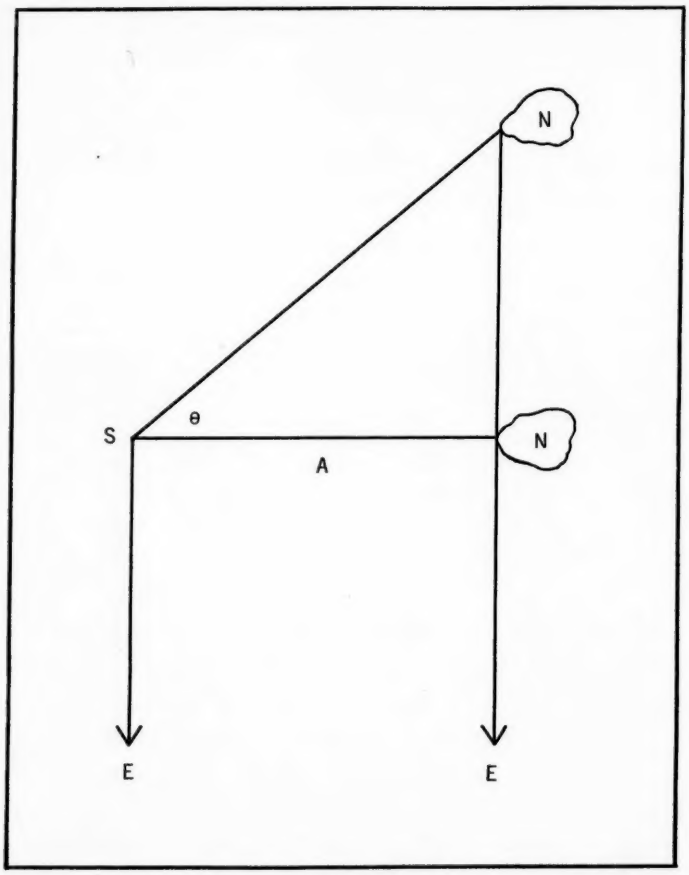

FIG. 1.—A is the projected distance in light-years from γ Cassiopeiae (S) to the nearer nebula, N. The true distance is approximately A sec θ; the lag in time, observed at the earth E, between the stellar outburst and its effect on the nebula is approximately A (sec θ+tan θ).

sible effects on the two diffuse nebulosities which are situated close to the star. There can be little doubt that the nebulae owe their luminosity to the radiation of γ Cassiopeiae, and it seems likely that the approximate doubling in the light of the latter would result in an appreciable increase in the brightness of the nebulae themselves.

From similarity with Be stars observed by Trumpler[1] in the cluster χ Persei and in the Pleiades we can assume that the photographic absolute magnitude of γ Cassiopeiae probably lies between -1 mag. and -3 mag. On the assumption that its apparent photographic magnitude is 2, its distance from the earth lies between 40 and 100 parsecs.

If there is no foreshortening, the light of the star will reach the nebula (Fig. 1) A years later and will also be observed at the earth A years after the original outburst. If foreshortening is present, the true direction of the nebula makes an angle θ with A, and the light from the nebula will reach the earth approximately

$$A(\sec\theta + \tan\theta) \qquad [+90^\circ > \theta > -90^\circ]$$

years later than the observed rise in γ Cassiopeiae.

From the apparent observed shapes of the two nebulae it seems rather unlikely that $\theta > 45^\circ$. As the angular distance from the vertex of the nearer nebula to the star is $20'$, the elapsed times at the earth between the observed rise in the star's brightness and a possible effect in the nebula are:

θ	D_{E-*}=40 Parsecs	D_{E-*}=100 Parsecs
-45°	0.3 years	0.8 years
0	0.7	1.9
$+45$	1.6	4.5

Accurate photometric measures of the nebulae during the next few years may therefore show an increase in their brightness as a result of the increased strength of the radiation of γ Cassiopeiae.

W. W. MORGAN

YERKES OBSERVATORY
April 21, 1937

[1] *Pub. A.S.P.*, **38**, 350, 1926.

NOTE ON THE DUPLICITY OF NOVA HERCULIS

ABSTRACT

Micrometer measures and the visual appearance of the components of the nova are discussed, together with some conclusions derived therefrom.

After the writer had found the nova to be a close double star in the 36-inch telescope of the Lick Observatory, micrometer measures were published by him[1] and by Voûte,[2] Van Biesbroeck,[3] Aitken,[4] and Simonov.[5] The last author states that his images were only slightly elongated, and his distances are accordingly not reliable.[6] His results have not been used.

The normal points representing these observations are given in Table 1. The two recent averages by the writer are from unpublished measures, which are in the table below. The observations made with seeing 3 are given half-weight. The angles and distances

TABLE 1

1935.515	130°.6	0″.212	Δm =	0.4	4	*n* K	36-inch
1935.531	128.0	.168		.5	5	*n* VB	40-inch
1935.588	131.5	.224		.4	5	*n* K	36-inch
1935.598	131.6	.204	−	.2	5	*n* Vou	24-inch
1935.746	128.3	.194		.6	5	*n* VB	40-inch
1936.740	131.1	.505		.4	3, 2*n*	K	40-inch
1936.747	136.9	.39		.5	1	*n* A	36-inch
1937.202	131.7	.62		.1	3	*n* K	40-inch

1936.687	131°.6	0″.50	Δm = 0.3	40, 1340 ×	seeing 4
1936.726	131.9	....		40, 1340 ×	3
1936.799	130.2	0.51	0.4	40, 960 ×	4
1936.740	131.1	0.505	0.4	3,2*n*	
1936.980	135°.2	0″.70	Δm = 0.4	40, 700 ×	seeing 3
1937.241	130.7	.55	.0	40, 960, 1340 ×	4
1937.274	131.0	0.65	0.0	40, 960 ×	4
1937.202	131.7	0.62	0.1	3*n*	

[1] *Pub. A.S.P.*, **47**, 228 and 267, 1935.

[2] *Ibid.*, p. 270.

[3] *Ap. J.*, **82**, 433, 1935.

[4] *Pub. A.S.P.*, **48**, 340, 1936.

[5] *A.N.*, **259**, 81, 1936.

[6] *Ibid.*, **256**, 300, 1935.

in Table 1 are represented in Figure 1. My measures make the angles sensibly constant. The difference of 3° between these and Van Biesbroeck's is certainly small for a pair of only 0".2 separation. Dr. Aitken's result is, unfortunately, only a single night's measure, with "seeing not of the very best, ... at least 3."

The distances appear to increase linearly with the time. I have drawn in the diagram a straight line which, in my opinion, is the

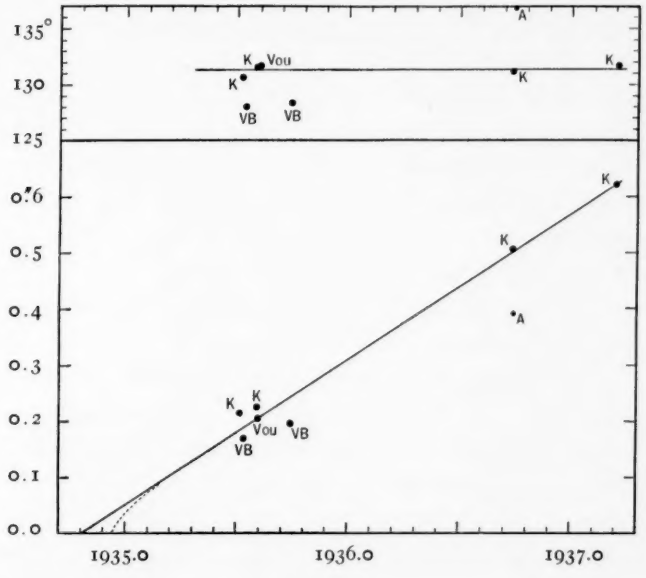

FIG. 1

best that may be derived from the measures. It intersects the time axis at about 1934.82, which precedes the outburst on December 12[7] = 1934.94 by 0.12 years. But this small difference is not considered significant. If it is possible to follow the nova for at least two more years, the reality of this difference may be discussed to advantage. The explanation of a difference of this nature would obviously be the gravitational deceleration of the two masses.

Many papers have discussed models which would explain the observed spectral features. For mathematical reasons a spherical model is attractive and has been frequently used. But the visual observa-

[7] For instance, A. Beer, *M.N.*, **97**, 242, 1936.

tions show this to be very far from the truth. We shall discuss the visual observations of the two components, without trying to interpret them, since it is found that more data are needed.

On July 3, 1935, when the duplicity was first noticed (I had looked in vain for possible duplicity on March 31, April 27, and June 10), the images in the 36-inch telescope were sharp in yellow light, being nearly monochromatic, and were apparently of small real diameter. This diameter could hardly have exceeded 0".05. Further, Δm was roughly the same for the various monochromatic emissions, indicating that the two bodies seen had nearly identical spectra.[8] This question was further examined in a second note,[9] describing the visual prismatic spectrum of the two components. Van Biesbroeck[10] has noticed the same features with the 40-inch telescope.

Recently Aitken[11] found the images "larger and less sharply defined when the focus was set for green rays than when it was adjusted for yellow light. In the latter focus the two nuclei were small and fairly sharp, but I should hardly call them stellar." The seeing was 3 during this observation.

In view of the importance of the matter, the writer has paid special attention to the appearance of the images whenever a first-class opportunity occurred. The following records were made immediately after the observations with the 40-inch telescope.

October 19, 1936.—Seeing 4. More than 95 per cent of the visual light is concentrated in the nebulium lines. The size of the components seems to be about 0".3 or 0".4 with power 960 ×, and the images seem nearly in contact. But with 1340 ×, sharp nuclei are visible—the true diameter of which cannot be larger than 0".10—which are surrounded by hazy disks, about 0".4 in diameter. The impression was that this larger disk (or blur) was due to the combined effect of imperfect correction of the 40-inch objective for blue light and of imperfect seeing. No continuous spectrum could be seen, or any nebulosity around the nova, with low power (460 ×).

March 29, 1937.—Seeing 4. The images are separated by at least three times their diameter. The image in the yellow plus red light is 4 to 5 mag. fainter than that in the "nebular" light. (Observation

[8] *Pub. A.S.P.*, **47**, 229, 1935.

[9] *Ibid.*, p. 269.

[10] *Loc. cit.*

[11] *Loc. cit.*

through a small prism held between the eyepiece and the eye.) The appearance of the yellow images, though faint, is sharp and stellar; the images in the nebular light look fuzzy, but that may be due to the objective.

April 10, 1937.—Seeing 4. The images in the yellow light are too faint to be measured. The "nebular" images are fairly sharp, separated by at least three times their diameter.

These observations are not conclusive as to the exact size of the images, but they indicate that the disks are not larger than $0''.2$, and are possibly only $0''.1$, in diameter. Further observations under the best conditions are required, and a comparison should be made with other objects having a similar spectrum.

G. P. KUIPER

YERKES OBSERVATORY
May 1937

REVIEWS

Die Fernröhre und Entfernungsmesser. By A. KÖNIG. 2d ed. Berlin: Julius Springer, 1936. Pp. v+242. Rm. 22.50.

The second edition of this book[1] contains an interesting new chapter on the history of the telescope from Lippershey to Porro. There is also a new section on instruments for measuring the altitudes of airplanes. There have been numerous other improvements in the text and in the illustrations.

A Textbook of Astrophysics and Stellar Astronomy (in Russian). Edited by B. P. GERASIMOVIČ. Vol. 1: *Methods of Astrophysical and Astrophotographic Investigation.* Leningrad: ONTI, 1934. Pp. 342. Rb. 4.20. Vol. 2: *The Physics of the Solar System and Stellar Astronomy.* Leningrad: ONTI, 1936, Pp. 579. Rb. 7.25.

Professor Gerasimovič, who is well known in America for his brilliant research work in astrophysics and who is now the director of Russia's largest observatory at Pulkovo, is to be congratulated for having edited an extraordinarily good advanced textbook of modern astrophysics. Russian students will have the advantage of learning from a treatise which contains a connected story of all phases of astrophysics. It is a pity that the book is not available in English. The well-known volumes by Russell, Dugan, and Stewart are unsurpassed as an introduction for the serious student; but these authors state in their Preface that "the preliminary knowledge assumed on the part of the student involves only the elements of mathematics and physics. Use of the calculus has been completely avoided. . . . . " The Russian books, on the other hand, use the mathematical form of exposition, although it would seem that they intentionally avoid the more difficult and specialized methods.

It cannot be too strongly emphasized that our universities are particularly in need of a textbook of the character of these volumes edited by Gerasimovič. Our students who specialize in astronomy rely at present upon Russell, Dugan, and Stewart for their general training. After that they begin the study of such highly specialized volumes as Eddington's

[1] *Ap. J.*, **60**, 78, 1924.

Internal Constitutions of the Stars, Rosseland's *Theoretical Astrophysics*, or Milne's and Pannekoek's articles in the *Handbuch der Astrophysik*. The step from the elementary general course to the specialized advanced study is difficult and frequently causes even good students to lose confidence in their ability to master the subject. The excellent book by the two Strömgrens, father and son, is a useful supplement, and it includes in its scope not only astrophysics but also positional astronomy and celestial mechanics; but it is at present not available in English.

The question arises why we have no suitable textbook which would serve as a link between Russell, Dugan, and Stewart and the specialized monographs. Is it because commercial publishers cannot make a sufficient profit from an advanced textbook in astronomy and because the various university presses are being operated on a profit basis? If so, we can perhaps make a serious effort to induce our universities, or their presses, to disregard the financial aspects and to publish for the few advanced students in astronomy the kinds of textbook they now lack.

The volumes under review consist of a series of chapters written by the leading Russian astronomers in each field.

Volume 1 begins with an Introduction by Ambarzumian on atomic physics. Balanovsky gives a short but complete account of the theory of the refractor and the reflector. Kostinsky discusses the chemical foundations of photography and contributes a long chapter on astrometric methods applied to photography. All necessary details are given for the reduction of star positions. Schlesinger's method of dependences is also described. Shajn contributes a splendid chapter on the methods of stellar spectroscopy. A student who has carefully read this chapter should be able to design a good spectrograph, test it, and use it for the determination of radial velocities. Balanovsky writes on photometry, while Kosirev discusses the methods and some of the results of spectrophotometry. The volume is concluded by a chapter on solar work written by Perepelkin.

Volume 2 contains a long chapter on the results of solar investigations by Perepelkin. The second chapter on the planetary system by Fessenkoff is especially valuable since it contains the fundamentals of theoretical photometry. Gerasimovič and Shajn collaborate in a chapter on "The Introduction to Stellar Astronomy." This is followed by Shajn on "Double Stars" and by Ambarzumian on "Stellar Atmospheres." Both chapters are authoritative as well as comprehensive. The remainder of the book is by Gerasimovič. It is devoted to variable stars, diffuse matter in interstellar space, clusters, the internal constitution of the stars, the

distribution of the stars in space, stellar motions, and extra-galactic nebulae.

It is regrettable that such a fine book is printed on the very poor grade of paper which is so familiar to those who make use of the Russian scientific literature. The halftone illustrations are quite unsatisfactory and in some cases fail to show the characteristic features of the objects which they are supposed to illustrate.

O. STRUVE

Arc Spectrum of Iron from λ 8388 to 2242 A. By A. GATTERER and J. JUNKES. Castel Gandolfo (Italy): Specola Vaticana, 1935. Pp. 10+21 illustrations.

Spark Spectrum of Iron from λ 4650 to 2242 A. By A. GATTERER and J. JUNKES. Castel Gandolfo (Italy): Specola Vaticana, 1935. Pp. 9+13 illustrations.

The first part of this publication represents a set of twenty-one photographic reproductions of the arc spectrum of iron. Approximately four thousand lines are shown and their wave-lengths, to the nearest 0.01 A, are indicated on the margins. The photographs were obtained with a prism spectrograph. The dispersion on the reproductions varies from 0.17 A/mm in the ultraviolet to 4.39 A/mm in the infrared.

The second part contains thirteen photographic reproductions of the spectrum of the iron spark from λ 4242 to λ 4650. Approximately two thousand lines are shown.

The plates will be found very useful for the rapid identification of the comparison lines in a slit spectrogram. It is especially convenient to have the exact wave-lengths in international angstroms without having to consult the tables of Kayser and Konen.

O. S.